



HAL
open science

Every entangled stuff has its own avatar

Mario Mastriani

► **To cite this version:**

| Mario Mastriani. Every entangled stuff has its own avatar. 2018. hal-01655231v3

HAL Id: hal-01655231

<https://hal.science/hal-01655231v3>

Preprint submitted on 28 Mar 2018 (v3), last revised 19 Aug 2019 (v13)

HAL is a multi-disciplinary open access archive for the deposit and dissemination of scientific research documents, whether they are published or not. The documents may come from teaching and research institutions in France or abroad, or from public or private research centers.

L'archive ouverte pluridisciplinaire **HAL**, est destinée au dépôt et à la diffusion de documents scientifiques de niveau recherche, publiés ou non, émanant des établissements d'enseignement et de recherche français ou étrangers, des laboratoires publics ou privés.

Quantum Communications, Relativistic Entanglement and the Theory of Dilated Locality

Mario Mastriani

Quantum Communications Group, Merx Communications LLC,
2875 NE 191 st, suite 801, Aventura, FL 33180, USA

mmastri@merxcomm.com

Since his famous discussions with Niels Bohr, Albert Einstein considered quantum entanglement (QE) as a spooky action at a distance, due to the violation of locality necessary so that two entangled particles can share this effect in an instantaneous way despite of being at a great distance from each other, i.e., not being local. In other words, a notification about the change of state in one of them could only cover the space that separates them at a speed superior to that of light, which we know is impossible according to the Theory of Relativity (TR). Besides, QE faces directly the two main pillars of Physics: TR and Quantum Theory (QT); becoming the bone of contention between both theories. Quite the contrary, in this work we will see that QE is the meeting point of both theories, so much so, that QE could be considered as the cornerstone of the Theory of Everything (TOE). Consistent with this, the entangled particles retain certain autonomy unknown to date, and in addition, they will have relativistically entangled alter-egos, which will hold the effect even when the original entangled particles are extremely separated from each other. These alter-egos can be considered as black holes (with their corresponding temperature and entropy) giving rise to a wormhole. This is possible since the locality dilates according to the Lorentz factor, which is accompanied by a contraction in the effective channel and in the temporal delay to cross that channel. All this takes place while space-time is curved (hyperspace) to generate the wormhole between both black holes. In other words, QE is a local effect of infinite range so it does not outpace the speed of light, and therefore QT is a complete theory that does not clash with TR. Finally, everything we have said has direct consequences on the link between entangled particles from the point of view of quantum communications in terms of the channel and its bandwidth, latency, capacity, robustness and security.

Keywords—Black holes; EPR paradox; locality; quantum channel; quantum communication; quantum entanglement; Quantum Theory; quasi-entanglement; Theory of Relativity; wormhole.

1 Introduction

Quantum entanglement -also known as the God effect- is a physical phenomenon which takes place between two or more particles (strictly speaking, their spins) that interact after their creation in such a way that the resulting quantum state corresponds to the effect itself and not to the individual particles that make it up [1]; even when such particles are separated by an astronomical distance. Consequently, the resulting quantum state acts as a whole [2] with a total loss of individuality on the part of the original states. Therefore, we will refer to the entanglement as a specific case of correlation between subsystems [3]. Also, several configurations for quantum entanglement which currently exist can be found, in particular: GHZ state due to D.M. Greenberger, M.A. Horne and A. Zeilinger [4,5] formed by 3 or more entangled particles and the so-called configuration W which is the perfect complement of the previous one [3]. Another interesting kind of entanglement is called Hyperentanglement [6] which is a promising resource in quantum information processing because of its inherent characteristic of high capacity; defined as the entanglement in multiple degrees of freedom (DOF) of a determined quantum system, such as polarization, spatial-mode, orbit-angular-momentum, time-bin and frequency DOF of photons [7]. Simultaneously, multidimensional entanglement quantum system confirms the existence of at least one dimension of 100-x-100 using spatial modes of photons [8]. On the other hand, distributed entanglement [9] is the polygamous nature present in multipartite systems with a strong unlocalizable character [10]. Recently, two extremely important experiments have been carried out: one being entanglement between photons that have never coexisted [11], i.e., entanglement in time, not only in space, and the other one being, a scheme that deterministically generates wave-particle entanglement of two photons [12].

Besides, at this point, it is important to mention two outstanding aspects of entanglement: distillation, and, swapping. In the first case, we get some number of almost pure Bell pairs from N copies of an arbitrary entangled state. This transformation happens using local operations and classical communication (LOCC). In other words, it is a powerful tool to cope with the negative influence produced by noise in quantum channels. Thanks to this previous transformation, the distillation is achieved by obtaining a smaller number of maximally entangled pairs (i.e., Bell states [1]) from less shared entangled pairs. As for swapping, it is a simple and illustrative example of Teleportation, which can be equally applied to pure and mixed states, and is considered as the state of a single subsystem of an entangled pair [1].

Moreover, quantum decoherence is the worst enemy of entanglement, and formally it is the loss of quantum coherence. In quantum mechanics, particles such as electrons also behave like waves and are described by a wavefunction. These waves can interfere, leading to the peculiar behavior of quantum particles. As long as there is a definite phase relation between different states, the system is said to be coherent [1].

Although quantum entanglement is a key piece in Quantum Information Processing [13-15] in general and Quantum Computing [14,16-20] in particular, it is in Quantum Communications [18,19,21-23] where the most exciting challenge is presented, which consists of the following problem: if we have two entangled particles and we separate them from each other at a distance similar to that existing between Earth and Mars; the theory of quantum entanglement tells us that any local change in the state of one of the particles causes the instantaneous change in the state of the other particle regardless of the distance between them, either because of the quantum measurement, or by a change in the polarization of the particle or in the magnetic field in which it is immersed.

However, if we consider the link between these particles as a quantum channel and the change in both states as a signal, then that signal should travel at a speed greater than light to perform such a feat. This fact collides head-on with the Theory of Relativity [24] and this results in the Einstein-Podolsky-Rosen (EPR) paradox [1,25-30] and even more, with No-Communication [31] and No-Cloning [1] Theorems (two No-Go Theorems [32]). At this point, a formidable debate on the basis of four possible alternatives breaks ground:

- 1) quantum entanglement [1] is not instantaneous, therefore, it makes no contribution in relation to the communications involved in the trip to Mars, and hence, it does not collide with the Theory of Relativity [24],
- 2) quantum entanglement is instantaneous, and we do not expect it to convey information, this is the present posture (or resignation) and from which no problem is derived,
- 3) quantum entanglement is instantaneous, and we intend to carry information, then, it collides with the Theory of Relativity, which represents a very unpleasant scenario because it deepens the gap between Quantum Theory and the Theory of Relativity,
- 4) lastly, quantum entanglement is instantaneous, and we intend to carry information, however, it does not collide with the Theory of Relativity. This is the hypothesis and the central objective of this work, moreover, this would be the ideal scenario, because Quantum Theory [1] would be a complete theory, being quantum entanglement an instantaneous effect, and all these advantages coexist simultaneously.

Regardless of the correct alternative, such a debate is the main pitfall of quantum communications involved in the trip to Mars.

On the other hand, in recent years, there have been significant efforts to formally link quantum entanglement with gravity in general [33-35], as well as with the entropy of black holes in particular [36-38]. This link is not trivial at all. If this was successful, it would give rise to a version of the theory of everything (TOE) [39], through which the Quantum Theory [40-43] and the Theory of Relativity [24] would coexist, neither doubting the completeness of the first (as happened from the EPR paradox [27]) nor exposing with marked discrimination the total inability of the second to explain the subatomic world; given that, the search for a formal nexus between both worlds definitely represents the central axis of Modern Physics, and the present work.

The principle of locality [44-45] establishes that an object can only be influenced by its immediate surroundings. A local theory must necessarily include the principle of locality. This is presented as an alternative to the deeply rooted concept of instantaneous *action at a distance* [1,25-29]. Since the days of Newton, the locality has overflowed its natural frame (i.e., Classical Physics), in particular, field

theories. Basically, the idea is the following: given two points A and B; if an action takes place on point A, then, the only way that this action could have influence on point B is that between them, there is a field that conveys such action. In other words, there must be a wave or particle that crosses the space between the two points so that they share that influence. The Special Theory of Relativity [24] establishes that the limit at which the mentioned influence can travel is that of the speed of light. A direct consequence of this is that an action at point A cannot simultaneously and instantaneously cause the same result at point B; since, the time it takes for the influence to cross the space between both points cannot be less than $t = d/c$, where d is the distance between the points, and c is the speed of light. In fact, in 1935 Albert Einstein, Boris Podolsky and Nathan Rosen published their work on the EPR paradox [1,25-30]. In this work they theorize about the possibility of non-local behavior of quantum mechanics. Their reasoning is based on the fact that, if we make a measurement on one of the constituent particles of an entangled pair, it simultaneously and instantaneously produces the collapse of the wave-function in both near and remote particles, incomprehensibly exceeding the speed of light. However, this violation of locality does not allow us to use it to transmit information faster than light [29,46,47], since the collapse of the wave-function has a probabilistic nature. In 1964, John Stewart Bell presented his famous theorem (the *Bell inequality* [1,25]), which was violated in several experiments implying, at least apparently, that quantum mechanics does not comply with locality and realism (or local-realism [1,27]). This principle, among others, is linked with values of unmeasured magnitudes. Then, the local-realism emerges as the resultant between locality principle (establishing the speed of light as the upper limit of any cause-and-effect) with the assumption that any physical magnitude must objectively have a real value before any possible measurement. As Albert Einstein said “I like to think that the moon is there even when I am not looking at it”.

The local realism is accepted by classical mechanics, and classical electrodynamics, but absolutely rejected by quantum mechanics. This rejection is based on the experiments carried out with remote entangled particles, in particular, that made by Aspect in 1982, which is apparently supported by the Bell's 1964 inequality theorem [1,25]: an interpretation that Einstein previously rejected (in form of a paradox). In the course of this work the reason why we say *apparently* will be unveiled. By definition, Quantum Mechanics violates either locality or realism. If an experiment shows quantum mechanics, it violates Bell's theorem. However, it is not clear if the 1982 experiment demonstrates a true violation, due to two reasons: experimental limits of the test and the complete inability to prove the sub-class of inequalities. Currently, several interpretations of quantum mechanics seem to violate various aspects of Local Realism, at least, apparently, since it can be wondered: Does the violation really happen? Is that interpretation correct? In fact, some interpretations only violate aspects of a related principle known as counter-factual definiteness [48] (CFD), i.e., it accepts the results of a measurement that was never made giving values that were never measured as valid.

The first experimental test about the Bell inequality was made by Alain Aspect in 1982 [30,49]. In such test, quantum mechanics seems to violate the inequality, so it follows that it must violate either locality or realism [1,27]. However, several scientists have noticed that these experiments contained “loopholes”, which do not allow an effective response to this question. Apparently, this problem seemed to have been solved in 2015 in the experiment of Dr. Ronald Hanson at Delft University, carrying out the first loophole-free experiment [50].

However, as it can be seen, the controversy continues although, at present, in a tone significantly lower than in the days of Albert Einstein, who fundamentally objected to the probabilistic nature of quantum mechanics and famously declared “I am convinced God does not play dice”. Einstein, Podolsky, and Rosen argued that “elements of reality” (in the form of hidden variables [1-3,51]) must be incorporated to quantum mechanics to explain entanglement without accepting action at a distance [1,52]. This led the authors to argue that Quantum Theory could not be considered a complete theory, although it was [27]. In other words, entanglement became the bone of contention between the two main theories of Physics. Later, Bell's theorem established that local hidden variables of certain types are impossible, and that this implies non-locality. Another famous non-local theory belongs to De Broglie–Bohm [1,2].

In a very short although extremely interesting paper [53], Prof. Alain Aspect raises doubts about what the problem is: locality or realism? Several experiments have been carried out throughout the last decades with the object of unmasking, or simply bringing out the truth in relation to this subject, including, of course, Bell's experiments. The most outstanding fact of these experiments takes place

based on the so-called CHSH inequalities, which are thanks to John Clauser, Michael Horne, Abner Shimony, and Richard Holt (CHSH), who described them in a much-cited paper published in 1969 [51].

Nowadays, a series of methods for local operations and classical communication [1,3] (LOCC) complete these concepts. The first one is LOCC itself which is employed in quantum information theory, and where a local operation (i.e., a product) is carried out on part of the system. The result of that operation is communicated classically to another part where another local operation is usually performed putting in evidence that two Bell pairs [25] would constitute an example of this. Another method is the so-called NLOCC [54], or noisy LOCC, by means of which local systems in maximally mixed states can only be added. That means that any other system must be considered in the initial state rather than in the processing stage. Lastly, the CLOCC or closed LOCC [55] method, which is a modification of the LOCC paradigm that disallows unrestricted consumption of local pure states. Horodecki *et al* [56] had previously obtained some limitations on this problem, both for the one-way and two-way CLOCC case.

Finally, and based on what we have said so far, it is clear that a reconciling theory is more necessary than a unifying one. That is the central idea of this work through the Theory of Dilated Locality developed in the next sections.

2 Results

2.1 Mutual information as a measure of correlations

For pure states, that is, states on the Bloch's sphere [13], any wave-function

$$|\psi\rangle = \alpha|0\rangle + \beta|1\rangle \quad (1)$$

arises from the superposition of so-called Computational Basis States (CBS) or qubit basis states, which are located at the poles of the already mentioned sphere with $|\alpha|^2 + |\beta|^2 = 1$, such that $\alpha \wedge \beta \in \mathbb{C}$,

$$\text{Spin up} = |\uparrow\rangle = |0\rangle = \text{North pole} \equiv \mu_{|0\rangle}, \quad (2)$$

$$\text{Spin down} = |\downarrow\rangle = |1\rangle = \text{South pole} \equiv \mu_{|1\rangle} = -\mu_{|0\rangle}, \quad (3)$$

where $\mu_{|0\rangle} = 1$ for photons, and $\frac{1}{2}$ for electrons, being $\mu_{|0\rangle}$ and $\mu_{|1\rangle}$ the scalar versions of the *spin up* $|0\rangle$ and the *spin down* $|1\rangle$, respectively, in such a way that the complete spin is conserved, i.e., $\mu_{|0\rangle} + \mu_{|1\rangle} = 0$, similarly when a spinless particle decays in two new entangled particles with opposite spins [1,2,13]. Therefore, in this paper, the letter μ will represent spin numbers in general, exclusively, and does not necessarily mean muon. Moreover, and based on CBS, we can define another basis, which will be very useful for the rest of this paper as well as for Quantum Information in general [1], and quantum teleportation and superdense coding in particular [28,57-59], taking into account the interaction of two subsystems A and B, and considering that its components are pure states and using their scalar versions too,

$$\begin{aligned} |0^A\rangle \otimes |0^B\rangle &= |0^A\rangle |0^B\rangle = |0^A, 0^B\rangle = |0^A 0^B\rangle \equiv \mu_{|00\rangle} = \mu_{|0\rangle}^2, \\ |0^A\rangle \otimes |1^B\rangle &= |0^A\rangle |1^B\rangle = |0^A, 1^B\rangle = |0^A 1^B\rangle \equiv \mu_{|01\rangle} = \mu_{|0\rangle} \mu_{|1\rangle}, \\ |1^A\rangle \otimes |0^B\rangle &= |1^A\rangle |0^B\rangle = |1^A, 0^B\rangle = |1^A 0^B\rangle \equiv \mu_{|10\rangle} = \mu_{|1\rangle} \mu_{|0\rangle}, \\ |1^A\rangle \otimes |1^B\rangle &= |1^A\rangle |1^B\rangle = |1^A, 1^B\rangle = |1^A 1^B\rangle \equiv \mu_{|11\rangle} = -\mu_{|1\rangle}^2, \end{aligned} \quad (4)$$

where \otimes is the Kronecker's product, and $\mu_{|00\rangle}$ and $\mu_{|11\rangle}$ are the scalar version of $|00\rangle$ and $|11\rangle$, respectively, with $\mu_{|00\rangle} + \mu_{|11\rangle} = 0$. The sign rules that support the equivalences and equalities of Eq.(4)

will be explained at the end of this section. From Eq.(4), we are going to build the famous Bell's bases [1-3], with 2-qubit vectors the combined Hilbert space will be $H^{A \cup B} = H_2^A \otimes H_2^B$, and then we will have the following four vectors,

$$|\Phi_{\pm}^{A \cup B}\rangle = \frac{1}{\sqrt{2}}(|0^A, 0^B\rangle \pm |1^A, 1^B\rangle), \quad |\Psi_{\pm}^{A \cup B}\rangle = \frac{1}{\sqrt{2}}(|0^A, 1^B\rangle \pm |1^A, 0^B\rangle). \quad (5)$$

At the same time, we will define the density matrix necessary to calculate the entropy for the complete set of the above-mentioned cases. We are going to begin with density matrix of the subsystems treated individually,

$$\rho^A = \rho^B = \frac{1}{2}(|0\rangle\langle 0| + |1\rangle\langle 1|) = \frac{1}{2}I = \frac{1}{2} \begin{bmatrix} 1 & 0 \\ 0 & 1 \end{bmatrix}, \quad (6)$$

where I is the identity matrix. While the scalar version of this operator will be

$$r^A = r^B = \frac{1}{2} \left(\frac{\mu_{|0\rangle}^2 + \mu_{|1\rangle}^2}{\eta} \right) = \frac{1}{2} \left(\frac{\mu_{|0\rangle}^2 + \mu_{|1\rangle}^2}{2} \right), \quad (7)$$

where η is the adjustment factor (necessary in the scalar version of the density matrix), which in the case of photons is equal to 2, since the scalar version is strongly dependent on the type of particle to which it represents. We must note that in the case of photons $r^A = r^B = 1/2$; which is consequent with the matrix nature of Eq.(6). However, with respect to the case of the system composed of two subsystems, its density matrix will depend on whether or not these subsystems are entangled. Therefore, for the non-entangled case

$$\rho^{A \cup B} = \rho^A \otimes \rho^B, \quad (8)$$

but for the entangled case, we will have,

$$\rho^{A \cup B} \neq \rho^A \otimes \rho^B. \quad (9)$$

Although this operator will depend on each of the 3 cases that will be analyzed in the next subsection: completely independent, classically-correlated, and entangled subsystems.

Now, with respect to the entropy, we can define it in two forms: tensor and scalar. The first one,

$$S^A = S^B = -tr \left[\rho^A \log(\rho^A) \right] = -tr \left[\rho^B \log(\rho^B) \right], \quad (10)$$

then, replacing Eq.(6) into Eq.(10), yield,

$$S^A = S^B = -tr \left[\frac{1}{2} \begin{bmatrix} 1 & 0 \\ 0 & 1 \end{bmatrix} \log \left(\frac{1}{2} \begin{bmatrix} 1 & 0 \\ 0 & 1 \end{bmatrix} \right) \right] = 1, \quad (11)$$

while the scalar version would be,

$$S^A = S^B = -\kappa \left[r^A \log(r^A) \right] = -\kappa \left[r^B \log(r^B) \right], \quad (12)$$

where, κ is an adjustment factor (necessary in the scalar version of the entropy). Then, replacing Eq.(7) into Eq.(12), and considering the case of photons: $\kappa = 2$ and $\mu_{|0\rangle} = -\mu_{|1\rangle} = 1$, yield,

$$S^A = S^B = -2 \left[\frac{1}{2} \log \left(\frac{1}{2} \right) \right] = 1. \quad (13)$$

In the same way, for a composed system, the entropy would be,

$$S^{A \cup B} = -\text{tr} \left[\rho^{A \cup B} \log \left(\rho^{A \cup B} \right) \right] = -\kappa \left[r^{A \cup B} \log \left(r^{A \cup B} \right) \right]. \quad (14)$$

In this case, κ depends on the degree of correlation between both subsystems: completely independent, classically-correlated, and entangled subsystems.

Besides, in both worlds: classical and quantum-mechanical, the correlations between the systems are those established by the additional information. In the case of composite quantum systems, the mutual information $S^{A \cap B}$ is introduced to quantify that additional information, allowing us to obtain the degree of correlation between both subsystems [1],

$$S^{A \cap B} = S^A + S^B - S^{A \cup B} \geq 0. \quad (15)$$

Therefore, the entropy of the composite system $S^{A \cap B}$ indicates us that the uncertainty of a state $\rho^{A \cup B}$ is less than the two subsystems S^A and S^B added together. In other words, $S^{A \cap B}$ tells us how much more information the composite system can store compared to the individual subsystems. Besides, $S^{A \cap B}$ measures the distance between the state $\rho^{A \cup B}$ and the non-entangled state [1] $\rho^A \otimes \rho^B$.

The entropy of the subsystems S^A and S^B is equal to one in all cases (i.e., $S^A = S^B = 1$); while the entropy of the composite system $S^{A \cup B}$ will have different values for each and every of the three cases. For the sake of simplicity, the subsystems are expressed in qubits. Making use of Eq.(15), the main idea is to relate correlations and entanglement to the entropy, and in particular, to the mutual information $S^{A \cap B}$.

Then, we present the mutual information of the three types of subsystems: completely independent, classically correlated, and entangled, where the last one is critical for the development of both the alter-egos involved in the relativistic entanglement and the Theory of Dilated Locality.

2.2 Completely independent subsystems

In this case, both subsystems have absolute and complete independence between them, i.e., $\rho^{A \cup B}$ is a Kronecker's product of density matrices like Eq.(8), as we can see in Fig.1. Therefore, there are no correlations between such subsystems.

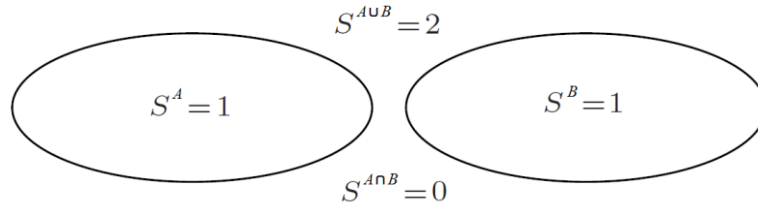


Fig. 1 Completely independent.

In the computational basis of $H^A \otimes H^B$, $\rho^{A \cup B}$ takes the following form,

$$\rho^{A \cup B} = \frac{1}{4} \left(|0^A, 0^B\rangle \langle 0^A, 0^B| + |0^A, 1^B\rangle \langle 0^A, 1^B| + |1^A, 0^B\rangle \langle 1^A, 0^B| + |1^A, 1^B\rangle \langle 1^A, 1^B| \right) = \frac{1}{4} I^{4 \times 4}, \quad (16)$$

where $I^{4 \times 4}$ is a 4x4 identity matrix. Therefore, replacing Eq.(16) into Eq.(14), $S^{A \cup B}$ will be

$$S^{A \cup B} = -tr \left\{ \frac{1}{4} \begin{bmatrix} 1 & 0 & 0 & 0 \\ 0 & 1 & 0 & 0 \\ 0 & 0 & 1 & 0 \\ 0 & 0 & 0 & 1 \end{bmatrix} \log \left(\frac{1}{4} \begin{bmatrix} 1 & 0 & 0 & 0 \\ 0 & 1 & 0 & 0 \\ 0 & 0 & 1 & 0 \\ 0 & 0 & 0 & 1 \end{bmatrix} \right) \right\} = 2. \quad (17)$$

Now, introducing the results of Eq.(13) and (17) into Eq.(15),

$$S^{A \cap B} = S^A + S^B - S^{A \cup B} = 1 + 1 - 2 = 0. \quad (18)$$

The result of the Eq.(18) ratifies the complete independence of the subsystems. At this point, if we remember the equivalences of Eq.(4), then, the scalar version of Eq.(16) will be,

$$\begin{aligned} r^{A \cup B} &= \frac{1}{4} \left(\frac{\mu_{|00\rangle} \mu_{|00\rangle} + \mu_{|01\rangle} \mu_{|01\rangle} + \mu_{|10\rangle} \mu_{|10\rangle} + \mu_{|11\rangle} \mu_{|11\rangle}}{\eta} \right) \\ &= \frac{1}{4} \left(\frac{\mu_{|0\rangle}^2 \mu_{|0\rangle}^2 + (\mu_{|0\rangle} \mu_{|1\rangle}) (\mu_{|0\rangle} \mu_{|1\rangle}) + (\mu_{|1\rangle} \mu_{|0\rangle}) (\mu_{|1\rangle} \mu_{|0\rangle}) + (-\mu_{|1\rangle}^2) (-\mu_{|1\rangle}^2)}{4} \right), \quad (19) \\ &= \frac{1}{4} \left(\frac{\mu_{|0\rangle}^4 + \mu_{|0\rangle}^2 \mu_{|1\rangle}^2 + \mu_{|1\rangle}^2 \mu_{|0\rangle}^2 + \mu_{|1\rangle}^4}{\eta} \right) = \left(\frac{\mu_{|0\rangle}^4 + 2\mu_{|0\rangle}^2 \mu_{|1\rangle}^2 + \mu_{|1\rangle}^4}{4^2} \right) = \left(\frac{\mu_{|0\rangle}^2 + \mu_{|1\rangle}^2}{4} \right)^2 \end{aligned}$$

where η will be equal to 4 for the purpose of adjusting its subsequent use into entropy, and considering that, we will make the following deduction for the case of photons: $\mu_{|0\rangle}^2 = \mu_{|1\rangle}^2 = 1$. Then, replacing Eq.(19) into the scalar version of Eq.(14) with $\kappa = 4$, and $S^{A \cup B} = 2$ from Eq.(17), we will have,

$$S^{A \cup B} = 2 = -\kappa \left[r^{A \cup B} \log(r^{A \cup B}) \right] = -4 \left[\left(\frac{\mu_{|0\rangle}^2 + \mu_{|1\rangle}^2}{4} \right)^2 \log \left(\left(\frac{\mu_{|0\rangle}^2 + \mu_{|1\rangle}^2}{4} \right)^2 \right) \right]. \quad (20)$$

Replacing $\mu_{|0\rangle}^2 = \mu_{|1\rangle}^2 = 1$ outside logarithm, and making additions and subtractions that do not alter Eq.(20),

$$\begin{aligned} 1 &= -\log \left(\frac{\mu_{|0\rangle}^2 + \mu_{|1\rangle}^2}{4} \right) + \log \left(\frac{\mu_{|0\rangle}^2}{2} \right) - \log \left(\frac{\mu_{|0\rangle}^2}{2} \right) + \log \left(\frac{\mu_{|1\rangle}^2}{2} \right) - \log \left(\frac{\mu_{|1\rangle}^2}{2} \right), \quad (21) \\ &= -\log \left(\frac{\mu_{|0\rangle}^2 + \mu_{|1\rangle}^2}{4} \right) + \log \left(\frac{\mu_{|0\rangle}^2}{2} \right) + 1 + \log \left(\frac{\mu_{|1\rangle}^2}{2} \right) + 1 \end{aligned}$$

and,

$$-1 = -\log \left(\frac{\mu_{|0\rangle}^2 + \mu_{|1\rangle}^2}{4} \right) + \log \left(\frac{\mu_{|0\rangle}^2}{2} \right) + \log \left(\frac{\mu_{|1\rangle}^2}{2} \right) = \log \left(\frac{\mu_{|0\rangle}^2 \mu_{|1\rangle}^2}{\mu_{|0\rangle}^2 + \mu_{|1\rangle}^2} \right) = \log(\mu_{|\uparrow\uparrow\rangle}) = \log(\mu_{|\uparrow\rangle}^2). \quad (22)$$

Finally,

$$\mu_{|\uparrow\uparrow\rangle}^2 = \mu_{|\uparrow\rangle}^2 = \frac{\mu_{|0\rangle}^2 \mu_{|1\rangle}^2}{\mu_{|0\rangle}^2 + \mu_{|1\rangle}^2} = \mu_{|0\rangle}^2 // \mu_{|1\rangle}^2 = 2^{-1} = \frac{1}{2}. \quad (23)$$

where “//” is the parallel operator, and $\mu_{|\uparrow\rangle}$ is the equivalent spin for completely independent subsystems, which would have been impossible to deduce with the traditional tensor (original) analysis [1]. The graphic interpretation of Eq.(23) can be seen in Fig.2 where $\mu_{|0\rangle}^2$ in red is in position A, and $\mu_{|1\rangle}^2$ in blue is in position B, where, the pink line is parallel to the thick black line of the base and perpendicular to the spins' arrows.

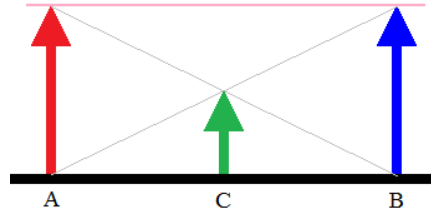


Fig. 2 Parallel operator for completely independent subsystems.

Then, as $\mu_{|\uparrow\rangle}^2 = \mu_{|0\rangle}^2 // \mu_{|1\rangle}^2$ according to Eq.(23), $\mu_{|\uparrow\rangle}^2 = \frac{1}{2}$ in green is in position C, that is to say, at the intersections of two gray lines, one connects the upper part of $\mu_{|0\rangle}^2$ (in red) with the base of $\mu_{|1\rangle}^2$ (in blue) and the other connects the base $\mu_{|0\rangle}^2$ (in red) with the upper part of $\mu_{|1\rangle}^2$ (in blue). In short, this is - in itself - the geometric interpretation of the parallel operator.

In Fig.3, if we move $\mu_{|1\rangle}^2$ (in blue) to position B', and we leave $\mu_{|0\rangle}^2$ (in red) in its original position A, and reapply the parallel operator to this new configuration, we will see that a new $\mu_{|\uparrow\rangle}^2$ (in green) appears as a result of the two new intersected gray lines, but now in position C', which has a value of $\frac{1}{2}$ again, i.e., similar to the previous case of Fig.2. We can see this new result in Fig.3, where, the pink lines are parallel to the thick black line of the base and perpendicular to the arrows (red, blue and green) representing the spins. In other words, the lines of pink color indicate that heights are preserved regardless of the distance between both particles (red and blue) on which the parallel operator is applied. This indicates that the parallel operator is insensitive to the distance between the two spins (red and blue).

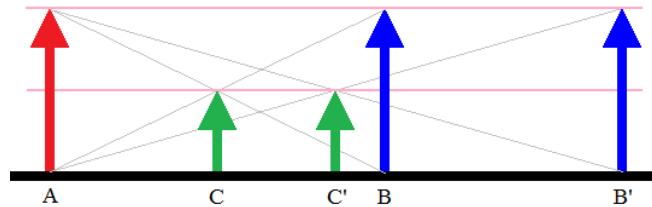


Fig. 3 Parallel operator for completely independent subsystems with an increase in separation between original spins.

Now, if we apply square root to both sides of Eq.(23), we obtain the final value of the equivalent spin $\mu_{|\uparrow\rangle}$

$$\mu_{|\hat{n}\rangle} = \sqrt{\mu_{|\hat{n}\rangle}^2} = \sqrt{\mu_{|0\rangle}^2 // \mu_{|1\rangle}^2} = \sqrt{\frac{\mu_{|0\rangle}^2 \mu_{|1\rangle}^2}{\mu_{|0\rangle}^2 + \mu_{|1\rangle}^2}} = \frac{\mu_{|0\rangle}}{\sqrt{1 + \left(\frac{\mu_{|0\rangle}}{\mu_{|1\rangle}}\right)^2}} = \frac{1}{\sqrt{2}}. \quad (24)$$

Finally, in the Section called Methods, the position of the spin $\mu_{|\hat{n}\rangle}$ will be analyzed.

2.3 Classically-correlated subsystems

In this case, see Fig. 4, it is possible to create correlations without obtaining entanglement for $S^{A \cap B} \neq 0$. For example, let's do this with the *separable mixture* of pure product states.

$$\rho^{A \cup B} = \frac{1}{2} \left(|0^A, 0^B\rangle \langle 0^A, 0^B| + |1^A, 1^B\rangle \langle 1^A, 1^B| \right). \quad (25)$$

As we can see, $\rho^{A \cup B}$ of Eq.(25) contains fewer terms than the case of completely independent of Eq.(16).

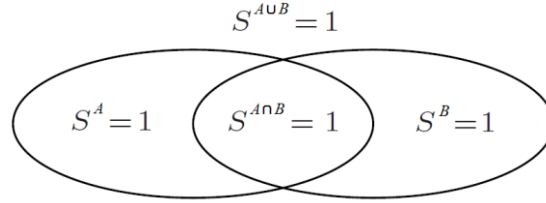


Fig. 4 Classically-correlated.

In the computational basis of $H^A \otimes H^B$, $\rho^{A \cup B}$ will be:

$$\rho^{A \cup B} = \frac{1}{2} \begin{bmatrix} 1 & 0 & 0 & 0 \\ 0 & 0 & 0 & 0 \\ 0 & 0 & 0 & 0 \\ 0 & 0 & 0 & 1 \end{bmatrix}. \quad (26)$$

Therefore, replacing Eq.(26) into Eq.(14), $S^{A \cup B}$ will be

$$S^{A \cup B} = -tr \left\{ \frac{1}{2} \begin{bmatrix} 1 & 0 & 0 & 0 \\ 0 & 0 & 0 & 0 \\ 0 & 0 & 0 & 0 \\ 0 & 0 & 0 & 1 \end{bmatrix} \log \left(\frac{1}{2} \begin{bmatrix} 1 & 0 & 0 & 0 \\ 0 & 0 & 0 & 0 \\ 0 & 0 & 0 & 0 \\ 0 & 0 & 0 & 1 \end{bmatrix} \right) \right\} = 1. \quad (27)$$

Next, introducing the results of Eq.(13) and (27) into Eq.(15), yields the following

$$S^{A \cap B} = S^A + S^B - S^{A \cup B} = 1 + 1 - 1 = 1. \quad (28)$$

This result brings out a certain degree of correlation between the subsystems. Then, if we remember the equivalences of Eq.(4), the scalar version of Eq.(25) will be,

$$\begin{aligned}
r^{A \cup B} &= \frac{1}{2} \left(\frac{\mu_{|00}\mu_{|00} + \mu_{|11}\mu_{|11}}{\eta} \right) = \frac{1}{2} \left(\frac{\mu_{|0}^2\mu_{|0}^2 + (-\mu_{|1}^2)(-\mu_{|1}^2)}{4} \right), \\
&= \frac{1}{2} \left(\frac{\mu_{|0}^4 + \mu_{|1}^4}{4} \right) = \frac{1}{2} \left(\frac{\mu_{|0}^4 + \mu_{|1}^4}{4} \right) = \frac{\mu_{|0}^4 + \mu_{|1}^4}{8}
\end{aligned} \tag{29}$$

where $\eta = 4$ for the same reasons as for the completely independent case, where we also consider the use of photons: $\mu_{|0}^2 = \mu_{|1}^2 = 1$. Then, replacing Eq.(29) into the scalar version of Eq.(14) with $\kappa = 2$, and $S^{A \cup B} = 1$ from Eq.(27), we will have,

$$S^{A \cup B} = 1 = -\kappa \left[r^{A \cup B} \log(r^{A \cup B}) \right] = -2 \left[\left(\frac{\mu_{|0}^4 + \mu_{|1}^4}{8} \right) \log \left(\left(\frac{\mu_{|0}^4 + \mu_{|1}^4}{8} \right) \right) \right]. \tag{30}$$

Replacing $\mu_{|0}^2 = \mu_{|1}^2 = 1$ outside logarithm,

$$2 = -\log \left(\frac{\mu_{|0}^4 + \mu_{|1}^4}{8} \right) = -\log(\mu_{|0}^4 + \mu_{|1}^4) + 3. \tag{31}$$

Simplifying and making additions and subtractions that do not alter Eq.(31),

$$-1 = -\log(\mu_{|0}^4 + \mu_{|1}^4) + \log(\mu_{|0}^4) - \log(\mu_{|0}^4) + \log(\mu_{|1}^4) - \log(\mu_{|1}^4), \tag{32}$$

being $-\log(\mu_{|0}^4) = -\log(\mu_{|1}^4) = 0$, then,

$$-1 = \log \left(\frac{\mu_{|0}^4 \mu_{|1}^4}{\mu_{|0}^4 + \mu_{|1}^4} \right) = \log(\mu_{|\hat{n}\hat{n}}^2) = \log(\mu_{|\hat{n}}^4), \tag{33}$$

Finally,

$$\mu_{|\hat{n}}^2 = \mu_{|\hat{n}}^4 = \frac{\mu_{|0}^4 \mu_{|1}^4}{\mu_{|0}^4 + \mu_{|1}^4} = \mu_{|0}^4 // \mu_{|1}^4 = 2^{-1} = \frac{1}{2}. \tag{34}$$

Anew, this would have remained hidden if not for this treatment: the scalar version. Besides, and as for the previous case (completely independent), the equivalent spin $\mu_{|\hat{n}}$ represents (in some way) the original spins involved with a similar analysis to the one made for Fig.3, and with a similar result, because, in this case too, the parallel operator is completely insensitive to the distance between the spins. Then, if we apply the fourth root to both sides of Eq.(34), we obtain the final value of the equivalent spin $\mu_{|\hat{n}}$

$$\mu_{|\hat{n}} = \sqrt[4]{\mu_{|\hat{n}}^2} = \sqrt[4]{\mu_{|0}^4 // \mu_{|1}^4} = \sqrt[4]{\frac{\mu_{|0}^4 \mu_{|1}^4}{\mu_{|0}^4 + \mu_{|1}^4}} = \frac{\mu_{|0}}{\sqrt[4]{1 + \left(\frac{\mu_{|0}}{\mu_{|1}} \right)^4}} = \frac{1}{\sqrt[4]{2}}. \tag{35}$$

2.4 Entangled subsystems

For this case (see Fig.5) we will take one of the Bell states of Eq.(5) as an example, specifically $|\Phi_+^{A\cup B}\rangle$, which is a pure state, with $\rho^{A\cup B}$ from Eq.(36),

$$\rho^{A\cup B} = \frac{1}{4} \left(|0^A, 0^B\rangle\langle 0^A, 0^B| + |0^A, 0^B\rangle\langle 1^A, 1^B| + |1^A, 1^B\rangle\langle 0^A, 0^B| + |1^A, 1^B\rangle\langle 1^A, 1^B| \right). \quad (36)$$

In this case [1], $S^{A\cup B} = 0$, then, introducing this value and the results of Eq.(13) into Eq.(15), we will obtain

$$S^{A\cap B} = S^A + S^B - S^{A\cup B} = 1 + 1 - 0 = 2. \quad (37)$$

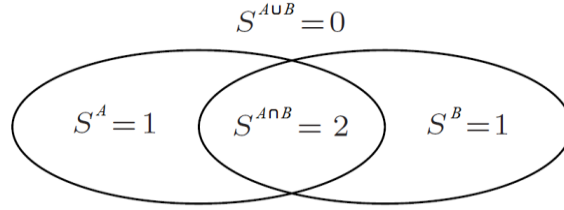


Fig. 5 Entangled subsystems.

Therefore, we will go directly to the calculation of $r^{A\cup B}$,

$$\begin{aligned} r^{A\cup B} &= \frac{1}{4} \left(\frac{\mu_{|00\rangle}\mu_{|00\rangle} + \mu_{|00\rangle}\mu_{|11\rangle} + \mu_{|11\rangle}\mu_{|00\rangle} + \mu_{|11\rangle}\mu_{|11\rangle}}{\eta} \right) \\ &= 4 \left(\frac{\mu_{|0\rangle}^2\mu_{|0\rangle}^2 + \mu_{|0\rangle}^2(-\mu_{|1\rangle}^2) + (-\mu_{|1\rangle}^2)\mu_{|0\rangle}^2 + (-\mu_{|1\rangle}^2)(-\mu_{|1\rangle}^2)}{4} \right), \\ &= \frac{1}{4} \left(\frac{\mu_{|0\rangle}^4 - 2\mu_{|0\rangle}^2\mu_{|1\rangle}^2 + \mu_{|1\rangle}^4}{4} \right) = \left(\frac{\mu_{|0\rangle}^2 - \mu_{|1\rangle}^2}{4} \right)^2, \end{aligned} \quad (38)$$

where $\eta = 4$ for the same reasons that we applied to the previous cases, where we also considered the use of photons: $\mu_{|0\rangle}^2 = \mu_{|1\rangle}^2 = 1$. Then, replacing Eq.(38) into the scalar version of Eq.(14) with $\kappa = 4$, we will have,

$$\begin{aligned} S^{A\cup B} = 0 &= -\kappa \left[r^{A\cup B} \log(r^{A\cup B}) \right] = -4 \left[\left(\frac{\mu_{|0\rangle}^2 - \mu_{|1\rangle}^2}{4} \right)^2 \log \left(\left(\frac{\mu_{|0\rangle}^2 - \mu_{|1\rangle}^2}{4} \right)^2 \right) \right] \\ &= -\frac{1}{2} \left[\left(\mu_{|0\rangle}^2 - \mu_{|1\rangle}^2 \right)^2 \log \left(\frac{\mu_{|0\rangle}^2 - \mu_{|1\rangle}^2}{4} \right) \right] \end{aligned} \quad (39)$$

Clearing Eq.(39) appropriately,

$$\frac{0}{\frac{1}{2} \left(\mu_{|0\rangle}^2 - \mu_{|1\rangle}^2 \right)^2} = \infty = -\log \left(\frac{\mu_{|0\rangle}^2 - \mu_{|1\rangle}^2}{4} \right). \quad (40)$$

That is, on the left side of Eq.(40), denominator tends to zero with more power than the numerator. In fact, the right side verifies it, because, $-\log(0) = \infty$. Now, doing additions and subtractions that do not alter Eq.(40)

$$\begin{aligned} \infty &= -\log\left(\frac{\mu_{|0\rangle}^2 - \mu_{|1\rangle}^2}{4}\right) + \log\left(\frac{\mu_{|0\rangle}^2}{2}\right) - \log\left(\frac{\mu_{|0\rangle}^2}{2}\right) + \log\left(\frac{\mu_{|1\rangle}^2}{2}\right) - \log\left(\frac{\mu_{|1\rangle}^2}{2}\right) \\ &= -\log\left(\frac{\mu_{|0\rangle}^2 - \mu_{|1\rangle}^2}{4}\right) + \log\left(\frac{\mu_{|0\rangle}^2}{2}\right) + 1 + \log\left(\frac{\mu_{|1\rangle}^2}{2}\right) + 1 \end{aligned} \quad (41)$$

Then,

$$\begin{aligned} \infty - 2 &= \infty = -\log\left(\frac{\mu_{|0\rangle}^2 - \mu_{|1\rangle}^2}{4}\right) + \log\left(\frac{\mu_{|0\rangle}^2}{2}\right) + \log\left(\frac{\mu_{|1\rangle}^2}{2}\right) \\ &= \log\left(\frac{\frac{\mu_{|0\rangle}^2}{2} \frac{\mu_{|1\rangle}^2}{2}}{\frac{\mu_{|0\rangle}^2 - \mu_{|1\rangle}^2}{4}}\right) = \log\left(\frac{\mu_{|0\rangle}^2 \mu_{|1\rangle}^2}{\mu_{|0\rangle}^2 - \mu_{|1\rangle}^2}\right) = \log\left(\mu_{|\uparrow\uparrow\rangle}\right) = \log\left(\mu_{|\uparrow\uparrow\rangle}^2\right) \end{aligned} \quad (42)$$

Finally,

$$\mu_{|\uparrow\uparrow\rangle} = \mu_{|\uparrow\uparrow\rangle}^2 = \frac{\mu_{|0\rangle}^2 \mu_{|1\rangle}^2}{\mu_{|0\rangle}^2 - \mu_{|1\rangle}^2} = \frac{\mu_{|00\rangle}(-\mu_{|11\rangle})}{\mu_{|00\rangle} - (-\mu_{|11\rangle})} = \frac{-\mu_{|00\rangle}\mu_{|11\rangle}}{\mu_{|00\rangle} + \mu_{|11\rangle}} = \mu_{|0\rangle}^2 // \mu_{|1\rangle}^2 = \mu_{|00\rangle} // (-\mu_{|11\rangle}) = 2^\infty = +\infty. \quad (43)$$

Actually, Eq.(43) has two possible values: $\pm\infty$, see Eq.44 and Fig.6. Equation (43) represents one of a pair of super-spins, and this result justifies in itself the whole paper and in a few words tells us that the parts are infinitely superior to the whole. Then, another super-spin will be,

$$\mu_{|\downarrow\downarrow\rangle} = -\mu_{|\downarrow\downarrow\rangle}^2 = -\infty, \quad (44)$$

therefore, $\mu_{|\downarrow\downarrow\rangle} + \mu_{|\uparrow\uparrow\rangle} = 0$. The attribute of these last two equations was hidden with the traditional treatment [1] and through them, we will try to explain the exceptional attributes of entanglement. Clearly, the value of these spins infinitely exceeds the value of the original spins. The traditional analysis [1] based on vector or tensor notation is unable to detect this scenario, in fact, the expressions based on scalar notation (Equations 38 and 39) are key, which leads to the equation as it could have never been possible with the original version, i.e., Eq.(36) and $S^{A \cup B}$ based on Eq.(36). On the other hand, Fig.6 shows us the geometric representation of Eq.(43) with $\mu_{|00\rangle}$ (in red) in position A and $\mu_{|11\rangle}$ (in blue) in position B.

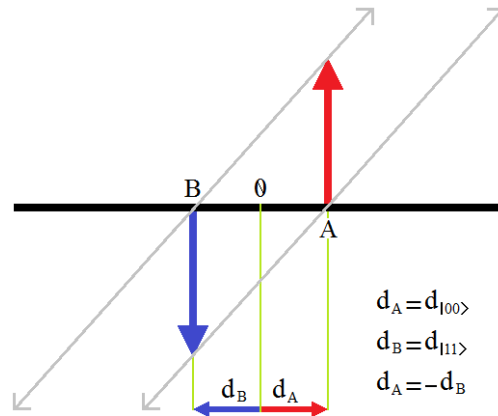


Fig.6 Parallel operator for entangled subsystems.

Figure 6 shows that $\mu_{|\downarrow\downarrow\rangle}$ and $\mu_{|\uparrow\uparrow\rangle}$ are in the positions $-\infty$ and $+\infty$, respectively, i.e., to both ends of the figure, namely, where both gray lines intersect. Therefore, it seems as if the positions were also entangled,

$$d_{|\uparrow\uparrow\rangle} = d_A + \frac{\mu_A d_{BA}}{\mu_A + \mu_B} = d_{|00\rangle} + \frac{\mu_{|00\rangle}(d_{|11\rangle} - d_{|00\rangle})}{\mu_{|00\rangle} + \mu_{|11\rangle}} = +\infty, \quad (45)$$

$$d_{|\downarrow\downarrow\rangle} = d_B + \frac{\mu_B d_{AB}}{\mu_A + \mu_B} = d_{|11\rangle} + \frac{\mu_{|11\rangle}(d_{|00\rangle} - d_{|11\rangle})}{\mu_{|00\rangle} + \mu_{|11\rangle}} = -\infty, \quad (46)$$

Equations (45) and (46) will be analyzed in depth in the section called Methods. They keep the same relationship as in the case of spins: $d_{|\downarrow\downarrow\rangle} + d_{|\uparrow\uparrow\rangle} = 0$.

In Fig.7, if we move $\mu_{|00\rangle}$ from position A to position A', we will have $\mu_{|\uparrow\uparrow\rangle} = +\infty$ and $\mu_{|\downarrow\downarrow\rangle} = -\infty$ again. Besides, and as in the case of completely independent subsystems, Fig.7 shows that $\mu_{|\uparrow\uparrow\rangle}$ and $\mu_{|\downarrow\downarrow\rangle}$ are absolutely insensitive to the distance between the original spins, as long as $\mu_{|00\rangle}$ and $\mu_{|11\rangle}$ do not change neither in modulus nor in its orientation (polarization). Regardless how much they separate from each other, such displacement does not alter the final result; in this case, $\mu_{|\downarrow\downarrow\rangle} = -\infty$ and $\mu_{|\uparrow\uparrow\rangle} = +\infty$. This confirms the success of the parallel operator since it attempts to model the entanglement, and as we know from several laboratory experiences, it does not seem to care about the distance between the entangled particles.

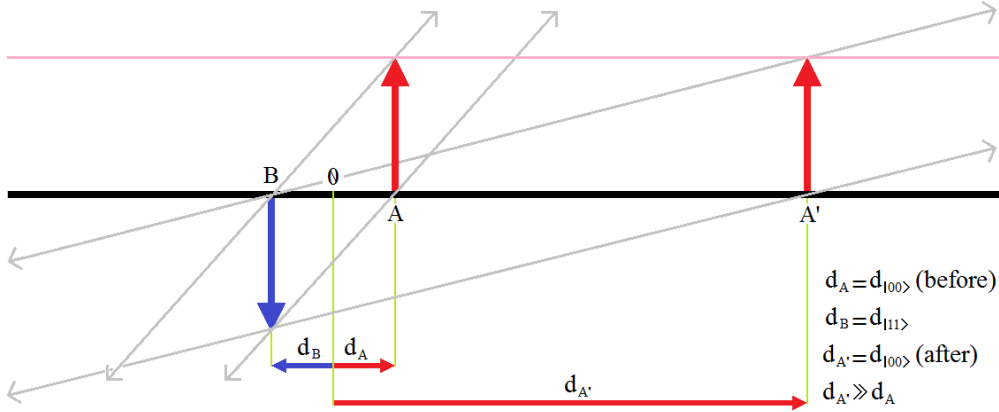


Fig.7 Parallel operator for entangled subsystems with an increase in the inter-spin separation.

Finally, if we apply square root to both sides of Eq.(45), we obtain the final value of the resulting spin

$$\mu_{|\uparrow\rangle} = \sqrt{\frac{\mu_{|0\rangle}^2 \mu_{|1\rangle}^2}{\mu_{|0\rangle}^2 - \mu_{|1\rangle}^2}} = \frac{|\mu_{|1\rangle}|}{\sqrt{1 - \left(\frac{\mu_{|1\rangle}}{\mu_{|0\rangle}}\right)^2}} = \mu_{|0\rangle}, \quad \gamma = +\infty, \quad (47)$$

with $\mu_{|\downarrow\rangle} = \mu_{|1\rangle}$, $\gamma = -\infty$, $|\mu_{|1\rangle}| = \mu_{|0\rangle} = -\mu_{|1\rangle}$, and, $\mu_{|\uparrow\rangle} + \mu_{|\downarrow\rangle} = 0$, and where,

$$\gamma = \frac{1}{\sqrt{1 - \left(\frac{v}{c}\right)^2}} = \frac{1}{\sqrt{1 - \left(\frac{\mu_{|1\rangle}}{\mu_{|0\rangle}}\right)^2}} = \frac{1}{\sqrt{1 - \left(\frac{\mu_{|0\rangle}}{\mu_{|1\rangle}}\right)^2}}, \quad (48)$$

is the Lorentz factor when the speed $v = c$ (speed of light). In a generic way, we will have: $\mu_{|X\rangle} = \mu_{|x\rangle} \gamma$, where, X is the subscript of the alter-egos, which can be \uparrow or \downarrow , while, x is the subscript of the original spins, respectively, which can be 0 or 1. In this way, we arrive at a unified effect equation. This is the first testimony of the relativistic nature of spins involved in quantum entanglement. In fact, both spins are relativistic. These are the alter-egos. The same situation applies with the locations of these alter-egos,

$$d_{|\uparrow\uparrow\rangle} = d_{|\uparrow\rangle}^2 = d_A + \gamma^2 d_{BA} = d_{|00\rangle} + \gamma^2 (d_{|11\rangle} - d_{|00\rangle}) = +\infty \quad (49)$$

$$d_{|\downarrow\downarrow\rangle} = -d_{|\downarrow\rangle}^2 = d_B + \gamma^2 d_{AB} = d_{|11\rangle} + \gamma^2 (d_{|00\rangle} - d_{|11\rangle}) = -\infty \quad (50)$$

Equations (49) and (50) will also be analyzed in depth in the section called Methods. This tells us that both the spins resulting from the entanglement and their locations suffer a dilation according to the Theory of Relativity [24].

On the other hand, the original spins and their alter-egos form a spatial homothety between them, where the alter-egos are the shadows of the original spins projected to the infinite with the same morphology (in this case, the orientation or polarization of the spins) but with infinite magnitude.

2.5 Spatiotemporal analysis

Figures 6 and 7 show us the case analyzed so far, where the coordinates of point A are (d_A, t_A) , while those of point B are (d_B, t_B) , this means, same time but different space. However, the model allows an entanglement between spins that have never coexisted before [11]. See Fig.8. In this figure, it can also be seen that the model is insensitive to inter-spin temporal separation as it is in the case of spatial separation. In this case, we have same space but a different time since A is in the future and B is in the past.

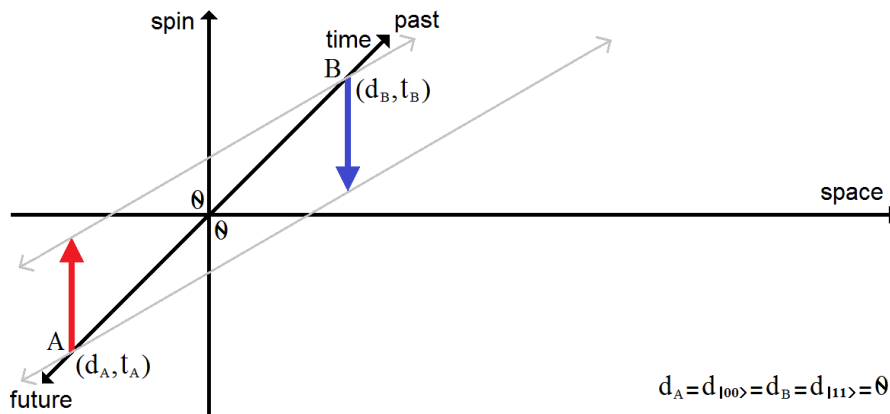


Fig.8 Entanglement between particles that have never coexisted before.

Finally, Figures 9 and 10 show us the spin A in the present in the position d_A , while spin B is in the position d_B , in the past in Fig.9 and in the future in Fig.10.

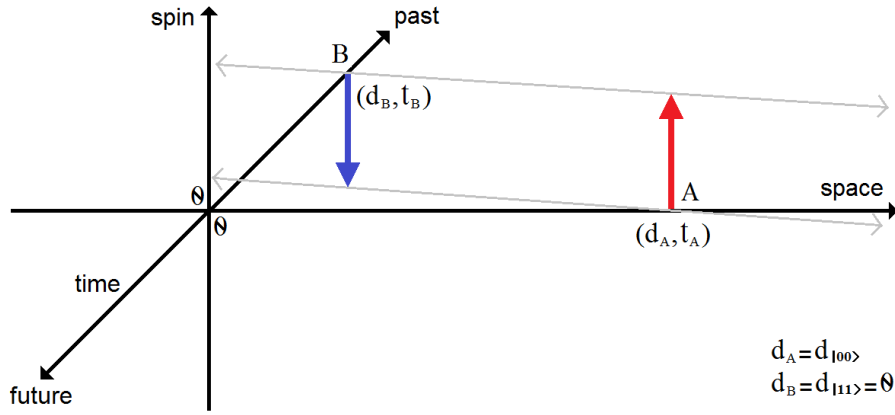


Fig.9 Particle A in the present in position d_A , and particle B in the past in position d_B .

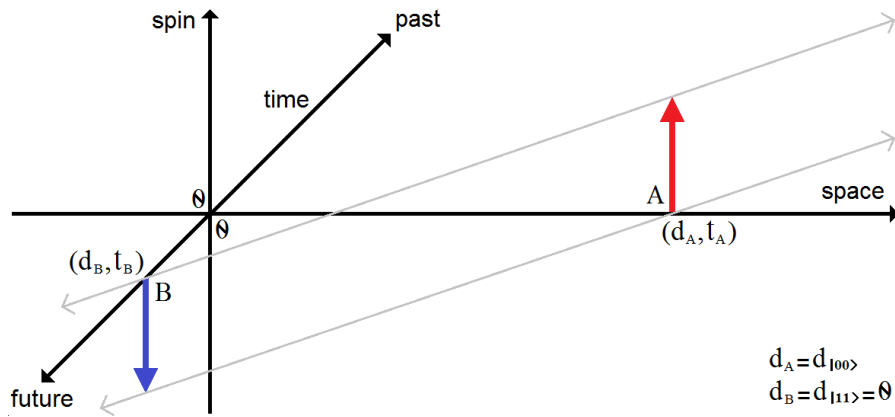


Fig.10 Particle A in the present in position d_A , and particle B in the future in position d_B .

2.6 Final thoughts on this section

The alter-egos of Equations (43 and 44) were obtained from Eq.(39), i.e., the scalar version of $S^{A \cup B}$. We would have never found the alter-egos with the original tensor notation (no scalar) since with that notation values, signs and polarizations (or orientations) of spins are blurred; which is not advisable, in particular, when we try to study different degree of correlations between them. All this is particularly important considering that the spin is the most conspicuous element of Quantum Physics. Besides, Table 1 shows us some attributes of the parallel operator “//” employed in Eq.(23, 34 and 43) which will be taken into account later.

//	0	x	∞	$-x$	$-\infty$
0	0	0	0	0	0
x	0	$x/2$	x	$\pm\infty$	x
∞	0	x	∞	$-x$	$\pm\infty$
$-x$	0	$\pm\infty$	$-x$	$-x/2$	$-x$
$-\infty$	0	x	$\pm\infty$	$-x$	$-\infty$

Where x is a scalar and has generic value.

On the other hand, the model for the representation of the entanglement based on the parallel operator “//” predicts strange configurations which have not been tested in the laboratory yet. That is the case of three spins oriented according to a single axis z , which we can see in Fig.11. The spin numbers of these particles are $(1, 1, -1/2)$.

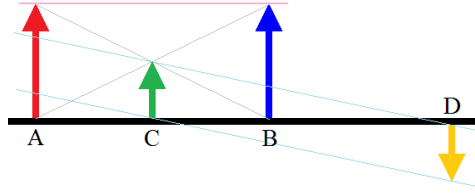


Fig.11 Two completely independent spins (μ_A and μ_B) are entangled with a third spin μ_D .

These spins do not comply with the Principle of Spin Conservation since $1+1-1/2 \neq 0$. The first two (μ_A and μ_B) are completely independent (red and blue in Fig.11); however, their resulting spin, in green, obtained after the application of Eq.(23) is μ_C , which is entangled with another spin in position D: μ_D in yellow. According to the model, the result is a perfect entanglement between μ_C and μ_D . This can only take place as long as the spins in C and D are equal in modulus and opposite in orientation. In other words, both parallel lines in light blue, that link both spins through the parallel operator, intersect between each other at $+\infty$ and $-\infty$ to both sides of the Fig.11 and to infinite distances of the original spins. The literature about entanglement, curiously, does not mention anything about it, maybe because it does not exist in reality.

Additionally, the same model also predicts the existence of quasi-entanglement when we have two opposite spins oriented respect to the same axis but with different spin numbers, see Fig.12.

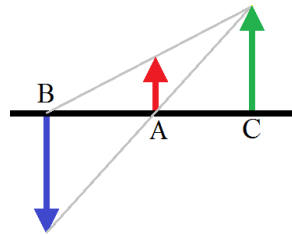


Fig.12 Quasi-entanglement of two opposite spins (μ_A in red and μ_B in blue) oriented according to the same axis but with different spin numbers, produces the resulting spin μ_C in green.

As we can see in Fig.12, the resulting spin of quasi-entangled subsystems is on the same side and has the same sign as the spin of the smaller modulus. That is to say, by the mere fact that μ_A and μ_B have a different modulus: $|\mu_A| \neq |\mu_B|$, we obtain, $|\mu_C| = \infty$. We are going to analyze the position of the spin μ_C in the Section called Methods. Besides, as it was seen in the cases of completely independent, classically-correlated, and entangled spins; the results of the application of the parallel operator “//” to quasi-entangled subsystems is completely insensitive to the distance between original spins, i.e., to the inter-spin distance. See Fig.13.

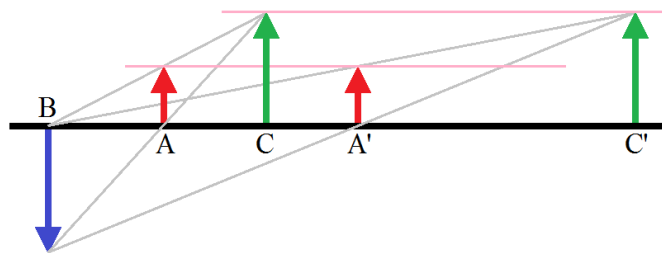


Fig.13 When spin μ_A is displaced from position A to position A', the result of the quasi-entanglement gives us a new resulting spin μ_C in a new position C'. This tells us that just as in the case of entanglement, here also, the inter-spin distances are entangled and that μ_C will have much-smaller-than-infinity modulus.

Table 2 compares two attributes (quantity and size) of the resulting spin after applying the parallel operator “//” to the four viewed cases, depending on the degree of correlation between both spins (μ_A and μ_B): completely independent, classically-correlated, entangled, and quasi-entangled. As we can see in Table 2, in the case of entangled spins two resulting spins are generated only, i.e., both alter-egos have infinitely large modulus, whereas, in the other cases, a single spin is generated and it has finite modulus.

Table 2. Attributes (quantity and size) of the spins resulting from applying the parallel operator “//” according to the degree of correlation of such spins.				
attribute	independent	correlated	entangled	quasi-entangled
quantity	1	1	2	1
size	finite	finite	infinite	finite

In the case of quasi-entangled spins, the resulting one is on the same side and has the same sign (orientation) as the spin of smaller modulus, as shown in Figures 12 and 13.

But, at this point, a question automatically arises: What does each resulting spin represent physically for each of the 4 cases? We can go in an ascendant order of importance. First, in the completely independent case, the resulting spin is a kind of figurehead or representative of the population of spins involved, and without being in the least tied to some kind of correlation between them. In this case, the parallel operator is only the instrument that conveys the finding of the resulting spin. A similar case appears in some diatomic molecules, where if classical physics were applicable, the nuclei would have energy [62],

$$E_{classical} = \frac{p_1^2}{2m_1} + \frac{p_2^2}{2m_2} + \frac{1}{2}kx^2 \quad (51)$$

where m_1 and m_2 are the masses of the nuclei, p_1 and p_2 are the magnitudes of its momenta, k is a constant and x denotes displacement or distance. In the *center-of-mass* frame, we can set $p_1 = p_2 = p$ and, by introducing the reduced mass (resulting and equivalent mass) through the parallel operator

$$\mu = \frac{m_1 m_2}{m_1 + m_2} = m_1 // m_2. \quad (52)$$

Then, we will obtain

$$E_{classical} = \frac{p^2}{2\mu} + \frac{1}{2}kx^2. \quad (53)$$

It is clear that both masses do not have any kind of correlation between them. Instead, in the second and third cases corresponding to Figures 12 and 13 (quasi-entangled), as well as in the case of classically-correlated of Eq.(34), respectively, and even in the curious case of Fig.11, all of them possess a witness of the correlation between the original spins in the resulting one.

However, in the fourth case, the entanglement, the resulting spins have a deeper (ontological) philosophical and physical meaning. As we will see in the following section both alter-egos are the ones that support the effect; since they generate a locality aisle that involves all the mentioned spins, i.e., originals and alter-egos, which will be developed later on. It is the alter-egos that will give rise to all the extraordinary attributes of entanglement.

On the other hand, it is important to make clear the sign rules for the scalar spins of Eq.(4), with

$$\text{sign}(\mu_{|0\rangle}) > 0 \quad (54a)$$

$$\text{sign}(\mu_{|1\rangle}) < 0 \quad (54b)$$

$$\mu_{|xy\rangle} = \mu_{|x\rangle} \mu_{|y\rangle} \quad (55a)$$

$$-\mu_{|xy\rangle} = -\mu_{|x\rangle} \mu_{|y\rangle} \quad (55b)$$

where $\text{sign}(\bullet)$ means *sign of* (\bullet), and x and y can only be 0 or 1. Such rules are

Rule #1: $\forall \mu_{|xy\rangle}$

if $x = 0$,

$$\text{sign}(\mu_{|x\rangle}) > 0$$

else

$$\text{sign}(\mu_{|x\rangle}) < 0$$

$$\text{sign}(\mu_{|y\rangle}) = -\text{sign}(\mu_{|y\rangle})$$

end if

Rule #2: $\forall \mu_{|xy\rangle}$

$$\text{sign}(\mu_{|xy\rangle}) = -\text{sign}(\mu_{|\bar{y}\bar{x}\rangle})$$

where \bar{x} and \bar{y} mean inverse of x and y (e.g., if $x = 0$, then $\bar{x} = 1$, and vice-versa).

Rule #3: $\forall -\mu_{|xy\rangle}$

$$\text{sign}(-\mu_{|xy\rangle}) = -\text{sign}(-\mu_{|\bar{y}\bar{x}\rangle})$$

Therefore,

$$\mu_{|00\rangle} = \mu_{|0\rangle}^2 \quad (56a)$$

$$\mu_{|11\rangle} = -\mu_{|1\rangle}^2 \quad (56b)$$

$$\mu_{|00\rangle} + \mu_{|11\rangle} = 0 \quad (57a)$$

$$\mu_{|01\rangle} + \mu_{|10\rangle} = 0 \quad (57b)$$

In this way, the rules of the signs necessary for their use in the deduction of Equations (23, 34 and 43) are completed.

Finally, in today's Physics, we employ the following syllogism:

Major premiss:

The Theory of Relativity [24] says that any instantaneous phenomenon can only be local since it cannot have a speed that outpaces the speed of light [29,46,47,60]; and if there is an instantaneous nonlocal phenomenon, this cannot transport information.

Minor premiss:

In Quantum Theory [4,26,42], the works of Bell [4,5,25,30,44,48-50], CHSH [51], Aspect [30], Zeller [58], and many others, establish that the entanglement is a nonlocal effect, like another phenomenon predicted by the Theory of Relativity: the ER bridge [61] (by Einstein and Rosen) also known as wormhole between two black holes.

Therefore:

There is no instantaneous transmission of information thanks to the entanglement or through the interior of a wormhole.

However, and from what has been seen so far in this work, it is logical to ask ourselves: what is the impact of this work on both theories and the apparent crack that separates them? As we have said before, the truth is that a reconciling and binding theory is not only needed to close the gap between both pillar theories of Physics but also to test the earlier syllogism. In fact, this work will show that there is a problem of interpretation with the results of the experiments cited in the *minor premiss*, since at their time the information provided by this work was unavailable. This is what we will try to do throughout the following sections.

3 Discussion

3.1 Dilated Locality

Equations (43 and 47) tell us about two new spins (alter-egos) that arise as a consequence of the quantum entanglement, whose values are infinite in modulus and are at infinite distances from the center of origin (at opposite ends of the universe). From the previous analysis, we cannot deduce anything about the respective eventual masses of both spins. In fact, there are two possibilities:

- their masses are null, i.e., $m_{|\uparrow\uparrow\rangle} = m_{|\downarrow\downarrow\rangle} = 0$, and
- their masses (finite or infinite) have opposite signs, in such a way that $m_{|\uparrow\uparrow\rangle} + m_{|\downarrow\downarrow\rangle} = 0$.

From here to the rest of this section, we will work with the first ponder idea. This possibility is very interesting because if a massless spin with infinite modulus could bend the space-time, then, a large number of pairs of these spins but with opposite signs (alter-egos) could be responsible for several facts in the visible and invisible universe. This fact would constitute something extremely important in the field of Physics, since, as we know from the Theory of Relativity [63-69] a big mass curves the space-time diverting the path of light beam composed by massless photons which have finite spin equal to $\frac{1}{2}$, but there is still no evidence that space-time is curved by a massless spin, even if this one has infinite modulus. If the above is correct, we could conjecture that a pair of such extravagantly immense spins (even if they do not have mass) could divert the trajectory of elements with and without mass, attracting and/or repelling them directly. A direct consequence of some of these possibilities would be that a large number of entangled spins can be responsible for the expansion of the universe. Besides, in a section called Methods, we are going to analyze the second ponder idea, i.e., different to zero masses (finite or infinite) with opposite signs.

On the other hand, in literature there are numerous works about particles with infinite spins [70-75], whose existence has not yet been discovered. There are also works on massless particles with infinite spin [74,76-84] with identical considerations as the previous ones regarding their eventual existence, which can also be found under the name of massless continuous spin [72,85-89], although of course, all these works are mere theoretical speculations. We must not forget the contribution of the Vasiliev Higher-Spin theory [90-95], which is a minimal extension of gravity with (massless, Gauge) fields of spin $s > 2$. It is a higher-derivative completion of gravity that has good chances of being a consistent theory of quantum gravity (without super-symmetries and extra dimensions). The idea of a relativistic spin [96-104] was not born with the present work, and as a consequence of this, a relativistic entanglement [105-117] comes to light. Besides, in recent years numerous works have appeared linking entanglement with the Theory of Relativity [118-128] directly or indirectly, some of which pose an entanglement between black holes (giving rise to an ER bridge or wormhole, even if temporarily) and others instead explore the relativistic consequences of entanglement.

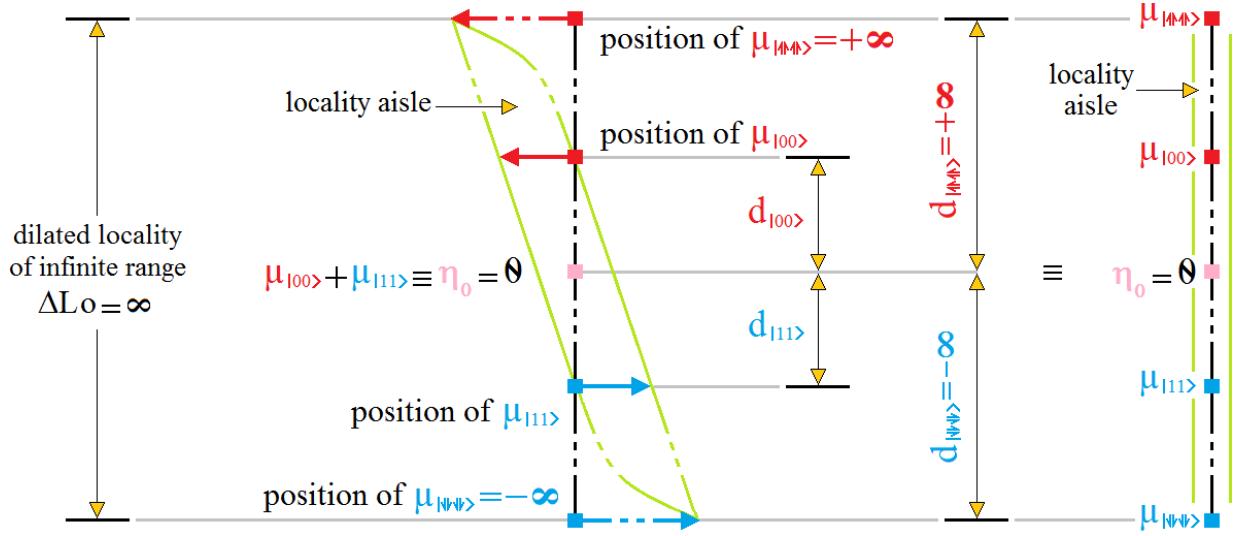


Fig.14 On the left, the dilation of the locality with an infinite range. In the middle, the locality aisle between two parallel green lines which is curved in the vicinity of the alter-egos since the graph is not in scale. And, on the right, a simplified version of the graphic, where η_0 means neutral meson which sometimes decays into two opposed charged muons, and $\eta_0 = 0$ represents the spin baseline.

The above concerns can be channeled through an exhaustive analysis of Fig.7, which is the key to the whole effect, given that this figure shows the immunity of entanglement to the distance between the original spins to obtain the same alter-egos with their same locations, i.e., at infinity. In other words, even if we modify at will the separation between $\mu_{|00\rangle}$ and $\mu_{|11\rangle}$, the distance between $\mu_{|\uparrow\uparrow\rangle}$ and $\mu_{|\downarrow\downarrow\rangle}$ will always be the same (based on Equations 49 and 50 and considering for simplicity $d_{|11\rangle} + d_{|00\rangle} = 0$), and it is represented in Fig.14, as

$$\begin{aligned}
 d_{|\uparrow\uparrow\rangle} - d_{|\downarrow\downarrow\rangle} &= d_{|00\rangle} + \gamma^2 (d_{|11\rangle} - d_{|00\rangle}) - (d_{|11\rangle} + \gamma^2 (d_{|00\rangle} - d_{|11\rangle})) \\
 &= d_{|00\rangle} + \gamma^2 (d_{|11\rangle} - d_{|00\rangle}) - (-d_{|00\rangle} - \gamma^2 (d_{|11\rangle} - d_{|00\rangle})) \\
 &= d_{|00\rangle} + \gamma^2 (d_{|11\rangle} - d_{|00\rangle}) + (d_{|00\rangle} + \gamma^2 (d_{|11\rangle} - d_{|00\rangle})) \\
 &= 2(d_{|00\rangle} + \gamma^2 (d_{|11\rangle} - d_{|00\rangle})) = 2d_{|\uparrow\uparrow\rangle} = 2\infty = \infty
 \end{aligned} \tag{58}$$

This follows from Eq.(49) where $d_{|\uparrow\rangle} = +\infty$ and $d_{|\downarrow\rangle} = -\infty$, with $d_{|\uparrow\uparrow\rangle} = d_{|\uparrow\rangle}^2$ and $d_{|\downarrow\downarrow\rangle} = -d_{|\downarrow\rangle}^2$, which represents a case identical to the rule of the signs of the spins seen above. In the middle of Fig.14, we can see the original spins and their alter-egos linked by two green parallel lines which intersect exactly in the alter-egos. These lines have been drawn curved in the vicinity of the alter-egos since it is impossible to graph infinite values in such figure. As we can see, both green lines define among themselves a locality aisle whose range is infinite and is determined by Eq.(58). Let's test that statement with a simple mental experiment (*Gedankenexperiment* - in german) based on Fig.7:

- if the distance between $\mu_{|00\rangle}$ and $\mu_{|11\rangle}$ is so small that the experiment may be considered local, then, the application of Eq.(43) will give the same alter-egos (i.e., $\pm\infty$) and the Eq.(45 and 46) will give the same locations (i.e., $\pm\infty$), now,

- if we start to separate $\mu_{|00\rangle}$ and $\mu_{|11\rangle}$ until the experiment may be considered non local by our knowledge of the works of Bell [4,5,25,30,44,48-50], CHSH [51], Aspect [30], Zeller [58], and many others, then, the application of Eq.(43) will give the same alter-egos (i.e., $\pm\infty$) and the Eq.(45) and (46) will give the same locations (i.e., $\pm\infty$) again.

At this point, there is an apparent contradiction given that in one case the experiment is local, and in the other case it is non-local, however, the effect is the same with identical results. How is it possible? If the effect is the same, then both times the experiment is local or both times it is not local. But the same effect cannot be disguised as different things according to the occasion. It is clear that something happens with the locality, as well as the fact that the alter-egos are under the same area of the effect caused by the original spins when they are entangled according to Eq.(43). On the other hand, if in the first case the original spins are so close that the measurement instruments of the experiment overlap, while in the second case the original spins can be as far apart as the alter-egos and even more being part of the same area of influence of the effect (i.e., inside locality aisle or locality alley) which involves the above mentioned alter-egos, then, the only explanation is that in both cases the experiment is local with a significant influence on the locality, which translates into a dilation of locality infinitely until sheltering, containing or covering the alter-egos. In other words, in both cases, the locality contains the alter-egos despite the distance between the original spins. Therefore, based on Eq.(58), the locality is stretched like a chewing gum. Then, this dilation of the locality can be represented by the following equation

$$\Delta L_o = d_{|\uparrow\uparrow\rangle} - d_{|\downarrow\downarrow\rangle} = 2\left(d_{|00\rangle} + \gamma^2(d_{|11\rangle} - d_{|00\rangle})\right) = 2d_{|\uparrow\uparrow\rangle} = 2\infty = \infty. \quad (59)$$

ΔL_o is represented on the left of Fig.14. Besides, on the right of this figure, we have an equivalent simplification of the central scheme which will help us better understand the concepts developed in relation to Fig.15. Finally, η_0 means neutral meson which sometimes decays into two opposite charged muons, and it represents the spin baseline. It is also a simply reference which establishes the value of spin equal to zero.

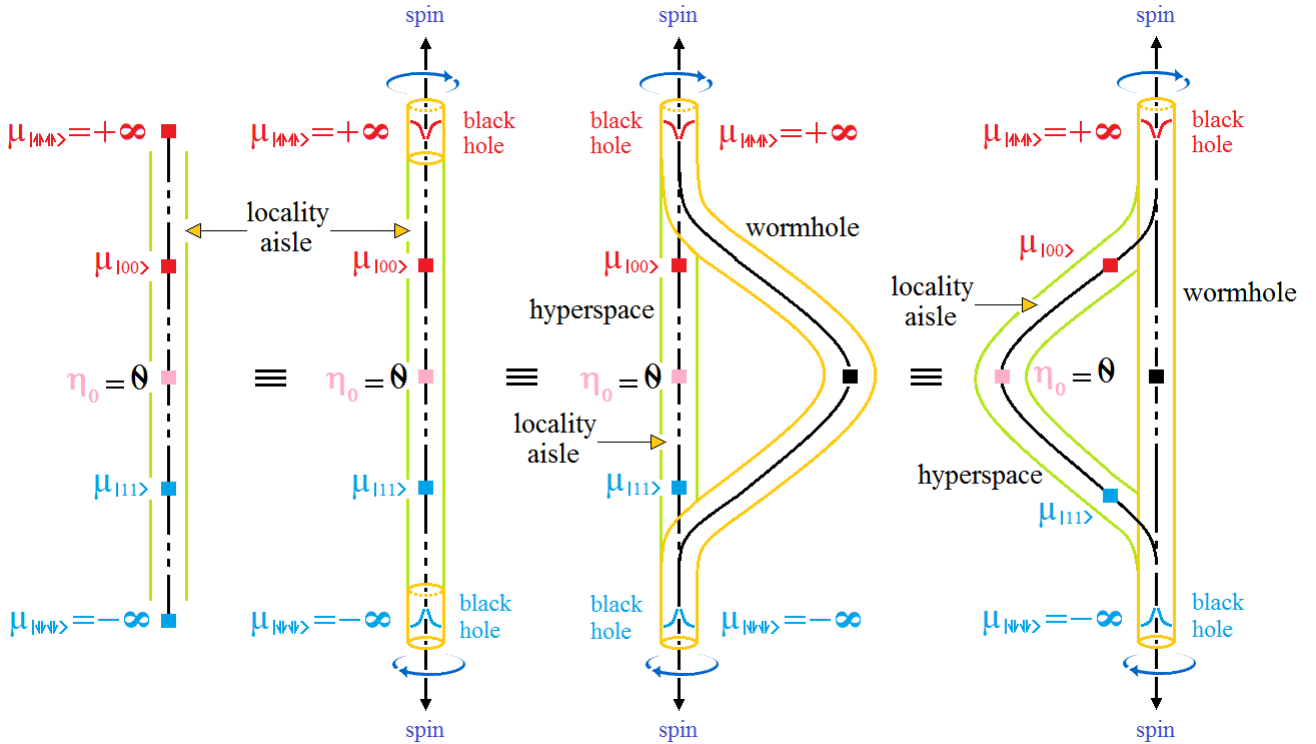


Fig.15 From bipartite entanglement to wormhole where the locality aisle curves according to the Theory of Relativity forming the hyperspace.

The graph on the right of Fig.14 is the same graph on the left of Fig.15, and this -in turn- is equivalent to the graph on its right, which interprets the alter-egos as two massless black holes [129-133] (massless, at least for the moment). The alter-egos are entangled with each other forming an EPR bridge or wormhole (in yellow) which can be seen in the third and fourth graph (from the left to the right) of Fig.15. In these graphs we can see that the locality aisle becomes the hyperspace (in green) when bending according to the Theory of Relativity [63-69] and the entanglement of the two massless black holes (alter-egos) forms a particular case of wormhole, which has already been vastly treated in the literature although with a slightly different approach [36,38,126,134-136], particularly in the works of Susskind [36,126] and Maldacena [36,37].

Evidently, the alter-egos are entangled with each other, in fact, as entangled as the original spins to each other in Eq.(43). Then and taking into account everything seen so far

$$\begin{aligned}\mu_{|\hat{n}\hat{n}\rangle_2} &= \mu_{|\hat{n}\hat{n}\rangle} // \mu_{|\hat{u}\hat{u}\rangle} = \frac{\mu_{|\hat{n}\hat{n}\rangle} \mu_{|\hat{u}\hat{u}\rangle}}{\mu_{|\hat{n}\hat{n}\rangle} + \mu_{|\hat{u}\hat{u}\rangle}} = \frac{\mu_{|\hat{n}\rangle}^2 (-\mu_{|\hat{u}\rangle}^2)}{\mu_{|\hat{n}\rangle}^2 + (-\mu_{|\hat{u}\rangle}^2)} = \frac{\mu_{|\hat{n}\rangle}^2}{1 - \left(\frac{\mu_{|\hat{n}\rangle}}{\mu_{|\hat{u}\rangle}}\right)^2} \\ &= \frac{\mu_{|0\rangle}^2 \gamma^2}{1 - \left(\frac{\mu_{|0\rangle} \gamma}{\mu_{|1\rangle}}\right)^2} = \frac{\mu_{|0\rangle}^2 \gamma^2}{1 - \left(\frac{\mu_{|0\rangle}}{\mu_{|1\rangle}}\right)^2} = \mu_{|0\rangle}^2 \gamma^4 = \mu_{|\hat{n}\rangle}^2 \gamma^2\end{aligned}\quad (60)$$

where, $\mu_{|\hat{n}\hat{n}\rangle_2}$ means second level entanglement, with,

$$\mu_{|\hat{n}\rangle_2} = \sqrt{\mu_{|\hat{n}\hat{n}\rangle} // \mu_{|\hat{u}\hat{u}\rangle}} = \mu_{|0\rangle} \gamma^2 = \mu_{|\hat{n}\rangle} \gamma \quad (61)$$

Therefore, Eq.(47, 49, 58 and 61) constitute an approximation to the Theory of Everything [39], e.g., in the case of Eq.(61) we can see that this equation is a perfect balance between a spin (being the spin the fifth essence of Quantum Theory) and the Lorentz's factor (which is a central tool in the Theory of Relativity); i.e., entanglement generates relativistic spins and hence relativistic entanglement. The negative complement of Eq.(61) will be

$$\mu_{|\hat{u}\rangle_2} = \mu_{|\hat{u}\rangle} \gamma = -\left|\mu_{|\hat{u}\rangle}\right| \gamma \quad (62)$$

Thus, Eq.(61) and its negative complement Eq. (62) represent an ER bridge or wormhole, where the spin of Eq.(47), i.e., $\mu_{|\hat{n}\rangle} = \mu_{|0\rangle} \gamma$ and its negative complement $\mu_{|\hat{u}\rangle} = \mu_{|1\rangle} \gamma$ are the massless black holes of Fig.15, which when entangled generate the spins of the Eq.(61 and 62) as a result. In other words, a domino effect takes place, being each time more and more pronounced, getting alter-egos from alter-egos. The main role of the alter-egos in the entanglement and, in consequence, an eventual quantum communication through a wormhole are clear at this point. To do justice to the importance of alter-egos in the entanglement we propose the following mental experiment (*Gedankenexperiment* - in german) based on Fig.7 again. Let's define the following rates spin/distance-from-center

$$\mu_{|00\rangle}^{\cdot} = \frac{\mu_{|00\rangle} \times [\text{units of distance}]}{d_{|00\rangle}} \quad \text{and} \quad \mu_{|11\rangle}^{\cdot} = \frac{\mu_{|11\rangle} \times [\text{units of distance}]}{d_{|11\rangle}} \quad (63)$$

where $\mu_{|00\rangle}^{\cdot}$ and $\mu_{|11\rangle}^{\cdot}$ do not have physical units (like spins). Then, if we start with both spins relatively close (and this statement can be as arbitrary as we want), and we separate them, both ratios of Eq.(63) start deteriorating (i.e., they are approaching zero), therefore, and according to Fig.7 and

Eq.(43) the alter-egos remain intact in magnitude and position, while the ratios of Eq.(63) disappear, which clearly indicates that the alter-egos sustain the effect, that is, the entanglement, even more so than the original spins themselves, which give existence to the alter-egos. Evidence of this can be obtained by replacing the alter-egos and their positions in Eq.(63); in this case, the ratios will always be equal to 1, regardless of the position occupied by the original spins, i.e., these new ratios do not degrade with the positions of the original spins.

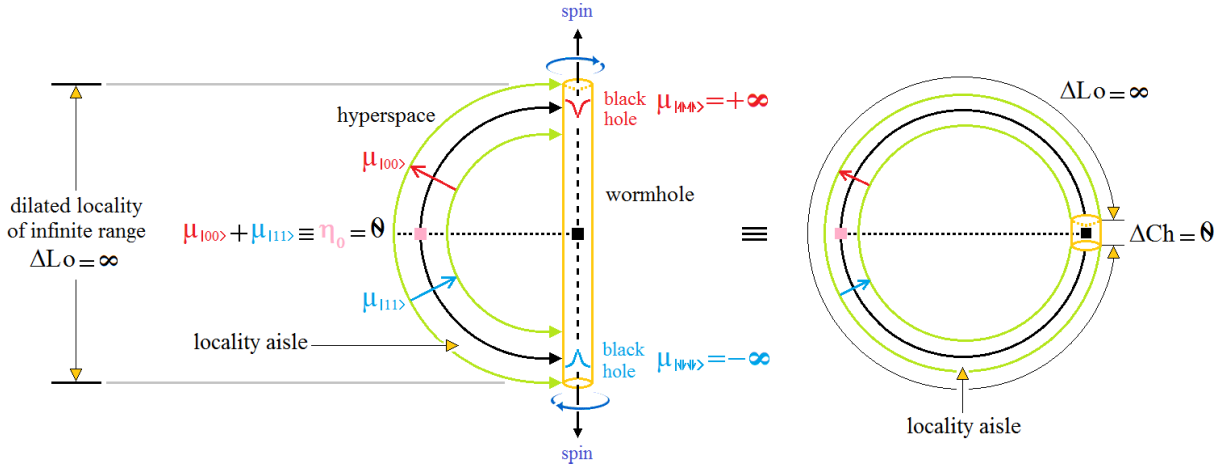


Fig.16 Graph on the left is a continuity of Fig.15, with a very pronounced curvature of hyperspace (locality aisle) according to Equations (60 and 61). The graph on the right shows us the complete curvature of hyperspace to the point of provoking a super-compression (or overshinking) on the channel (ER bridge or wormhole). This last graphic is the platform to analyze the virtues of entanglement in communications.

On the other hand, the graph on the right of Fig.15 (the last one) is equivalent to the graph on the left of Fig.16 (the first one), with a pronounced curvature of hyperspace (or locality aisle).

Equations (60 and 61) tell us that as the alter-egos are entangled, then the curvature of space-time becomes extravagantly exaggerated to the point of completely closing in a perfect circle (infinite stretching of the locality aisle) crushing the ER bridge or wormhole to a null trajectory or channel length with dramatic consequences. The most relevant of these consequences consists of the appearance of a trade-off between the range of the locality ΔL_o (see Eq.59) and the length of the channel (ER bridge or wormhole) ΔCh , both in meters

$$\Delta L_o \Delta Ch \geq \frac{l_p^2}{4\pi} \quad (64)$$

where $l_p = 1.616229(38) \times 10^{-35}$ is the Planck length in meters. Equation (64) will be called *entanglement's uncertainty principle* and will be deduced formally in a future section called Method. The most outstanding thing to highlight at this moment is that, as the locality stretches to infinity, the channel is compressed (shrunk) to zero. This phenomenon is of vital importance when we later deduce the attributes of entanglement from the point of view of quantum communications: bandwidth, latency and channel capacity.

3.2 Final thoughts on this section

Although Eq.(59) shows a dilation of the locality directly proportional to γ^2 instead of γ (from the point of view of an eventual communication between both alter-egos), everything is local, i.e., the link behaves operatively as a point. In fact, and as we have seen, the channel has null length. This last characteristic has surprising implications since the main argument by which we could not transmit useful information thanks to a link based on the entanglement, is that -given its instantaneousness- any transmission at such a distance d , such that if we divide that distance by a time $t = 0$, such ratio would

result in a velocity greater than the speed of light, i.e., $v > c$. This would automatically imply that the information traveled faster than c , which results in an inconceivable concept being in clear opposition to what is established by the Theory of Relativity. Namely, what is questioned is not the instantaneousness (null latency) of entanglement but the fact that it could beat the speed of light to transmit useful information. However, and based on what is seen here in this work, particularly, if we look at the graph on the right of Fig.16, and relate it to Eq.(64) we can carry out another mental experiment (*Gedankenexperiment* - in german). Imagine a turtle (*Dermodochelys coriacea*) crossing the length channel $\Delta Ch = 0$ at a speed

$$v_{turtle} = .09 \left[\frac{meter}{sec} \right] \ll c \approx 300,000,000 \left[\frac{meter}{sec} \right]. \quad (65)$$

How long would it take the turtle to cross that channel?

$$Latency = \frac{\Delta Ch}{v_{turtle}} = \frac{0 \left[meter \right]}{.09 \left[\frac{meter}{sec} \right]} = 0 \text{ sec}. \quad (66)$$

That is to say, and to exemplify it, the trip of a turtle through a channel (ER bridge or wormhole) of null length is instantaneous even when the speed used by the turtle is much less than c . In this way, the entanglement retains its main attribute without contradicting the Theory of Relativity, because it is a local effect of infinite range, and as we have already said, it is also the key to the TOE [39], given that if we rewrite Eq.(5) based on the original spins we will have

$$\begin{aligned} |\Phi_{\pm}^{A \cup B}\rangle &= \frac{1}{\sqrt{2}} \left(|\mu_{|0\rangle}^A, \mu_{|0\rangle}^B \rangle \pm |\mu_{|1\rangle}^A, \mu_{|1\rangle}^B \rangle \right) = \frac{1}{\sqrt{2}} \left(|\mu_{|00\rangle} \rangle \pm |\mu_{|11\rangle} \rangle \right), \\ |\Psi_{\pm}^{A \cup B}\rangle &= \frac{1}{\sqrt{2}} \left(|\mu_{|0\rangle}^A, \mu_{|1\rangle}^B \rangle \pm |\mu_{|1\rangle}^A, \mu_{|0\rangle}^B \rangle \right) = \frac{1}{\sqrt{2}} \left(|\mu_{|01\rangle} \rangle \pm |\mu_{|10\rangle} \rangle \right) \end{aligned} \quad (67)$$

we can define symbolically the entanglement between both black holes of Fig.16 based on the Eq.(67)

$$\begin{aligned} |\Phi_{\pm}^{black\ holes}\rangle &= \frac{1}{\sqrt{2}} \left(|\mu_{|\uparrow\uparrow}\rangle \pm |\mu_{|\downarrow\downarrow}\rangle \right) = \frac{1}{\sqrt{2}} \left(|\mu_{|00\rangle} \rangle \pm |\mu_{|11\rangle} \rangle \right) \gamma^2 = |\Phi_{\pm}^{A \cup B}\rangle \gamma^2, \\ |\Psi_{\pm}^{black\ holes}\rangle &= \frac{1}{\sqrt{2}} \left(|\mu_{|\uparrow\downarrow}\rangle \pm |\mu_{|\downarrow\uparrow}\rangle \right) = \frac{1}{\sqrt{2}} \left(|\mu_{|01\rangle} \rangle \pm |\mu_{|10\rangle} \rangle \right) \gamma^2 = |\Psi_{\pm}^{A \cup B}\rangle \gamma^2 \end{aligned} \quad (68)$$

Then, Eq.(68) represents the essence of the TOE, where their last terms have on the left the original Bell's bases, which constitute a main role in Quantum Theory and, on the right the Lorentz factor as its counterpart in the Relativity Theory. In fact, Eq.(68) is the relativistic version of the Bell's bases.

Thanks to the Theory of Dilated Locality (TDL) there is no confrontation between the Theory of Relativity and Quantum Theory because of the entanglement. On the contrary, there is a union since the Theory of Relativity assists entanglement with a super curvature of space-time and, so TDL demonstrates that entanglement does not violate the Theory of Relativity, even when the entanglement carries useful information. In other words, it is the Theory of Relativity itself that collaborates with entanglement so as not to be violated by the entanglement itself.

Besides, if the channel is reduced to a point (that is, no channel) and the information is completely shared, it is clear that the following principle is applied: *What You Put is What You Get* (WYPIWYG). Therefore, the bandwidth of a link via entanglement is infinite, and as there is no channel then there is no noise, at least, there is no channel noise, therefore, with infinite bandwidth and without noise, we will have a channel capacity which is also infinite. And finally, at this point, the most important finding is that *it is impossible to attack, intercept or hack a channel that does not exist*, i.e., thanks to the entanglement we can manipulate data without the need of using compression or encryption. In fact, in this context, the compression and Cryptography of data will not be useful any more.

Furthermore, TDL shows that the channel is reduced to a point, so instead of talking about transmitting information we prefer to talk about sharing information at that point. In other words, it is even as if there was no a signal involved. The arguments mentioned above and the following ones are those that avoid violating the No-Communications Theorem [31,137-141] in the case of a transmission of information through a link based on entanglement, thus, we will start with a simple analysis about this important theorem. The No-Communication Theorem works with the Kraus matrices which satisfy certain conditions and their means –for example– that Alice's measurement apparatus does not influence Bob's subsystem, i.e., it starts from the non-locality established by Bell's theorem, CHSH and the apparent experimental verifications of such non-locality carried out by Aspect and others. We say “apparent experimental verifications” because such experiments were consistent with a preconception which is completely displaced in this work. Then, the mentioned Kraus matrices continue being manipulated until they reach a scalar on which the theorem says: *from this scalar, we can argue that, statistically, Bob cannot discern the difference between what Alice did and a random measurement (or if she just did something)*. That is, everything begins from the assumption that non-locality is the only reality around entanglement; but as we have seen throughout this work; the entanglement is a local phenomenon of infinite range, however, it does not violate the No-Communication Theorem. Besides, entanglement does not need a transmission at a speed $v > c$ to share information instantaneously. As we have previously seen, in relation to the Eq.(63) it is the alter-egos that sustain the effect and, in fact, they are the only ones that can communicate among themselves. Moreover, since they are located in the same point, we could say that they share information by default, because the channel has zero length. In other words, it is as if they would communicate between themselves even without intentionally doing so. Therefore, the No-Communication Theorem does not apply to alter-egos, which are the only ones that manipulate information without violating the Theory of Relativity. Furthermore, in relation to entanglement we can draw three interesting conclusions:

- it is a local phenomenon of infinite range,
- the original spins do not communicate among each other but they do it through their representatives, i.e., their alter-egos, and
- in every experiment related to the entanglement, the measured entangled pairs are those of Eq.(5) also known as singlet states, Bell bases, or simply the bases of Eq.(5), and they are based on the original spins of Eq.(4), since the alter-egos has never been measured (for obvious reasons). However, if such thing as measuring an alter-ego was possible, in fact, if we measured one, we would be measuring the other one as well because they share the same place (i.e., in this case the channel is a point).

Therefore, there is not the slightest inkling of limitation or impediment to the instantaneous sharing of useful information via a link based on entanglement. At least until the entanglement is destroyed, for example, through a quantum measurement.

So far, it should be clear that entanglement is the meeting point and not the cause of disagreement between the two main pillars of Physics (Theory of Relativity and Quantum Theory). Moreover, it is the cornerstone or instrument that ends up amalgamating everything. This is extremely positive since a better understanding of entanglement could lead us to convert a measurement into a message itself. Since if Alice and Bob share a pair of entangled spins, and are far away from each other, being Alice in a fort which could be attacked but previously she had agreed with Bob that if she was attacked, the polarity of her spin would change. Otherwise, if she was not attacked, then her spin would be intact. The only way for Bob to realize whether Alice's fort was assaulted is to measure his spin. Therefore, this is a clear example where the message is transmitted despite of the fact that the entanglement is destroyed. Techniques to recovering entanglement after a quantum measurement are shown in Appendix A.6. This better understanding of the entanglement sheds light on the potential it has in quantum communications in general, and in a possible interplanetary communication in particular, such as for the much-mentioned trip to Mars. Besides, thanks to the present work three types of communication systems are revealed:

- classic (via an electromagnetic transmission), for disambiguation in a quantum information transmission, e.g., Teleportation [1-3, 58],

- quantum (via optical fiber), for a classic information transmission, e.g., Superdense Coding [28, 57-59], and
- quantum (via entanglement exclusively), which will give rise to a new communication system with links that do not have obstacles that interrupt it, neither fading nor vanishing it. Moreover, with the real possibility of developing new protocols for Teleportation, which will allow a disambiguation without the use of a classic channel (like the traditional Teleportation protocol) but using a second entanglement link, instead. This would allow a completely instantaneous Teleportation without violating the Theory of Relativity. What is more, it could not only have an impact over the interpretation on the theory of black holes [142] and the Hawking's radiation [38,142,143], but also the Information Paradox [14,38].

On the other hand, and since the entanglement is "monogamous" (a third party cannot participate unless it is part of the original entangled particles) and taking into account that the channel is a point (i.e., there is not a channel or $\Delta Ch = 0$), the security of the link should be completely preserved. However, the impact on Teleportation and Superdense coding goes much further since under the parallel operator of Eq.(43) we could think about protocols considering not only an exclusive wave-function representative of entanglement (as we know from the literature on this subject [1-3]) but also, recognizing more individuality to the original spins involved in that eventual protocol, that is to say, a new protocol where Alice and Bob do not lose their individualities. Moreover, and already in the terrain of Figures 15 and 16, a possible teleportation based on the entanglement of both black holes could be thought as a distribution of an entangled pair of the type of Eq.(68) between Alice and Bob, instead of sharing pairs of the type of Eq.(67). This opens up a whole new world of possibilities to Teleportation protocols of another type, which to date are mere speculations.

Furthermore, from Eq.(43), it is easier to understand why there is no entanglement in the classical world. The reason is that in the world of the macroscopic (whether natural or man-made) there are not two perfectly equal things in such a way that with opposite signs they can be entangled by some means and reproduce an effect as extraordinary as the case of the entanglement between quantum spins. Even more, if two classic elements were perfectly equal, then they could cancel the denominator of the Eq.(43) and give infinite alter-egos, with everything that that entails. In other words, everything is reduced to the Eq.(43), where if two things in nature were perfectly equal and with opposite signs, they could make the denominator of Eq.(43) equal to zero, and in this way, there would be entanglement.

For the option chosen in this section, we conclude that the alter-egos do not emit Hawking's radiation [38,142,143], precisely because they are massless black holes and such radiation depends on the mass of a black hole.

Although we have taken the decision to completely strip this paper of all complicated symbolic logic so that the physical effect and its attributes survive above everything else, several questions remain to be answered:

- What attributes of the original spins are transferred to alter-egos? Since these spins are one of the so many attributes of a particle to which the spin belongs, e.g., if the original spins are photons (bosons) with mass = 0, electric charge = 0, mean lifetime = stable, among others, all this seems to be transferred from the originals to the alter-egos, except for the spin value which in photons are ± 1 and in the alter-egos are $\pm \infty$, precisely since the latter are reached by the relativistic dilation, which is ∞ too, and
- What kind of black holes are the alter-egos? We know that they are massless infinite spins, but what else? What about their linear momentum?

These questions will remain for an upcoming work, however, in the next section, we will delve into the relationship between alter-egos and black holes in order to verify the attributes of entanglement for quantum communications.

4 Methods

In this section, we will develop the necessary method for the verification of the concepts conceived in the previous sections, in particular, regarding the main attributes of entanglement in quantum communications: bandwidth and latency. This method is called Quantum Spectral Analysis-Frequency in Time (QSA-FIT) [144,145]. Also, we will demonstrate some theorems related to the

projection of the aforementioned attributes in communications. Besides, we will develop a new deduction of the alter-egos but this time from the Hamiltonian of entanglement. Finally, we will expose the possibility that a pair of alter-egos may have equal masses with opposite signs.

4.1 Prolegomena to Quantum Spectral Analysis-Frequency in Time

A unitary operator U can transform a quantum state into another one, with, $U: H \rightarrow H$ on a Hilbert space H , where U will be a unitary operator if it satisfies the condition: $U^\dagger U = U U^\dagger = I$. Besides, $(\bullet)^\dagger$ is the adjoint of (\bullet) , and I is the identity matrix. Such condition is required to preserve inner products, inasmuch as, we can transform $|\chi\rangle$ and $|\psi\rangle$ to $U|\chi\rangle$ and $U|\psi\rangle$, respectively, thus $\langle\chi|U^\dagger U|\psi\rangle = \langle\chi|\psi\rangle$. In particular, unitary operators preserve lengths:

$$\langle\psi|U^\dagger U|\psi\rangle = \langle\psi|\psi\rangle = \begin{bmatrix} \alpha^* & \beta^* \end{bmatrix} \begin{bmatrix} \alpha \\ \beta \end{bmatrix} = |\alpha|^2 + |\beta|^2 = 1, \quad (69)$$

Besides, the unitary operator satisfies the following differential equation known as the Schrödinger equation [13, 16, 17]:

$$\frac{d}{dt} U(t + \Delta t, t) = \frac{-i \hat{H}}{\hbar} U(t + \Delta t, t) \quad (70)$$

where \hat{H} represents the Hamiltonian matrix of the Schrödinger equation, while $i = \sqrt{-1}$, and \hbar is the reduced Planck constant: $\hbar = h/2\pi$. Multiplying both sides of Eq.(70) by $|\psi(t)\rangle$ and setting

$$|\psi(t + \Delta t)\rangle = U(t + \Delta t, t)|\psi(t)\rangle \quad (71)$$

Being $U(t + \Delta t, t) = U(t + \Delta t - t) = U(\Delta t)$ a unitary transform (operator and matrix), yields

$$\frac{d}{dt} |\psi(t)\rangle = \frac{-i \hat{H}}{\hbar} |\psi(t)\rangle \quad (72)$$

The Hamiltonian operator represents the total energy of the system and controls the evolution process. In most of the cases, the Hamiltonian is formed by kinetic and potential energy. However, if the particle is stationary thus the kinetic energy is cancelled, it will only leave the potential energy which is the only one that will be linked to external forces applied to this particle. Thus the control of the external forces is at the same time the control of the evolution of the states of the system [1, 2, 13, 16, 17, 146, 147]. For example, in the case of bosons (in particular, photons), they possess an integer spin ($\mu = 1$). Besides, we would have a momentum,

$$\sigma \cdot P = \begin{pmatrix} P_z & P_x - iP_y \\ P_x + iP_y & -P_z \end{pmatrix}, \quad (73)$$

being $\sigma = (\sigma_x, \sigma_y, \sigma_z)$ the Pauli's matrices,

$$\sigma_x = \begin{pmatrix} 0 & 1 \\ 1 & 0 \end{pmatrix}, \quad \sigma_y = \begin{pmatrix} 0 & -i \\ i & 0 \end{pmatrix}, \quad \sigma_z = \begin{pmatrix} 1 & 0 \\ 0 & -1 \end{pmatrix}, \quad (74)$$

while the spin will be,

$$S = \hbar \sigma = \hbar \mu \sigma = \hbar \mu (\sigma_x, \sigma_y, \sigma_z). \quad (75)$$

Then, the Hamiltonian takes the following form,

$$H = \frac{cS \cdot P}{h} = \frac{c\mu h \sigma \cdot P}{h} = \frac{c\mu h}{h} \begin{pmatrix} P_z & P_x - iP_y \\ P_x + iP_y & -P_z \end{pmatrix} = h\mu\Omega \quad (76)$$

being c the speed of light, Ω will result in this case,

$$\Omega = \frac{c}{h} \begin{pmatrix} P_z & P_x - iP_y \\ P_x + iP_y & -P_z \end{pmatrix} \quad (77)$$

At this point, if we consider a polarization of spin regarding the z -axis exclusively, thus,

$$\Omega_z = \frac{c}{h} \begin{pmatrix} P_z & 0 \\ 0 & -P_z \end{pmatrix} = \frac{c}{h} P_z \begin{pmatrix} 1 & 0 \\ 0 & -1 \end{pmatrix} = \frac{c}{h} P_z \sigma_z \quad (78)$$

with a Hamiltonian,

$$H = h\mu\Omega_z = h\mu \frac{c}{h} P_z \sigma_z = h\mu\omega \sigma_z \quad (79)$$

where ω is the angular frequency, which is the same in all directions since we will consider Ω as spatially isotropic and homogeneous.

Finally, solving Eq.(72) depending on the Hamiltonian of Eq.(79), we will have the solution to Schrödinger equation based on the exponential matrix of the Hamiltonian's,

$$|\psi(t + \Delta t)\rangle = e^{\frac{-i\hat{H}\Delta t}{h}} |\psi(t)\rangle \quad (\text{if Hamiltonian is not time-dependent}) \quad (80)$$

$$|\psi(t + \Delta t)\rangle = e^{\frac{-i}{h} \int_t^{t+\Delta t} \hat{H} dt} |\psi(t)\rangle \quad (\text{if Hamiltonian is time dependent}) \quad (81)$$

Discrete versions of Equations (80) and (81) for a time-dependent (or not) Hamiltonian, being k the discrete time. With,

$$|\psi_{k+\Delta k}\rangle = e^{\frac{-i\hat{H}\Delta k}{h}} |\psi_k\rangle = e^{-i\mu\omega_k \sigma_z \Delta k} |\psi_k\rangle \quad (\text{if Hamiltonian is not time-dependent}) \quad (82)$$

$$|\psi_{k+\Delta k}\rangle = e^{\frac{-i}{h} \sum_k^{k+\Delta k} \hat{H}_k} |\psi_k\rangle = e^{-i\mu\sigma_z \sum_k^{k+\Delta k} \omega_k} |\psi_k\rangle \quad (\text{if Hamiltonian is time-dependent}) \quad (83)$$

$$|\psi_{k+1}\rangle = e^{-i\mu\sigma_z \sum_{i=1}^{k+1} \omega_i} |\psi_0\rangle \quad (\text{with } \Delta k = 1, \text{ and starting from initial state [13] } |\psi_0\rangle) \quad (84)$$

Moreover, replacing Eq.(79) into Eq.(80) and (81), we will have another main equations for this paper,

$$|\psi(t + \Delta t)\rangle = e^{-i\mu\omega(t) \sigma_z \Delta t} |\psi(t)\rangle, \quad (85)$$

$$|\psi(t + \Delta t)\rangle = e^{-i\mu\sigma_z \int_t^{t+\Delta t} \omega(t) dt} |\psi(t)\rangle. \quad (86)$$

Finally, and considering an incremental approximation of Eq.(72) as well as in its discrete version, and considering the proper replacements of Eq.(79), both versions of Schrödinger's equation will take the following form respectively,

$$\frac{|\Delta\Psi(t+\Delta t)\rangle}{\Delta t} = -i\mu\omega(t)\sigma_z|\Psi(t+\Delta t)\rangle \quad (87)$$

and

$$|\Delta\Psi_{k+\Delta k}\rangle = \frac{|\Psi_{k+\Delta k+1} - \Psi_{k+\Delta k-1}\rangle}{2} = -i\mu\omega_k\sigma_z|\Psi_{k+\Delta k}\rangle \quad (88)$$

4.2 Quantum Spectral Analysis-Frequency in Time (QSA-FIT)

This tool plays a main role in the development of this section. Besides, it is highly important when it is applied in signal analysis, in particular for the practical calculation of the bandwidth of any type of signal in a much more direct way than the Fourier theory [148-150]. In fact, a *quantum time-dependent spectrum analysis*, or simply, quantum spectral analysis: frequency in time (QSA-FIT) complements and completes the Fourier theory, especially its maximum exponent: the fast Fourier transform (FFT) [151-154]. For all the above, QSA-FIT constitutes a practical temporal-spectral bridge [144,145]. Finally, QSA-FIT is a metric which assesses the impact of the flanks of a signal on its frequency spectrum at each instant, which is not taken into account by the Fourier theory and, let alone, in real time. This is the reason why they must both work together.

Next, we are going to deduce this operator in its continuous and discrete forms for a quantum state. There are several versions of QSA-FIT [144,145], in this case, we will deduce this operator in its continuous and discrete versions of Equations (87) and (88), respectively. Therefore, if we multiply by $\langle\Psi|$ both sides of Eq.(87), we will have,

$$\langle\Psi(t)|\frac{\Delta\Psi(t)}{\Delta t}\rangle = -i\mu\omega(t)\langle\Psi(t)|\sigma_z|\Psi(t)\rangle \quad (89)$$

then,

$$\Delta\omega(t) = \mu\omega(t) = i\frac{1}{\langle\Psi(t)|\sigma_z|\Psi(t)\rangle}\langle\Psi(t)|\frac{\Delta\Psi(t)}{\Delta t}\rangle \quad (90)$$

Now, if we multiply both sides of Eq.(88) by $\langle\Psi_k|$, we will have,

$$\frac{\langle\Psi_k|\Psi_{k+1} - \Psi_{k-1}\rangle}{2} = -i\mu\omega_k\langle\Psi_k|\sigma_z|\Psi_k\rangle \quad (91)$$

then,

$$\Delta\omega_k = \mu\omega_k = i\frac{\langle\Psi_k|\Psi_{k+1} - \Psi_{k-1}\rangle}{2\langle\Psi_k|\sigma_z|\Psi_k\rangle} = i\frac{(\langle\Psi_k|\Psi_{k+1}\rangle - \langle\Psi_k|\Psi_{k-1}\rangle)}{2\langle\Psi_k|\sigma_z|\Psi_k\rangle} \quad (92)$$

Summarizing, we are going to have a $\Delta\omega$ at each instant of the signal (continuous or discrete, classical or quantum). Another interesting attribute of this operator is that it is not affected by the quantum measurement problem, because its output is a classical scalar, i.e., it can be measured with complete accuracy. In fact, the operator $\Delta\omega$ arises from a hybrid algorithm with quantum and classical parts, as we can see in Fig.17 where a single fine line represents I or N qubits, while a single thick line represents I or N classical bits. Moreover, the quantum part of the operator $\Delta\omega$ must respect the concept of reversibility because it is closely related to energy consumption, and consequently to the Landauer's Principle [13], for this reason, $|\Psi_k\rangle$ also appears on the way out. Thus,

Quantum part:

$$a_k = \langle\Psi_k|\Psi_{k+1}\rangle, \quad b_k = \langle\Psi_k|\Psi_{k-1}\rangle, \quad c_k = \langle\Psi_k|\sigma_z|\Psi_k\rangle \quad (93)$$

Classical part:

$$\Delta\omega_k = \mu \omega_k = i \frac{(a_k - b_k)}{2c_k} \quad (94)$$

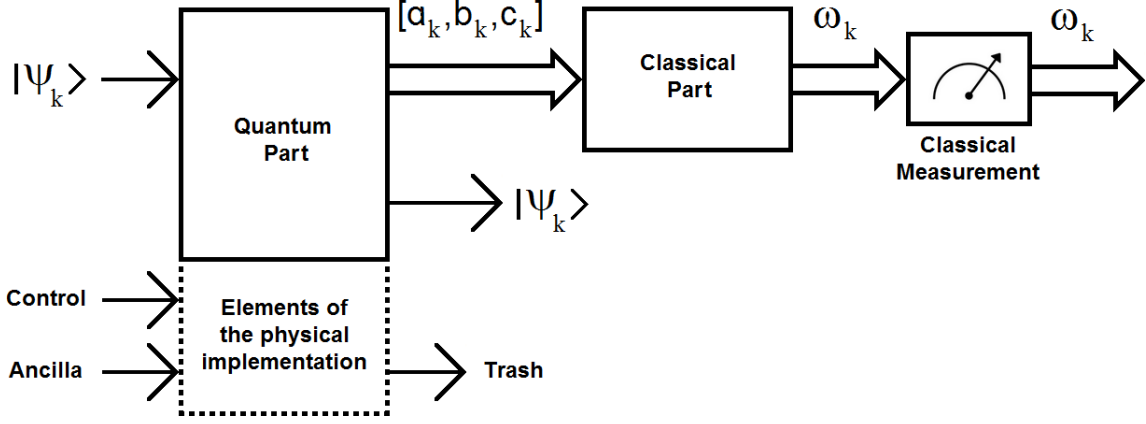


Fig. 17 A hybrid algorithm with quantum and classical parts.

Finally, for all mentioned cases (continuous or discrete, classical or quantum signals) the bandwidth BW will result from the difference between the maximum and the minimum frequency of such signal,

$$BW = f_{\max} - f_{\min} = \frac{1}{2\pi} (\Delta\omega_{\max} - \Delta\omega_{\min}) \quad (95)$$

A practical example will make things clearer. This is the case of the application of QSA-FIT to a classical signal. There are several versions and ways to apply QSA-FIT to a classical signal [144,145]. For any signal (in general) it is necessary to equalize it and calibrate it in quadrature with FFT [144,145], but for a pure tone this procedure is unnecessary, so we can access the result in a much simpler way. Therefore, the direct classical continuous version of Equations (90) and (92) will be,

$$\omega(t) = \frac{\eta}{s(t)} \frac{ds(t)}{dt}, \quad (96)$$

where $s(t)$ is the signal, and η is an adjustment factor. While the discrete version will be,

$$\omega_k = \frac{\eta}{s_k} \frac{(s_{k+1} - s_{k-1})}{2}. \quad (97)$$

The problem with Equations (96) and (97) consists in the indeterminacy of $\Delta\omega$ when the signal is null at that instant. Then, we will use a modified version of the signal called *baselineless* (BLL) which consists of,

$$\omega(t) = \frac{1}{s_{BLL}} \frac{ds(t)}{dt}, \quad (98)$$

with $\eta = 1$, where,

$$s_{BLL} = \frac{s_{\max} - s_{\min}}{2}, \quad (99)$$

then, ω , f_{max} and f_{min} will be

$$\omega(t) = \frac{1}{\left(\frac{s_{max} - s_{min}}{2}\right)} \frac{ds(t)}{dt}, \quad (100)$$

$$f_{max} = \frac{1}{2\pi} \frac{1}{\left(\frac{s_{max} - s_{min}}{2}\right)} \left(\frac{ds(t)}{dt}\right)_{max} = \frac{(ds(t)/dt)_{max}}{\pi(s_{max} - s_{min})}, \quad (101)$$

$$f_{min} = \frac{1}{2\pi} \frac{1}{\left(\frac{s_{max} - s_{min}}{2}\right)} \left(\frac{ds(t)}{dt}\right)_{min} = \frac{(ds(t)/dt)_{min}}{\pi(s_{max} - s_{min})}, \quad (102)$$

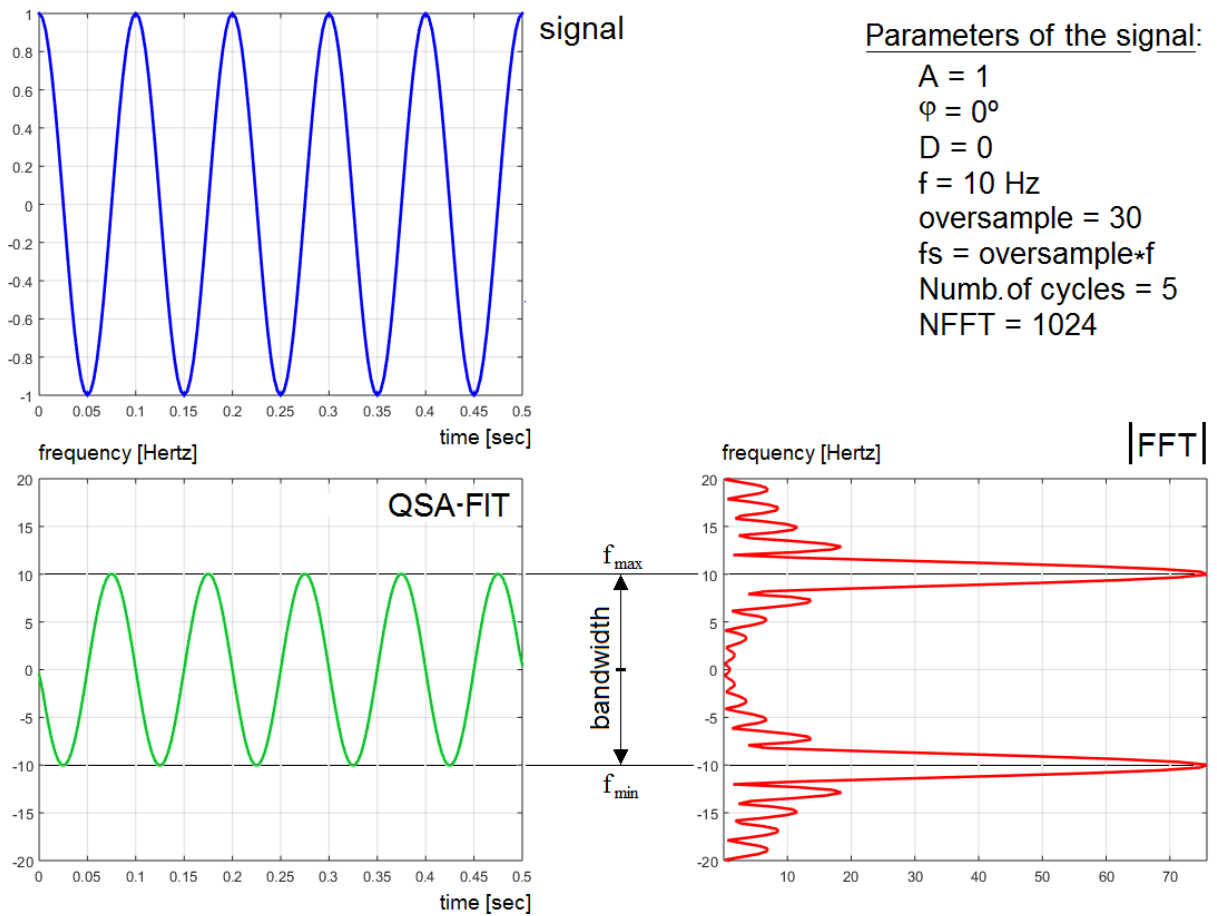


Fig. 18 Example of signal (in blue), QSA-FIT (in green), and |FFT| (in red) of cosine.

Now, if we consider a signal like Fig.18 (in blue),

$$s(t) = A \cos(\omega t + \varphi) + B, \quad (103)$$

where A is the amplitude, φ is the phase, and B is the baseline, with,

$$\frac{ds(t)}{dt} = -A \omega \sin(\omega t + \varphi), \quad (104)$$

then,

$$s_{\max} = A + B, \quad s_{\min} = -A + B. \quad (105)$$

Now, replacing Equations (104) and (105) into (100), we will have,

$$\omega(t) = \frac{1}{\left(\frac{(A+B) - (-A+B)}{2}\right)} (-A \omega \sin(\omega t + \varphi)) = -\omega \sin(\omega t + \varphi) \quad (106)$$

in green in Fig.18, then,

$$f_{\max} = \frac{\omega}{2\pi} = \frac{2\pi f}{2\pi} = f, \quad f_{\min} = \frac{-\omega}{2\pi} = \frac{-2\pi f}{2\pi} = -f. \quad (107)$$

Then, replacing Eq.(107) into (95), we will have,

$$BW = f_{\max} - f_{\min} = f - (-f) = 2f. \quad (108)$$

This result can be seen in the lower part of Fig.18 between QSA-FIT and |FFT|, which is the total aperture of QSA-FIT (in green) and at the same time, the distance between the peaks of |FFT| (in red).

Now, we are going to calculate the spectral analysis of one of the original spins thanks to the operator QSA-FIT. Therefore, if we resort to Eq.(87) but for one of the bases of Eq.(4), e.g., $|00\rangle$

$$\frac{d|00\rangle}{dt} = (-i \mu_{|00\rangle} \omega) [\sigma_z \cdot \oplus \sigma_z] |00\rangle. \quad (109)$$

In Eq.(109) we used a new operator “ $\cdot \oplus$ ” (which is easy to generalize) on the Pauli matrix σ_z of Eq.(74), this new operator is the only substantial difference between the Equations (87) and (109), and accounts for the dimensional difference between the two equations. So that if

$$A = \begin{bmatrix} a_{11} & a_{12} \\ a_{21} & a_{22} \end{bmatrix}, \quad \text{and} \quad B = \begin{bmatrix} b_{11} & b_{12} \\ b_{21} & b_{22} \end{bmatrix}, \quad \text{therefore}$$

$$\begin{aligned} A \cdot \oplus B &= \begin{bmatrix} a_{11} & a_{12} \\ a_{21} & a_{22} \end{bmatrix} \cdot \oplus \begin{bmatrix} b_{11} & b_{12} \\ b_{21} & b_{22} \end{bmatrix} = \left[\begin{bmatrix} a_{11} & a_{12} \\ a_{21} & a_{22} \end{bmatrix} + b_{11} \begin{bmatrix} a_{11} & a_{12} \\ a_{21} & a_{22} \end{bmatrix} + b_{12} \begin{bmatrix} a_{11} & a_{12} \\ a_{21} & a_{22} \end{bmatrix} \right. \\ &\quad \left. + b_{21} \begin{bmatrix} a_{11} & a_{12} \\ a_{21} & a_{22} \end{bmatrix} + b_{22} \begin{bmatrix} a_{11} & a_{12} \\ a_{21} & a_{22} \end{bmatrix} \right] \\ &= \begin{bmatrix} a_{11} + b_{11} & a_{12} + b_{11} \\ a_{21} + b_{11} & a_{22} + b_{11} \end{bmatrix} \begin{bmatrix} a_{11} + b_{12} & a_{12} + b_{12} \\ a_{21} + b_{12} & a_{22} + b_{12} \end{bmatrix} \\ &= \begin{bmatrix} a_{11} + b_{21} & a_{12} + b_{21} \\ a_{21} + b_{21} & a_{22} + b_{21} \end{bmatrix} \begin{bmatrix} a_{11} + b_{22} & a_{12} + b_{22} \\ a_{21} + b_{22} & a_{22} + b_{22} \end{bmatrix} \\ &= \begin{bmatrix} a_{11} + b_{11} & a_{12} + b_{11} & a_{11} + b_{12} & a_{12} + b_{12} \\ a_{21} + b_{11} & a_{22} + b_{11} & a_{21} + b_{12} & a_{22} + b_{12} \\ a_{11} + b_{21} & a_{12} + b_{21} & a_{11} + b_{22} & a_{12} + b_{22} \\ a_{21} + b_{21} & a_{22} + b_{21} & a_{21} + b_{22} & a_{22} + b_{22} \end{bmatrix} \end{aligned} \quad (110)$$

Now, applying the new operator on the Pauli matrices

$$\begin{aligned}
\sigma_z \cdot \oplus \sigma_z &= \begin{bmatrix} 1 & 0 \\ 0 & -1 \end{bmatrix} \cdot \oplus \begin{bmatrix} 1 & 0 \\ 0 & -1 \end{bmatrix} = \begin{bmatrix} \begin{bmatrix} 1 & 0 \\ 0 & -1 \end{bmatrix} + 1 & \begin{bmatrix} 1 & 0 \\ 0 & -1 \end{bmatrix} + 0 \\ \begin{bmatrix} 1 & 0 \\ 0 & -1 \end{bmatrix} + 0 & \begin{bmatrix} 1 & 0 \\ 0 & -1 \end{bmatrix} - 1 \end{bmatrix}, \\
&= \begin{bmatrix} \begin{bmatrix} 1+1 & 0+1 \\ 0+1 & -1+1 \end{bmatrix} & \begin{bmatrix} 1+0 & 0+0 \\ 0+0 & -1+0 \end{bmatrix} \\ \begin{bmatrix} 1+0 & 0+0 \\ 0+0 & -1+0 \end{bmatrix} & \begin{bmatrix} 1-1 & 0-1 \\ 0-1 & -1-1 \end{bmatrix} \end{bmatrix} = \begin{bmatrix} 2 & 1 & 1 & 0 \\ 1 & 0 & 0 & -1 \\ 1 & 0 & 0 & -1 \\ 0 & -1 & -1 & -2 \end{bmatrix},
\end{aligned} \tag{111}$$

Then, if we multiply both sides of the Eq.(109) by $\langle 00|$,

$$\langle 00|d^{00}/dt\rangle = (-i\mu_{|00\rangle}\omega)\langle 00|\sigma_z \cdot \oplus \sigma_z|00\rangle. \tag{112}$$

Then,

$$\Delta\omega_{\max} = \Delta\omega_{|00\rangle} = \mu_{|00\rangle}\omega = \mu_{|0\rangle}^2\omega = \omega = \frac{i\langle 00|d^{00}/dt\rangle}{\langle 00|\sigma_z \cdot \oplus \sigma_z|00\rangle}. \tag{113}$$

It can be seen that Equations (92) and (113) coincide in their form and it is clear that the spectral analysis for its counterpart independently of the term in the extreme right of Eq.(113) will be,

$$\Delta\omega_{\min} = \Delta\omega_{|11\rangle} = \mu_{|11\rangle}\omega = -\mu_{|1\rangle}^2\omega = -\omega, \tag{114}$$

Then, the bandwidth of the original entangled spins will be,

$$BW_{original} = \frac{1}{2\pi}(\Delta\omega_{\max} - \Delta\omega_{\min}) = \frac{1}{2\pi}(\omega - (-\omega)) = \frac{2\omega}{2\pi} = \frac{\omega}{\pi} \ll \infty. \tag{115}$$

Therefore, the bandwidth of the link between the original spins is finite. However, what happens with the bandwidth of the link between the alter-egos? We obtain the answer replacing the alter-egos in the Eq.(113),

$$\begin{aligned}
\Delta\omega_{\max} &= \Delta\omega_{|\uparrow\uparrow\rangle} = \mu_{|\uparrow\uparrow\rangle}\omega \\
\Delta\omega_{\min} &= \Delta\omega_{|\downarrow\downarrow\rangle} = \mu_{|\downarrow\downarrow\rangle}\omega
\end{aligned} \tag{116}$$

Then, the bandwidth will be

$$BW_{alter-egos} = \frac{1}{2\pi}(\Delta\omega_{|\uparrow\uparrow\rangle} - \Delta\omega_{|\downarrow\downarrow\rangle}) = \frac{1}{2\pi}(\infty - (-\infty)) = \frac{2\infty}{2\pi} = \frac{\infty}{\pi} = \infty = BW_{original}\gamma^2. \tag{117}$$

This result should not be surprising given the exceptional performance of the quantum entanglement and therefore of a quantum entanglement channel. But once again, it can be seen that it is the alter-egos that sustain not only the effect but also the exceptional attributes of such effect.

Now, if we consider that $\left| \frac{\Delta \hat{\uparrow}\hat{\uparrow}}{\Delta t} \right\rangle$ is a good approximation of $\left| \frac{d \hat{\uparrow}\hat{\uparrow}}{dt} \right\rangle$, since $|\hat{\uparrow}\hat{\uparrow}\rangle$ is a stationary wave-function, then

$$\Delta\omega \Delta t = \mu_{|\hat{\uparrow}\hat{\uparrow}\rangle} \omega \Delta t = \frac{i \langle \hat{\uparrow}\hat{\uparrow} | \Delta \hat{\uparrow}\hat{\uparrow} \rangle}{\langle \hat{\uparrow}\hat{\uparrow} | \sigma_z \oplus \sigma_z | \hat{\uparrow}\hat{\uparrow} \rangle}. \quad (118)$$

Equation (118) represents a trade-off, such that, if we consider the division by 2 of the derivative, and we take the modulus on the right side of the equality, then, the trade-off becomes

$$\Delta\omega \Delta t = \frac{1}{2} \left| \frac{i \langle \hat{\uparrow}\hat{\uparrow} | \Delta \hat{\uparrow}\hat{\uparrow} \rangle}{\langle \hat{\uparrow}\hat{\uparrow} | \sigma_z \oplus \sigma_z | \hat{\uparrow}\hat{\uparrow} \rangle} \right| = \frac{1}{2} |i| \left| \frac{\langle \hat{\uparrow}\hat{\uparrow} | \Delta \hat{\uparrow}\hat{\uparrow} \rangle}{\langle \hat{\uparrow}\hat{\uparrow} | \sigma_z \oplus \sigma_z | \hat{\uparrow}\hat{\uparrow} \rangle} \right| = \frac{1}{2} \{(i)^* (i)\}^{1/2} = \frac{1}{2} \{(-i)(i)\}^{1/2} \geq \frac{1}{2}, \quad (119)$$

which represents the famous Heisenberg Uncertainty Principle [1-3, 13], and it is the same for the original spins and for the alter-egos,

$$\Delta\omega_{alter-egos} \Delta t_{alter-egos} = \left(\Delta\omega_{originals} \gamma^2 \right) \left(\frac{\Delta t_{originals}}{\gamma^2} \right) = \Delta\omega_{originals} \Delta t_{originals} \geq \frac{1}{2}. \quad (120)$$

4.3 Entanglement and black holes

Next, we will try to verify the connection between Equations (64) and (119), since and as we can see, both equations represent a trade-off between their two respective components, i.e., if in Eq.(64) $\Delta L_o \rightarrow \infty$, then, $\Delta Ch \rightarrow 0$, and if in Eq.(119) $\Delta\omega \rightarrow \infty$, then, $\Delta t \rightarrow 0$. We will begin by demonstrating three theorems, which are key to this mission.

Perfect Quantum Channel Theorem (PQChT):

Theorem: A quantum channel with infinite bandwidth and then null time latency is a perfect quantum channel.

Proof: From Eq.(119), we know that if $\Delta\omega = \infty$, thus $\Delta t = 0$. Now, replacing $\Delta t = 0$ and $t = t_0$ into Eq.(71), we will have,

$$|\psi(t_0 + 0)\rangle = |\psi(t_0)\rangle = U(t_0 + 0, t_0) |\psi(t_0)\rangle = U(t_0 + 0 - t_0) |\psi(t_0)\rangle = U(0) |\psi(t_0)\rangle \quad (121)$$

It is easy to deduce that the only equality that admits Eq.(121) is when

$$U(0) = I \quad (122)$$

where I is the identity matrix. Consequently, Eq.(121) will be,

$$|\psi(t_0)\rangle = |\psi(t_0)\rangle \quad (123)$$

Therefore, we will obtain a perfect quantum channel U under these conditions. ■

No-Quantum Channel Theorem (NQChT):

Theorem: Every perfect quantum channel has null effective Euclidean dimensions.

Proof: If we do,

$$\Delta\omega = \frac{2\pi \Delta L_o C}{l_p^2} \quad (124)$$

and

$$\Delta t = \frac{\Delta Ch}{C} \quad (125)$$

where ΔL_o is the range or locality of the effect (quantum entanglement), $l_p = 1.616229(38) \times 10^{-35}$ is the Planck length, and ΔCh is the channel length (all of them in meters), and C is the speed of light, then, replacing Equations (124) and (125) into (119), we will have,

$$\Delta \omega \Delta t = \left(\frac{2\pi \Delta L_o C}{l_p^2} \right) \left(\frac{\Delta Ch}{C} \right) = 2\pi \left(\frac{\Delta L_o}{l_p} \right) \left(\frac{\Delta Ch}{l_p} \right) \geq 1/2 \quad (126)$$

with

$$2\pi \Delta l_o \Delta c_h \geq 1/2 \quad (127)$$

and then

$$\Delta l_o \Delta c_h \geq 1/4\pi \quad (128)$$

being Δl_o the range of effect (unitless) and Δc_h the channel length (unitless). Clearly, Eq.(128) holds the trade-off between Δl_o and Δc_h (like between $\Delta \omega$ and Δt), so, if $\Delta l_o \rightarrow \infty$, then, $\Delta c_h \rightarrow 0$. ■

This theorem does not tell us that there is no quantum channel but -under these conditions- there is a quantum channel of null dimension, that is, the quantum channel is reduced to a point. Besides, from Eq.(126) we can rearrange terms so that thanks to it we can deduce Eq.(64).

Moreover, in the two theorems developed up to this point we could have considered (in relation to the graph on the right of Fig.16) only the upper semicircle (or north arch) above the dotted line, that is, $(\Delta L_o/2)(\Delta Ch/2)$ instead of $\Delta L_o \Delta Ch$ (see Fig.19), although the final result for these two theorems would not have changed at all.

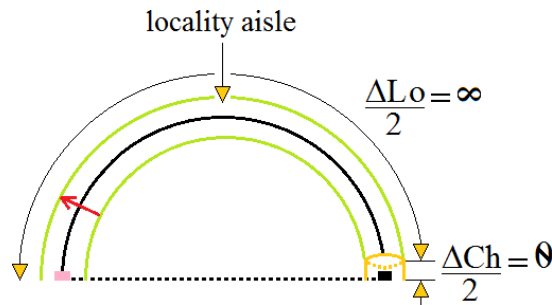


Fig.19 North arch of Fig.16.

Therefore, we will take Fig.19 into account for the following theorem. Besides, for the next theorem we will consider the remaining option with respect to the masses of the black holes of a bipartite entanglement, that is, both black holes have mass (finite or infinite) but of opposite sign. In particular, the following theorem exclusively involves the north arch, which has positive mass (finite or infinite), as we can see in Fig.19.

North Arch Theorem (NAT):

Theorem: The north arch of a bipartite quantum entanglement behaves like a black hole.

Proof: Let's start from Eq.(126), considering only the northern arch, and regrouping elements, we will have,

$$\Delta\omega \Delta t = 2 \frac{\left(\pi \Delta L_o / 2 \Delta C h / 2\right)}{l_p^2} \geq 1/2, \quad (129)$$

where the term inside parentheses represents the lateral area of the cylinder of Fig.20. In the following equation, A is the area of the event horizon, and the width of the channel is equal to its length since it is a point. Then,

$$\frac{A}{l_p^2} \geq \frac{1}{4} \quad (130)$$

where the lateral area $A = \pi \Delta L_o / 2 \Delta C h / 2$, being the diameter of the cylinder equivalent to $\Delta C h / 2$, and its length equal to $\Delta L_o / 2$, see Fig.20.

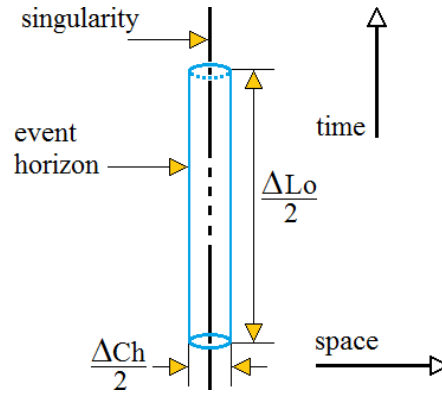


Fig.20 This cylinder contains the singularity of the entanglement black-hole whose lateral area contributes to the entropy of the effect, while such cylinder is its event horizon.

Now, if we divide both sides of the inequation (130) by 4 and multiply it by the Boltzmann's constant $k_B \approx 1.38064852(79) \times 10^{-23} J/K$, we will have the entropy of the entanglement black-hole,

$$S_{BH} = \frac{k_B A}{4 l_p^2} \geq \frac{k_B}{16}. \quad (131)$$

The central term of Eq.(131) represents the Bekenstein–Hawking [14, 38] formula for the entropy of a black hole. The subscript BH indiscriminately refers to "black hole" or "Bekenstein–Hawking". Now, if $l_p = \sqrt{\frac{G_N \hbar}{C^3}}$, where, G_N is Newton's gravitational constant, and if we replace them into Eq.(131), we will have,

$$S_{BH} = \frac{k_B A}{4 \left(\frac{G_N \hbar}{C^3}\right)} = \left(\frac{k_B C}{\hbar}\right) \left(\frac{A C^2}{4 G_N}\right) \geq \frac{k_B}{16}. \quad (132)$$

On the other hand, the Hawking temperature [155] for a black-hole is

$$T_H = \frac{h \kappa}{2\pi k_B C} = \frac{\kappa}{2\pi \left(\frac{k_B C}{h} \right)}, \quad (133)$$

where κ is the acceleration due to gravity at the horizon of the black-hole. Then,

$$\left(\frac{k_B C}{h} \right) = \frac{\kappa}{2\pi T_H}. \quad (134)$$

Now, replacing Eq.(134) into (132), we will have,

$$S_{BH} = \left(\frac{\kappa}{2\pi T_H} \right) \left(\frac{AC^2}{4G_N} \right) \geq \frac{k_B}{16}, \quad (135)$$

then,

$$T_H \leq \frac{2\kappa AC^2}{\pi k_B G_N}. \quad \blacksquare \quad (136)$$

It is evident that the north arch of a bipartite quantum entanglement behaves like a black hole because of the strict values that its temperature $\left(T_H = \frac{2\kappa AC^2}{\pi k_B G_N} \right)$ and its entropy $\left(S_{BH} = \frac{k_B}{16} \right)$ reach. It is a very particular black hole, but definitively, a black hole. However, a question immediately arises: What happens with the southern arch? Obviously, it is another black hole, but, how does it interact with the northern arch? They are mutually alter-egos of one another, and since both of them are in full contact (more precisely, one over the other) then, if the positive mass radiates, the other one will receive that radiation until both masses are annulled. If it does not happen instantly because the masses of the alter-egos are equal (finite or not) and of opposite sign, then, both black holes end up being massless black holes. The question that remains is whether in this case, the extinction of the radiation eliminates the entanglement, or if it is simply a scenario similar to the original case of massless black holes.

4.4 Deduction of parallel operator via a Hamiltonian analysis

We know from the literature [157] that the Hamiltonian of the entanglement has a form like the following

$$H = H^A \otimes I^B + I^A \otimes H^B. \quad (137)$$

But we also know [1] that a more consistent and complete model for entanglement is the following:

$$H^{AB} = H^A \otimes I^B + I^A \otimes H^B + H_{\text{int}}^{AB}, \quad (138)$$

where the interaction between both subsystems S^A and S^B is described by the Hamiltonian $H_{\text{int}}^{AB} \neq 0$ so that each individual subsystem is an *open* quantum system. The Hamiltonian as a whole, and under these circumstances, takes the form of Eq.(138). However, and considering two fundamental aspects:

- a greater approximation between the treatment based on entropy as well as that based on the Hamiltonian, and
- the possibility of working with a Hamiltonian model notably more simplified and at the same time closer to entanglement from the physical point of view, which is used with remarkable success [158], then, we understand that the best option is to use the following Hamiltonian,

$$H^{A \cup B} = H^A + H^B - H^{A \cap B} = H^A + H^B - \frac{1}{H''} H^A H^B \quad (139)$$

where,

$$H^A = \mu_{|00\rangle} \hbar \omega \sigma_z \quad (140a)$$

$$H^B = \mu_{|11\rangle} \hbar \omega \sigma_z \quad (140b)$$

$$H'' = \mu_{|\hat{n}\hat{n}\rangle} \hbar \omega \sigma_z \quad (140c)$$

$$H^{A \cup B} = (\mu_{|00\rangle} + \mu_{|11\rangle}) \hbar \omega \sigma_z = 0 \quad (140d)$$

Therefore, replacing Eq.(140) into (139) so that a pair of matrices σ_z cancel each other before being replaced in $H^{A \cup B}$, we will have,

$$0 = \mu_{|00\rangle} \hbar \omega \sigma_z + \mu_{|11\rangle} \hbar \omega \sigma_z - \frac{1}{\mu_{|\hat{n}\hat{n}\rangle} \hbar \omega} \mu_{|00\rangle} \hbar \omega \mu_{|11\rangle} \hbar \omega \sigma_z. \quad (141)$$

Thus,

$$\mu_{|\hat{n}\hat{n}\rangle} = \frac{\mu_{|00\rangle} \mu_{|11\rangle}}{\mu_{|00\rangle} + \mu_{|11\rangle}} = \frac{\mu_{|0\rangle}^2 (-\mu_{|1\rangle}^2)}{\mu_{|0\rangle}^2 - \mu_{|1\rangle}^2} = \frac{\mu_{|0\rangle}^2 \mu_{|1\rangle}^2}{\mu_{|1\rangle}^2 - \mu_{|0\rangle}^2} = \mu_{|\hat{n}\hat{n}\rangle}^2, \quad (142)$$

which coincides completely with Eq.(43). In fact, there are two more methods that converge to the same result and that have been omitted in this paper due to space issues and because they are considered unnecessary. Such coincidences clearly indicate the consistency in the genesis of alter-egos. Finally, we will see additional deductions of this operator based on others entropies in Appendix A.5.

4.5 Analysis of the positions of equivalent spins

In the case of two hypothetical and completely independent spins, we will use Eq.(23) for the calculation of the equivalent spin μ_C , and Eq.(45) for its position d_C

$$\mu_C = \frac{\mu_A \mu_B}{\mu_A + \mu_B} = \frac{12 \times 4}{12 + 4} = 3, \quad \text{and} \quad d_C = d_A + \frac{\mu_A d_{BA}}{\mu_A + \mu_B} = 5 \text{ cm} + \frac{12 \times (15 \text{ cm} - 5 \text{ cm})}{12 + 4} = 12.5 \text{ cm},$$

where $\mu_A = 12$, $\mu_B = 4$, $d_A = 5 \text{ cm}$, and $d_B = 15 \text{ cm}$. Besides, and although Fig.21 is not in scale, the proportions are preserved. In that figure, we can see that $d_{BA} = d_B - d_A$.

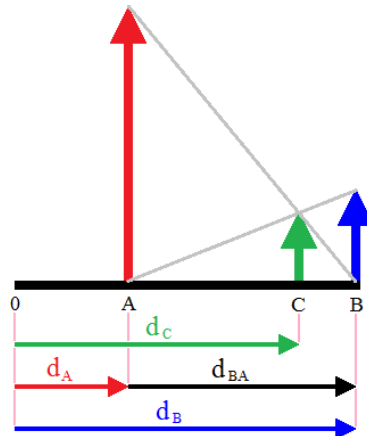


Fig.21 Sketch for the case of two hypothetical and completely independent spins.

We will apply the same equations of the previous figure to the case of two hypothetical quasi-entangled spins.

$$\mu_C = \frac{\mu_A \mu_B}{\mu_A + \mu_B} = \frac{-4 \times 8}{-4 + 8} = -8, \quad \text{and} \quad d_C = d_A + \frac{\mu_A d_{BA}}{\mu_A + \mu_B} = -4 \text{ cm} + \frac{-4 \times (8 \text{ cm} - (-4 \text{ cm}))}{-4 + 8} = -16 \text{ cm},$$

where $\mu_A = -4$, $\mu_B = 8$, $d_A = -4 \text{ cm}$, and $d_B = 8 \text{ cm}$. On the other hand, Fig.22 is not in scale, although, the proportions are preserved. However, it is the entangled case by far the most interesting one. Because of this we resort to Eq.(45) and (46). Making the convenient replacements in them, we will obtain the following:

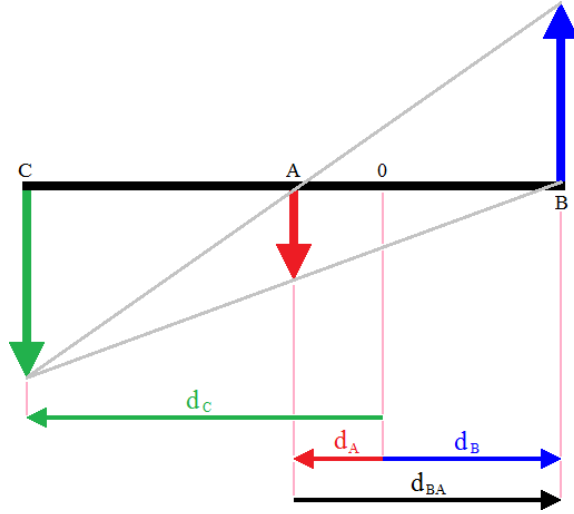


Fig.22 Sketch for the case of two hypothetical quasi-entangled spins.

$$\begin{aligned} d_{|\hat{n}\hat{n}\rangle} &= d_{|00\rangle} + \frac{\mu_{|00\rangle} (d_{|11\rangle} - d_{|00\rangle})}{\mu_{|00\rangle} + \mu_{|11\rangle}} = d_{|00\rangle} + \frac{\mu_{|00\rangle} (d_{|11\rangle} - d_{|00\rangle}) \mu_{|11\rangle}}{\mu_{|00\rangle} + \mu_{|11\rangle}}, \\ &= d_{|00\rangle} - \frac{\mu_{|\hat{n}\hat{n}\rangle} (d_{|11\rangle} - d_{|00\rangle})}{\mu_{|11\rangle}} = d_{|00\rangle} + \frac{\mu_{|11\rangle} \gamma^2 (d_{|11\rangle} - d_{|00\rangle})}{\mu_{|11\rangle}} = d_{|00\rangle} + \gamma^2 (d_{|11\rangle} - d_{|00\rangle}) = +\infty \end{aligned} \quad (143)$$

while,

$$\begin{aligned} d_{|u\bar{u}\rangle} &= d_{|11\rangle} + \frac{\mu_{|11\rangle} (d_{|00\rangle} - d_{|11\rangle})}{\mu_{|00\rangle} + \mu_{|11\rangle}} = d_{|11\rangle} + \frac{\mu_{|11\rangle} (d_{|00\rangle} - d_{|11\rangle}) \mu_{|00\rangle}}{\mu_{|00\rangle} + \mu_{|11\rangle}}, \\ &= d_{|11\rangle} - \frac{\mu_{|u\bar{u}\rangle} (d_{|00\rangle} - d_{|11\rangle})}{\mu_{|00\rangle}} = d_{|11\rangle} + \frac{\mu_{|00\rangle} \gamma^2 (d_{|00\rangle} - d_{|11\rangle})}{\mu_{|00\rangle}} = d_{|11\rangle} + \gamma^2 (d_{|00\rangle} - d_{|11\rangle}) = -\infty \end{aligned} \quad (144)$$

We can clearly see that Equations (143) and (144) are identical to Equations (49) and (50).

4.6 Final comments

As we have seen so far, the entanglement bandwidth is $BW = \infty$ (i.e., it is unlimited) and the length of the quantum link based on entanglement is null. A direct consequence of this is that the system interchanges information in a robust way, i.e., the link is immune to noise and could not be attacked,

that is be intercepted by an indiscreet third part. Besides, we must remember that a bipartite entanglement is a monogamous process [1-3]. However, what is the capacity of a quantum channel based on quantum entanglement? If we resort to a classical approach to the problem, e.g., the Shannon's Channel Capacity Theorem, then, we will have that the Shannon-Hartley Theorem [156] states that,

$$C = BW \log_2 \left(1 + \frac{S}{N} \right) \text{ [bits/sec]} \quad (145)$$

with these elements: C is the channel capacity, BW is the bandwidth in Hertz, S is the signal power and N is the noise power, $N_0 BW$ with $N_0/2$ is the two-sided noise Probability Density Function (PSD), and S/N is the ratio in watt/watt, not decibels. Then, C rises according to the increase of the available BW and the increase/improvement in S/N . Besides, Eq.(145) seems to tell us that as the BW increases, capacity C should increase proportionally. But this does not happen due to an increase in the bandwidth BW , because it also increases the noise power $N = N_0 BW$ giving:

$$\begin{aligned} C &= BW \log_2 \left(1 + \frac{S}{N} \right) = BW \log_2 \left(1 + \frac{S}{N_0 BW} \right) \\ &= \frac{S}{N_0} \frac{N_0 BW}{S} \log_2 \left(1 + \frac{S}{N_0 BW} \right) = \frac{S}{N_0} \log_2 \left(1 + \frac{S}{N_0 BW} \right)^{\frac{N_0 BW}{S}} \end{aligned} \quad (146)$$

Now, if $BW \rightarrow \infty$ then $\left(\frac{S}{N_0 BW} \right) \rightarrow 0$. On the other hand, the expression $\lim_{x \rightarrow 0} (1+x)^{1/x} = e$. This means that as $BW \rightarrow \infty$, $\left(\frac{S}{N_0 BW} \right) \rightarrow 0$, and $\left(1 + \frac{S}{N_0 BW} \right)^{\frac{N_0 BW}{S}} \rightarrow e$. Therefore, the channel capacity goes to:

$$\lim_{BW \rightarrow \infty} C = \lim_{BW \rightarrow \infty} \frac{S}{N_0} \log_2 \left(1 + \frac{S}{N_0 BW} \right)^{\frac{N_0 BW}{S}} = \frac{S}{N_0} \log_2 e = 1.44 \frac{S}{N_0} \quad (147)$$

If we do not have the channel, then, we do not have channel noise, therefore, when $BW \rightarrow \infty$ and $N_0 \rightarrow 0$, the channel capacity is also infinite. This is the last attribute of entanglement which is still to be explored in a context of absolute interest for quantum communications.

On the other hand, we rescue a particular equation, which constitutes a bridge between the Theory of Relativity and the Quantum Theory, and which constitutes a fundamental tool of the Theory of Everything,

$$\mu_{|\uparrow\uparrow\rangle} = \mu_{|00\rangle} \gamma^2, \quad \mu_{|\uparrow\downarrow\rangle} = \mu_{|01\rangle} \gamma^2, \quad \mu_{|\downarrow\uparrow\rangle} = \mu_{|10\rangle} \gamma^2, \quad \mu_{|\downarrow\downarrow\rangle} = \mu_{|11\rangle} \gamma^2. \quad (148)$$

In fact, we can consider a simplification like this,

$$\mu_{|XY\rangle} = \mu_{|xy\rangle} \gamma^2, \quad (149)$$

where, X and Y are the first and the second subscripts of the alter-egos, respectively, which can be \uparrow or \downarrow , while, x and y are the first and the second subscripts of the original spins, respectively, which can be 0 or 1. In this way, we arrive at a unified effect equation, which represents a super arching of space-time since γ^2 .

Finally, there is a large territory for the exploration of different questions and possibilities, namely:

- If we considered the case of alter-egos with masses different from zero and with opposite sign, and supposing that the masses did not cancel each other, a question arises: would the alter-egos repel each other? In Eq.(140) we can see that the sign of the energy is conditioned by the sign of the corresponding spin. Therefore, if one of the components of Eq.(140) has negative energy, we can suppose that this will have negative mass, given that $E = mc^2$.
- Could we consider an alter-ego constituted of matter and another one by anti-matter in the previous case? Would they annihilate each other?
- Could we picture a scenario where one black hole attracts and the other one repels?
- What is the relationship of the previous points with dark matter?
- Could a massless black hole with an infinite spin radiate foreign matter borrowed from its environment?
- Could a massless spin, especially if that spin is infinite, bend space-time?
- What is the relationship between alter-egos and an eventual black-hole/white-hole pair?
- Is the entanglement of a spin with itself possible? That is to say, is the self-entanglement a real possibility? See Fig.23.

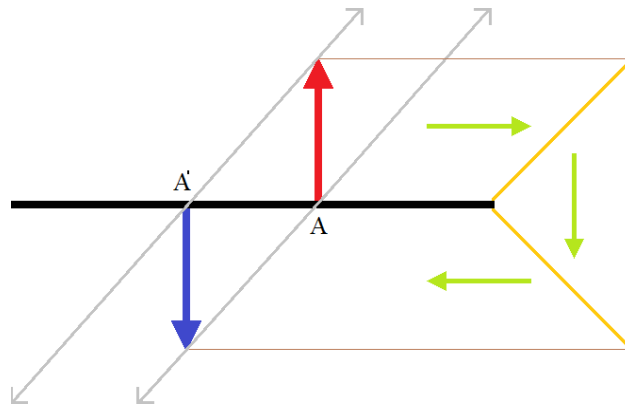


Fig.23 Symbolic sketch for a self-entanglement.

- Can we think in a Physics where the spin has more prominence than the mass when curving space-time?
- The entanglement is presented as a link system that does not allow a blocking of its effect by a third party, which is understandable given that it is impossible to block a channel that does not exist, then: Can we think of a communication system based on entanglement without antenna or transmission power? What is more, from the point of view of quantum communications: Can we think of Teleportation protocols that do not need to be disambiguated thanks to a classical channel?
- In [11] we can see entanglement between photons that have never coexisted temporarily, but, can two spins that have never coexisted spatially be entangled?
- From the General Theory of Relativity we know that it is not possible to use quantum entanglement to extract information from inside a black hole, but, in light of what it has been seen in this paper: what new conclusion can we draw from it?

These are just some of the questions that remain to be answered in the future. On the other hand, the following questions will be answered in Appendices below:

- What is the projection of this work in N -partite entanglement? See Appendix A.1.
- What is the incidence of decoherence in the analysis seen in this paper? See Appendix A.2.
- Is any type of entanglement between signals possible? See Appendix A.3.
- What is the N -dimensional analysis of entanglement according to this theory? See Appendix A.4.
- Is it possible to deduce the parallel operator for other entropies? See Appendix A.5.
- Is it possible to recover entanglement after its destruction by a quantum measurement? See Appendix A.6.

- Is it possible to deduce new protocols for Teleportation and Superdense Coding with a greater emphasis on the distinguishability of entangled particles based on the new theory?

In a future work, some concepts in the context of a practical quantum communication will have to be explored formally:

- If we need to distribute an EPR pair between Alice and Bob: what is the most convenient method to do it?
 - a) Take-out: using an adiabatic container, bottle or holder,
 - b) Sophisticated Delivery: using a laser cannon, or telescope
 - c) Simple Delivery: using a standard optical fiber (even in non-ideal conditions) as suggested in the simulations in [160].
- In light of this work: can we think of the following means of transmitting information?
 - a) Classical Channel: Internet, telephone, radiocommunication, etc.
 - b) Quantum Channel: optical fiber
 - c) Entanglement Link: this is a means, not a channel, in fact and as we could see in this work, thanks to the Theory of Dilated Locality there is no channel since the channel disappears at the expense of the locality. Therefore, useful information can be transmitted.
- In this paper the entanglement between atoms (matter) and photons (light) is pending.
- Throughout this work, we have assumed the absence of noise, i.e., we have considered a pure entanglement. An exhaustive analysis under noisy conditions remains pending.
- The symbolic logic has been simplified to the detriment of rigor in order to reach as many readers as possible, stripping the paper of all mathematical formalism in order to put the Physics of the problem above of such symbolic logic. To this end, the minimum symbolic and formal expressions necessary in order to respect the central idea of this work have been used.

Finally, this work highlighted fundamental concepts such as entanglement and spin which are the main actors in the Theory of Everything. Besides, the experiment where the thermodynamic arrow of time is reverses using quantum correlations in relation to a heat exchange [159] exposes the fact that there are negative and positive energies involved with a high degree of polarization on their parts. This concept is a key element involved in the very existence of the alter-egos which are the main essence of the present work, and hence, the experiment carried out in [159] supports all the predictions of the new theory presented in here.

Appendices: Theory of Dilated Locality contemplates all things related to entanglement

A.1 Multi-entanglement or N -partite analysis

In this appendix, six cases of entanglement will be analyzed according to the new perspective introduced by the Theory of Dilated Locality: 2-partite, 3-partite [1, 3] and 4-partite [3, 161] for GHZ and W states configurations. For this reason, we will introduce a couple of new tools:

- a polynomial of spins,
- and their corresponding complex root locus according to the canonicity of the state configuration: GHZ or W.

The complex adjective has a double meaning:

- a) the root locus has a Hermitian nature, but besides
- b) it has to do with the complexity of such root locus which depends on the order of the polynomial (whose roots are the spins) and the type of state configuration: GHZ or W.

2-partite GHZ states configuration: Fig.A.1.1a shows us this case. In fact, this is the case analyzed so far and on which all deductions were made. From Eq.(5) we have,

$$|\Phi_+^{A \cup B}\rangle = \frac{1}{\sqrt{2}}(|0^A, 0^B\rangle + |1^A, 1^B\rangle),$$

with the following polynomial of spins, where such spins are its roots,

$$P_2(\mu) = a_2 \mu^2 + a_1 \mu + a_0 = 0 \quad (\text{A.1.1})$$

where,

$$\begin{aligned} a_2 &= 1 \\ a_1 &= -(\mu_1 + \mu_2) = 0 = \mu_0 \quad (\text{this is the case of the meson}) \\ a_0 &= \mu_1 \mu_2 \end{aligned} \quad (\text{A.1.2})$$

We will use $\mu_1 = \mu_{|00\rangle}$ and $\mu_2 = \mu_{|11\rangle}$ (or $\mu_1 = \mu_{|0\rangle}$ and $\mu_2 = \mu_{|1\rangle}$, which in the case of photons are absolutely equivalent) for simplicity. In Fig.A.1.1a, we can see a black ring with μ_1 (on point A) and μ_2 (on point B) at 180 degrees from one another. Now, if we remember the Eq.(43), we will have,

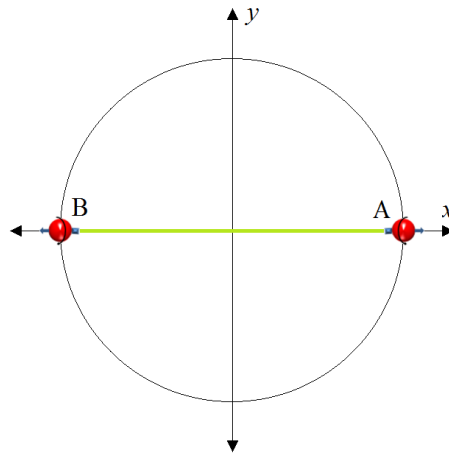


Figure A.1.1a. 2-partite GHZ states configuration.

$$\mu_{|\uparrow\uparrow\rangle} = \frac{\mu_1(-\mu_2)}{\mu_1 + \mu_2} = \frac{\mu_1 \mu_2}{-(\mu_1 + \mu_2)} = \frac{a_0}{a_1} = \pm\infty \quad (\text{A.1.3})$$

Besides, and how we have said, the denominator of Eq.(A.1.3) is the principle of spin conservation. If we make a rename,

$$\mu_{|\Rightarrow\rangle} = \mu_1 + \mu_2 = -a_1 = 0 = \mu_0 \quad (\text{A.1.4})$$

Then, the polynomial of the spins will be,

$$P_2(\mu) = \mu^2 + a_0 = 0 \quad (\text{A.1.5})$$

with roots,

$$\mu_{1,2} = \sqrt[2]{|a_0|} e^{i2\pi k/2} = \sqrt[2]{|a_0|} e^{i\pi k}, \quad \text{with } k \in [0,1] \quad (\text{A.1.6})$$

3-partite GHZ states configuration: Fig.A.1.1b shows us this case. In these circumstances, everything increases in one degree with respect to the previous case, that is,

$$|\Phi_+^{A \cup B \cup C}\rangle = \frac{1}{\sqrt{2}}(|0^A, 0^B, 0^C\rangle + |1^A, 1^B, 1^C\rangle),$$

with the following polynomial of spins,

$$P_3(\mu) = a_3 \mu^3 + a_2 \mu^2 + a_1 \mu + a_0 = 0 \quad (\text{A.1.7})$$

where,

$$\begin{aligned} a_3 &= 1 \\ a_2 &= -(\mu_1 + \mu_2 + \mu_3) = 0 \\ a_1 &= \mu_1 \mu_2 + \mu_1 \mu_3 + \mu_2 \mu_3 = 0 \\ a_0 &= -\mu_1 \mu_2 \mu_3 \end{aligned} \quad (\text{A.1.8})$$

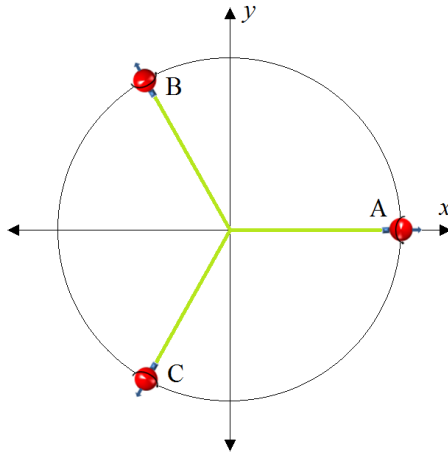


Figure A.1.1b. 3-partite GHZ states configuration.

In Fig.A.1.1b, we can see a black ring with μ_1 (on point A), μ_2 (on point B), and μ_3 (on point C) at 120 degrees from the next. Then, for this case, we will have,

$$\mu_{|\uparrow\uparrow\uparrow\rangle} = \sqrt[2]{\frac{\mu_1 \mu_2 \mu_3}{\mu_1 + \mu_2 + \mu_3}} = \sqrt[2]{\frac{a_0}{a_2}} = \pm\infty \quad (\text{A.1.9})$$

The degree of the root (i.e., 2) is equivalent to the jump between the degree of the numerator (i.e., 3) and the denominator (i.e., 1) under this root. Therefore, $\mu_{|\uparrow\uparrow\uparrow\rangle}$ has a degree equal to 1, in fact, this is what should always happen with $\mu_{|\uparrow\uparrow\uparrow\rangle}$. Besides, the denominator of Eq.(A.1.9) is the principle of spin conservation:

$$\mu_{|\Rightarrow\Rightarrow\Rightarrow\rangle} = \mu_1 + \mu_2 + \mu_3 = -a_2 = 0 = \mu_0 \quad (\text{A.1.10})$$

Then, the polynomial of the spins will be,

$$P_3(\mu) = \mu^3 + a_0 = 0 \quad (\text{A.1.11})$$

with roots,

$$\mu_{1,2,3} = \sqrt[3]{a_0} e^{i2\pi k/3}, \quad \text{with } k \in [0,1,2] \quad (\text{A.1.12})$$

4-partite GHZ states configuration: Fig.A.1.1c shows this last case. Here too, everything increases in one degree with respect to the previous cases, that is,

$$|\Phi_+^{A \cup B \cup C \cup D}\rangle = \frac{1}{\sqrt{2}} (|0^A, 0^B, 0^C, 0^D\rangle + |1^A, 1^B, 1^C, 1^D\rangle),$$

with the following polynomial of spins,

$$P_4(\mu) = a_4 \mu^4 + a_3 \mu^3 + a_2 \mu^2 + a_1 \mu + a_0 = 0 \quad (\text{A.1.13})$$

where,

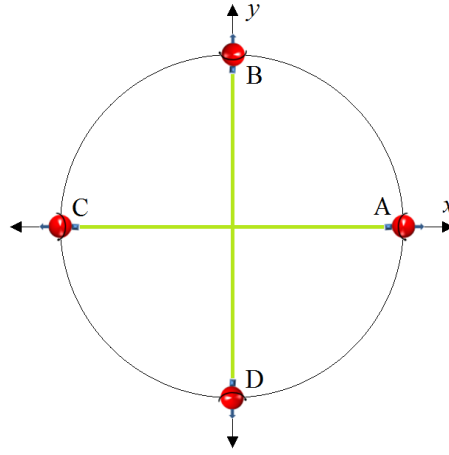


Figure A.1.1c. 4-partite GHZ states configuration.

$$\begin{aligned} a_4 &= 1 \\ a_3 &= -(\mu_1 + \mu_2 + \mu_3 + \mu_4) = 0 = \mu_0 \\ a_2 &= \mu_1 \mu_2 + \mu_1 \mu_3 + \mu_1 \mu_4 + \mu_2 \mu_3 + \mu_2 \mu_4 + \mu_3 \mu_4 = 0 \\ a_1 &= -(\mu_1 \mu_2 \mu_3 + \mu_1 \mu_2 \mu_4 + \mu_1 \mu_3 \mu_4 + \mu_2 \mu_3 \mu_4) = 0 \\ a_0 &= \mu_1 \mu_2 \mu_3 \mu_4 \end{aligned} \quad (\text{A.1.14})$$

In Fig.A.1.1c, we can see a black ring with μ_1 (on point A), μ_2 (on point B), μ_3 (on point C), and μ_4 (on point D), at 90 degrees from the next. Then, for this case, we will have,

$$\mu_{|\uparrow\uparrow\uparrow\rangle} = \sqrt[3]{\frac{\mu_1 \mu_2 \mu_3 \mu_4}{-(\mu_1 + \mu_2 + \mu_3 + \mu_4)}} = \sqrt[3]{\frac{a_0}{a_3}} = \pm\infty \quad (\text{A.1.15})$$

The degree of the root (i.e., 3) is equivalent to the jump between the degree of the numerator (i.e., 4) and the denominator (i.e., 1) under this root. Therefore, here again, $\mu_{|\uparrow\uparrow\uparrow\rangle}$ has a degree equal to 1. Besides, the denominator of Eq.(A.1.15) is the principle of spin conservation:

$$\mu_{|\Rightarrow\rangle} = \mu_1 + \mu_2 + \mu_3 + \mu_4 = -a_3 = 0 = \mu_0 \quad (\text{A.1.16})$$

Then, the polynomial of the spins were,

$$P_4(\mu) = \mu^4 + a_0 = 0 \quad (\text{A.1.17})$$

with roots,

$$\mu_{1,2,3,4} = \sqrt[4]{|a_0|} e^{i2\pi k/4} = \sqrt[4]{|a_0|} e^{i\pi k/2}, \quad \text{with } k \in [0,1,2,3] \quad (\text{A.1.18})$$

Summing-up for the N-partite GHZ states configuration: We will have,

$$P_N(\mu) = \sum_{n=0}^N a_n \mu^n = 0, \quad \forall a_n \in \mathbb{R}. \quad (\text{A.1.19})$$

$$\mu_{|\hat{n}\hat{n}\rangle} = N^{-1} \frac{\sqrt{\prod_{n=1}^N \mu_n}}{(-1)^{N-1} \sum_{n=1}^N \mu_n} = N^{-1} \sqrt{\frac{a_0}{a_{N-1}}} = \pm\infty \quad (\text{A.1.20})$$

$$\mu_{|\Rightarrow\rangle} = \sum_{n=1}^N \mu_n = -a_{N-1} = 0 = \mu_0 \quad (\text{A.1.21})$$

2-partite W states configuration: Fig.A.1.2a showcases this configuration. From Eq.(5) we have,

$$|\Psi_+^{A \cup B}\rangle = \frac{1}{\sqrt{2}} (|0^A, 1^B\rangle + |1^A, 0^B\rangle),$$

with,

$$\mu_{|\Rightarrow\rangle} = \mu_1 + \mu_2 = -a_1 = 0 = \mu_0, \quad (\text{this is the case of the meson}) \quad (\text{A.1.22})$$

and,

$$\mu_{|\hat{n}\hat{n}\rangle} = \frac{\mu_1(-\mu_2)}{\mu_1 + \mu_2} = \frac{\mu_1 \mu_2}{-(\mu_1 + \mu_2)} = \frac{a_0}{a_1} = \pm\infty. \quad (\text{A.1.23})$$

That is to say, for the 2-partite case, both models agree on the values of their spins $\mu_{|\Rightarrow\rangle}$ and $\mu_{|\hat{n}\hat{n}\rangle}$. For this case, we obtain the values of coefficients a_1 and a_0 from Eq.(A.1.2).

On the other hand, Fig.A.1.2a shows us a black ring with μ_1 (on point A) and μ_2 (on point B) at 180 degrees from one another. Besides, and clearly, Fig.A.1.2a allows to see a pink ring which represents the signal beam (i.e., vertical polarization), and a light blue ring which represents the idler beam (i.e., horizontal polarization). The two entangled particles correspond to the intersection points of the rings.

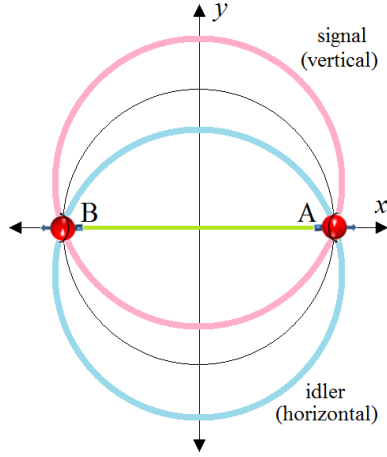


Figure A.1.2a. 2-partite W states configuration.

3-partite W states configuration: Fig.A.1.2b shows us this case. In these circumstances, everything increases in one degree with respect to the previous case, that is,

$$|\Psi_{+}^{A \cup B \cup C}\rangle = \frac{1}{\sqrt{3}} (|1^A, 0^B, 0^C\rangle + |0^A, 1^B, 0^C\rangle + |0^A, 0^B, 1^C\rangle),$$

with,

$$\mu_{|\Rightarrow\rangle} = \mu_1 \mu_2 + \mu_1 \mu_3 + \mu_2 \mu_3 = a_1 = 0, \quad (\text{A.1.24})$$

and

$$\mu_{|\uparrow\uparrow\rangle} = \frac{-\mu_1 \mu_2 \mu_3}{\mu_1 \mu_2 + \mu_1 \mu_3 + \mu_2 \mu_3} = \frac{a_0}{a_1} = \pm\infty. \quad (\text{A.1.25})$$

For this case, we obtain the values of the polynomial coefficients a_1 and a_0 from Eq.(A.1.8). On the other hand, Fig.A.1.2b displays this particular configuration.

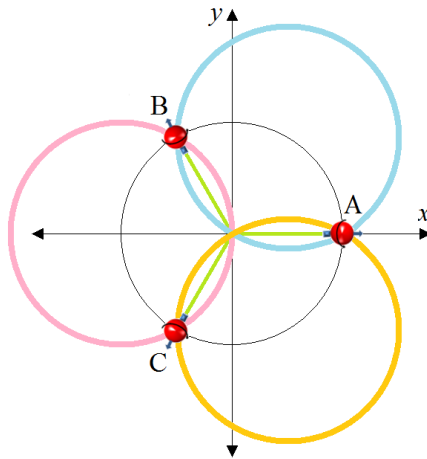


Figure A.1.2b. 3-partite W states configuration.

4-partite W states configuration: Fig.A.1.2c shows us this case. Here too, everything increases in one degree with respect to the previous case, that is,

$$|\Psi_{+}^{A \cup B \cup C \cup D}\rangle = \frac{1}{\sqrt{4}} (|1^A, 0^B, 0^C, 0^D\rangle + |0^A, 1^B, 0^C, 0^D\rangle + |0^A, 0^B, 1^C, 0^D\rangle + |0^A, 0^B, 0^C, 1^D\rangle),$$

with,

$$\mu_{|\Rightarrow\rangle} = \mu_1 \mu_2 \mu_3 + \mu_1 \mu_2 \mu_4 + \mu_1 \mu_3 \mu_4 + \mu_2 \mu_3 \mu_4 = -a_1 = 0, \quad (\text{A.1.26})$$

and

$$\mu_{|\hat{\uparrow}\hat{\uparrow}\rangle} = \frac{\mu_1 \mu_2 \mu_3 \mu_4}{-(\mu_1 \mu_2 \mu_3 + \mu_1 \mu_2 \mu_4 + \mu_1 \mu_3 \mu_4 + \mu_2 \mu_3 \mu_4)} = \frac{a_0}{a_1} = \pm\infty. \quad (\text{A.1.27})$$

For this case, we obtain the values of the polynomial coefficients a_1 and a_0 from Eq.(A.1.14). On the other hand, Fig.A.1.2c represents this particular configuration. It is too easy to extrapolate this case to another one of higher degrees.

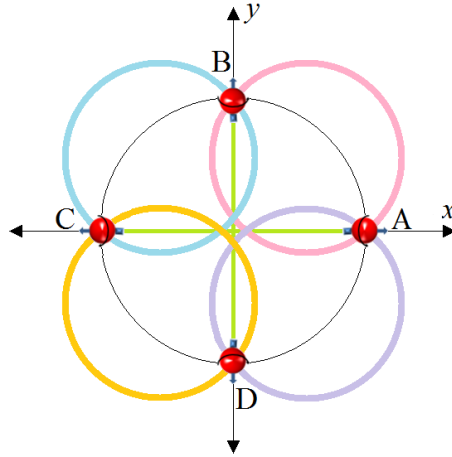


Figure A.1.2c. 4-partite W states configuration.

Summing-up for the W states configuration: In a generic manner and for this configuration we must remember the polynomial of the spins from Eq.(A.1.19), then,

$$\mu_{|\Rightarrow\rangle} = (-1)^{N-1} a_1 = 0, \quad (\text{A.1.28})$$

and

$$\mu_{|\hat{\uparrow}\hat{\uparrow}\rangle} = \frac{a_0}{a_1} = \pm\infty. \quad (\text{A.1.29})$$

Next, we will visualize the jumps of the GHZ states configuration from a purely graphic point of view for the cases: 2-partite, 3-partite, 4-partite and 5-partite. See Fig.A.1.3.

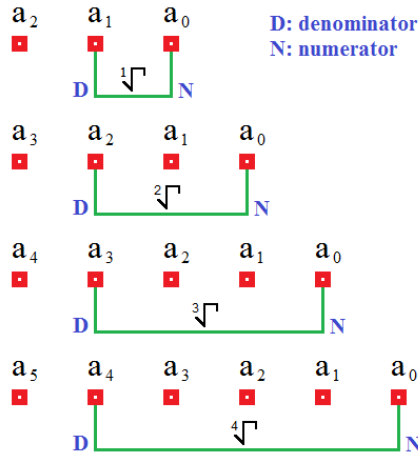


Figure A.1.3. Jumps for the configuration of GHZ states depending on the degree of the spins' polynomial.

As we can see in Fig.A.1.3, the jumps are equivalent to the difference of degree between a_{N-1} and a_0 , that is to say, $N-1$. Besides, $N-1$ is the difference between the subscript of a_{N-1} and a_0 , and at the same time, it is the degree of the radical that represents the corresponding jump. In Eq.(A.1.20) we can see this radical for the generic case, i.e., for N entangled spins of the GHZ configuration. We must remember that for this case all coefficients from a_{N-1} to a_1 are 0, where a_{N-1} represents the principle of spin conservation for this configuration, i.e., $\mu_{|\Rightarrow\rangle}$.

In Fig.A.1.4 instead, we can see the jumps for the W states configuration depending on the degree of the spins' polynomial. In this case, the jumps are the difference of degree between a_1 and a_0 , that is to say, always equal to 1. Besides, this configuration results from the intersection of different rings which represents several polarizations. In this regard, the simplest case is represented by the type 2-partite where one ring corresponds to the horizontal polarization while the other corresponds to the vertical polarization.

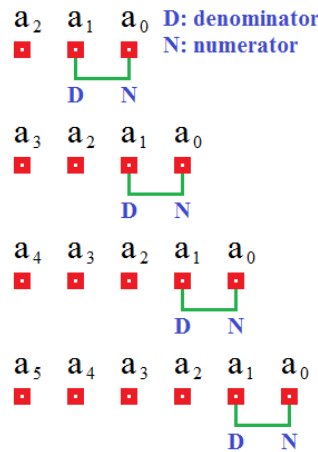


Figure A.1.4. Jumps for the W states configuration depending on the degree of the spins' polynomial.

A.2 Analysis of decoherence according to the Theory of Dilated Locality

The W states configuration (including the parallel operator) has its counterpart in electrical circuits, in particular, the so-called reactive circuits where they are composed, at first, by inductors (L) and capacitors (C). This will lead to the so-called entanglement circuits. This should not be surprising since Physics is frequently based in models. In fact, the parallel operator is repeated in several cases

inside Physics, e.g., we must remember Eq.(52) of Subsection 2.6 for the De Broglie wavelength as the centre-of-mass frame of a nuclei with two masses in the context of an energy treatment where $m_{eq} = m_1 // m_2$, see pp.136 of [62]. Another example in the use of this operator can be seen in Optics: if two lenses with focal length f_1 and f_2 placed next to each other are equivalent to a single lens with a focal length $f_{eq} = f_1 // f_2$, see pp.30 of [162]. Finally, the equivalent spin in W states configuration like Eq.(43) is also represented in RLC circuits [163].

On the other hand, in this appendix and with the same criterion of Appendix A.1, we are going to consider $X_L = \mu_{|00\rangle}$ and $X_C = \mu_{|11\rangle}$, or $X_L = \mu_{|0\rangle}$ and $X_C = \mu_{|1\rangle}$, which in the case of photons both pair of equalities are completely equivalent. In fact, if an inductive impedance is now associated with a spin up for a given frequency, we will have,

$$X_L = j\omega L = \mu_L, \quad (\text{A.2.1})$$

while the capacitive impedance will be,

$$X_C = \frac{-j}{\omega C} = \mu_C, \quad (\text{A.2.2})$$

then, the serial impedance will be the principle of spin conservation for entanglement, being this the left graphic of Fig.A.2.1,

$$Z_{|\Rightarrow\rangle} = X_L + X_C = j\omega L + \frac{-j}{\omega C} = j\left(\omega L - \frac{1}{\omega C}\right) = \mu_{|\Rightarrow\rangle} = \mu_L + \mu_C = 0, \quad (\text{A.2.3})$$

Now, for the resonance frequency, see Eq.(A.2.3), we will have,

$$\omega L = \frac{1}{\omega C}, \quad \omega^2 = \frac{1}{LC}, \quad \omega = \frac{1}{\sqrt{LC}}, \quad f = \frac{1}{2\pi\sqrt{LC}}. \quad (\text{A.2.4})$$

Besides, if we want to calculate the parallel impedance, this will be the super-spin for entanglement, being this the right graphic of Fig.A.2.1,

$$Z_{|\hat{m}\hat{m}\rangle} = \frac{X_L(-X_C)}{X_L + X_C} = \frac{j\omega L\left(-\left(-\frac{j}{\omega C}\right)\right)}{j\omega L + \left(-\frac{j}{\omega C}\right)} = \mu_{|\hat{m}\hat{m}\rangle} = \frac{\mu_L(-\mu_C)}{\mu_L + \mu_C} = \pm\infty, \quad (\text{A.2.5})$$

As we can see, Eq.(A.2.3) is similar to Eq.(A.1.22), whereas Eq.(A.2.5) is similar to Eq.(A.1.23). In Fig.A.2.1, we can see Eq.(A.2.3) on the left as a serial LC circuit which is the denominator of Eq.(A.2.5), while the complete version of Eq.(A.2.5) is on the right as a parallel LC circuit.

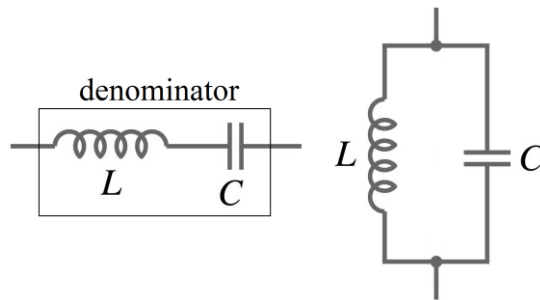


Figure A.2.1. On the left we have a serial LC circuit which is the denominator of Eq.(A.2.5), and on the right we have a parallel LC circuit.

This analogy resists even its application to the case of completely independent subsystems of Eq.(23), with

$$Z_{|\Rightarrow\rangle} = X_L + X_L = j\omega L + j\omega L = 2(j\omega L) = \mu_{|\Rightarrow\rangle} = \mu_L + \mu_L = 2\mu_L \neq 0, \quad (\text{A.2.6})$$

where Eq.(A.2.6) is the denominator of Eq.(A.2.7) and can be seen in the graphic on the left of Fig.A.2.2.

$$Z_{|\hat{m}\rangle} = \frac{j\omega L \ j\omega L}{j\omega L + j\omega L} = \frac{(j\omega L)^2}{2j\omega L} = \frac{j\omega L}{2} = \mu_{|\hat{m}\rangle} = \frac{\mu_L \mu_L}{\mu_L + \mu_L} = \frac{\mu_L}{2} \neq \infty. \quad (\text{A.2.7})$$

Equation (A.2.7) can be seen in the graphic on the right of Fig.A.2.2.

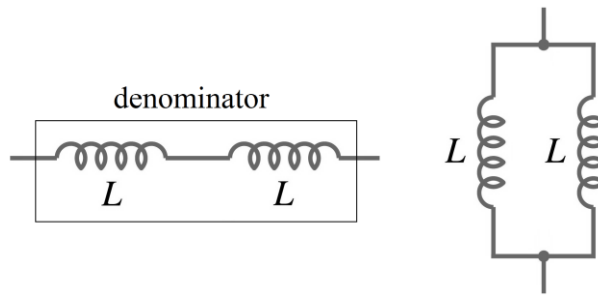


Figure A.2.2. An inductive version of completely independent subsystems.

The capacitive version of Fig.A.2.2 can be seen in Fig.A.2.3.

$$Z_{|\Rightarrow\rangle} = X_C + X_C = 2X_C = 2\left(\frac{-j}{\omega C}\right) = \mu_{|\Rightarrow\rangle} = \mu_C + \mu_C = 2\mu_C \neq 0, \quad (\text{A.2.8})$$

where Eq.(A.2.8) is the denominator of Eq.(A.2.9). Its graphic can be seen on the left of Fig.A.2.3.

$$Z_{|\hat{m}\rangle} = \frac{X_C \ X_C}{X_C + X_C} = \frac{(X_C)^2}{2X_C} = \frac{X_C}{2} = \frac{1}{2}\left(\frac{-j}{\omega C}\right) = \mu_{|\hat{m}\rangle} = \frac{\mu_C \mu_C}{\mu_C + \mu_C} = \frac{\mu_C}{2} \neq \infty. \quad (\text{A.2.9})$$

Equation (A.2.9) can be seen on the right of Fig.A.2.3.

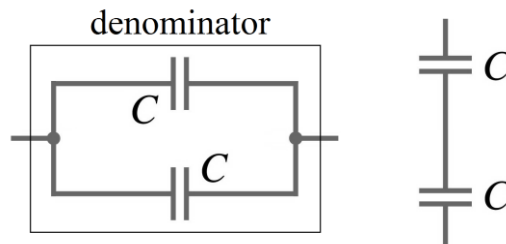


Figure A.2.3. A capacitive version of completely independent subsystems.

In Fig.11 we saw for the W states configuration that two completely independent particles can be entangled with another third particle. This example is showed in Fig.A.2.4 as an LC circuit. In this case, if the result of $X_L/X_L = X_L/2$ is equal and opposite to X_C , i.e., $X_L/2 + X_C = 0$, then, we will have entanglement. In other words, the last equation is the denominator of parallel operator and it is on the left of Fig.A.2.4.

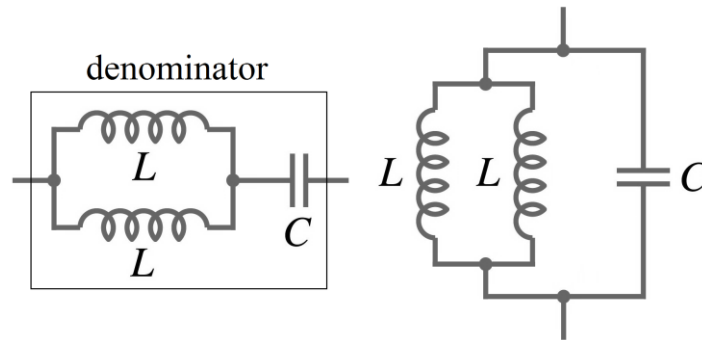


Figure A.2.4. Two completely independent particles are entangled with another third particle.

Including the most extreme cases, this analogy between spins and LC circuits fits the W states configuration, even under the effects of quantum measurement [164], however a question arises: what about the collapse of the wavefunction? It is a very interesting question, in fact, this analogy based on LC circuits for W states configuration resists the presence of decoherence. It is important to highlight that we can continue to use this analogy to represent the disturbed effect of entanglement intervened by the action of the environment since the scope is not adiabatic. The presence of decoherence is modelled via resistors in an RLC analogy in Fig.A.2.5, which represents both the degradation of the equivalent inductor and the capacitor simultaneously.

In other words, the presence of resistors degrades both the inductor and the capacitor leading us to present a theorem on decoherence based on the RLC analogy and its corresponding proof.

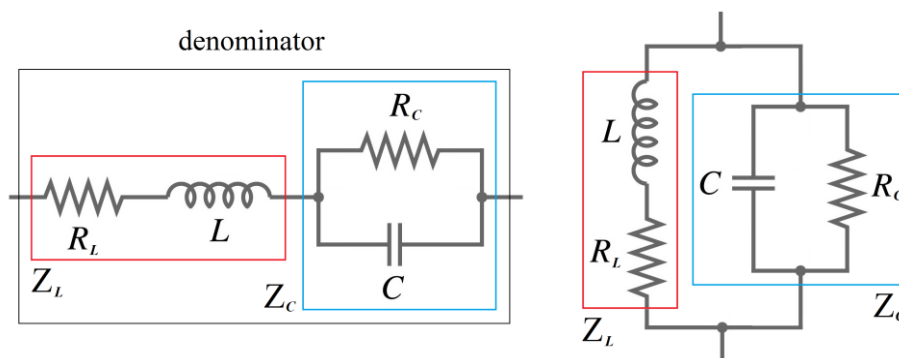


Figure A.2.5. Entanglement perturbed by decoherence represented with resistors.

Theorem: Decoherence converts two entangled spins into two new equivalent and completely independent spins.

Proof: First, we are going to simplify the RC tank circuit of Fig.A.2.5, which is framed in blue.

$$\begin{aligned}
Z_c &= \frac{R_c X_c}{R_c + X_c} = \frac{R_c \left(\frac{-j}{\omega C} \right)}{R_c - \frac{j}{\omega C}} = \frac{R_c \left(\frac{-j}{\omega C} \right) \left(R_c + \frac{j}{\omega C} \right)}{\left(R_c - \frac{j}{\omega C} \right) \left(R_c + \frac{j}{\omega C} \right)} = \frac{R_c^2 \left(\frac{-j}{\omega C} \right) + R_c \left(\frac{1}{\omega C} \right)^2}{R_c^2 + \left(\frac{1}{\omega C} \right)^2} \\
&= \frac{R_c \left(\frac{1}{\omega C} \right)^2 - j R_c^2 \omega C \left(\frac{1}{\omega C} \right)^2}{R_c^2 + \left(\frac{1}{\omega C} \right)^2} = \frac{R_c + (-j R_c^2 \omega C)}{1 + (\omega C R_c)^2} = \frac{R_c}{1 + (\omega C R_c)^2} + \frac{(-j R_c^2 \omega C)}{1 + (\omega C R_c)^2}, \quad (\text{A.2.10}) \\
&= R'_c + \left(\frac{-j}{\omega C'} \right)
\end{aligned}$$

where,

$$R'_c = \frac{R_c}{1 + (\omega C R_c)^2} \quad (\text{A.2.11})$$

and,

$$\frac{1}{\omega C'} = \frac{R_c^2 \omega C}{1 + (\omega C R_c)^2}, \quad \omega C' = \frac{1 + (\omega C R_c)^2}{R_c^2 \omega C}, \quad C' = \frac{1 + (\omega C R_c)^2}{R_c^2 \omega^2 C} \quad (\text{A.2.12})$$

Then, we will go from Fig.A.2.5 to Fig.A.2.6.

In consequence, the complete impedance of the graphic on the right of Fig.A.2.6 will be,

$$Z_{|\uparrow\uparrow)} = \frac{Z_L Z_C}{Z_L + Z_C} = \frac{(R_L + X_L)(R'_c + X'_c)}{(R_L + X_L) + (R'_c + X'_c)}, \quad (\text{A.2.13})$$

where its denominator will be,

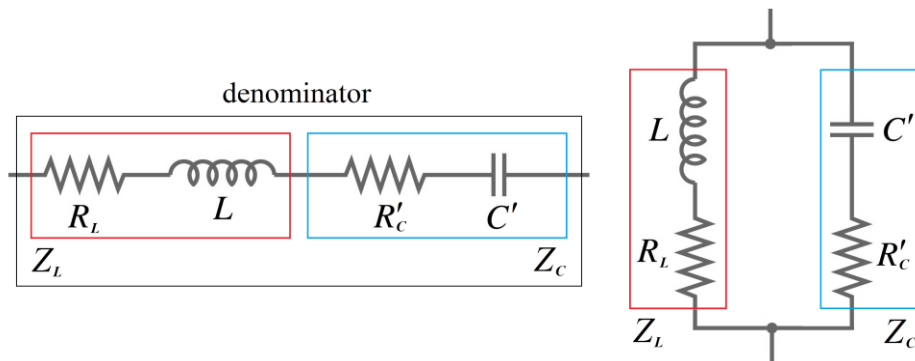


Figure A.2.6. RLC circuit of Fig.A.2.5 with a built-in simplification on the original RC circuit.

$$\begin{aligned}
Z_{|\Rightarrow\rangle} &= Z_L + Z_C = (R_L + X_L) + (R'_C + X'_C) = (R_L + R'_C) + (X_L + X'_C) \\
&= \left(R_L + \frac{R_C}{1 + (\omega C R_C)^2} \right) + \left(j\omega L + \frac{(-j R_C^2 \omega C)}{1 + (\omega C R_C)^2} \right) , \\
&= \left(R_L + \frac{R_C}{1 + (\omega C R_C)^2} \right) + j\omega \left(L - \frac{R_C^2 C}{1 + (\omega C R_C)^2} \right) \neq 0
\end{aligned} \tag{A.2.14}$$

The imaginary part of Eq.(A.2.14) may be canceled for some frequency, however, its real part will never be annulled, as we can see in Fig.A.2.7 where Z_L is in pink color while Z_C is in light blue and both of which shape $Z_{|\Rightarrow\rangle}$ in light green which will never be annulled. Therefore, we find ourselves facing a new 2-partite equivalent system of completely independent spins. ■

Note: this theorem, as well as its proof, is easily and completely generalizable to the N -partite case.

Therefore and undoubtedly, for this analogy, the resistors represent decoherence in the same way that they are associated with the energy expenditure by Joule effect in electrical circuits. Since in this analogy energy is lost in heat, the resistors will represent the loss of entanglement because of the interaction with the environment. If we consider that the ambit where the entangled particles are located is not adiabatic, they will be victims of the action of decoherence [1]. So much decoherence seems like the bad boy of the movie, however, it is an excellent tool to understand this analogy better.

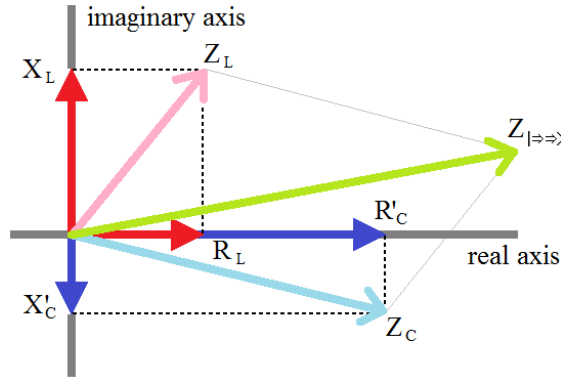


Figure A.2.7. The denominator of Eq.(A.2.13), which is the graphic on the left of Fig.A.2.6.

Finally, from Eq.(A.2.5)

$$Z_{|\uparrow\uparrow\rangle} = \frac{j\omega L}{1 - \omega^2 LC} = X_L \gamma^2 \equiv \mu_{|\uparrow\uparrow\rangle} = \mu_{|00\rangle} \gamma^2 , \tag{A.2.15}$$

where γ is the Lorentz's factor,

$$\gamma = \frac{1}{\sqrt{1 - \omega^2 LC}} . \tag{A.2.16}$$

Then,

$$Z_{|\uparrow\rangle} \equiv \mu_{|\uparrow\rangle} = \mu_{|0\rangle} \gamma , \tag{A.2.17}$$

where, Eq.(A.2.15) is equal to Eq.(48) and Eq.(A.2.17) is equal to Eq.(147).

A.3 Entanglement of Signals

If there is entanglement between particles, and between a particle and its wave duality [12], automatically two questions arise: can entanglement take place between two waves? If the answer to the first question was yes, then, how would such entanglement be according to both state configurations previously mentioned? We will try to answer both questions simultaneously. For example, if we choose two entangled waves regarding both states configuration (GHZ and W), we will have:

$$f = 2 \text{ [hertz]},$$

$$A = 1 \text{ (amplitude)},$$

$$D = 1 \text{ (baseline)},$$

$$N = 1000 \text{ (number of samples), and,}$$

$$t = 0:1/(N-1):1 \text{ (from 0 to 1 with a pass = } 1/(N-1)\text{)}, \text{ then,}$$

$$\begin{aligned} \mu_1 &= A \sin(2\pi f t) + D \\ \mu_2 &= A \sin(2\pi f t + \pi) + D \end{aligned} \tag{A.3.1}$$

In Fig.A.3.1 we can see both entangled signals μ_1 and μ_2 .

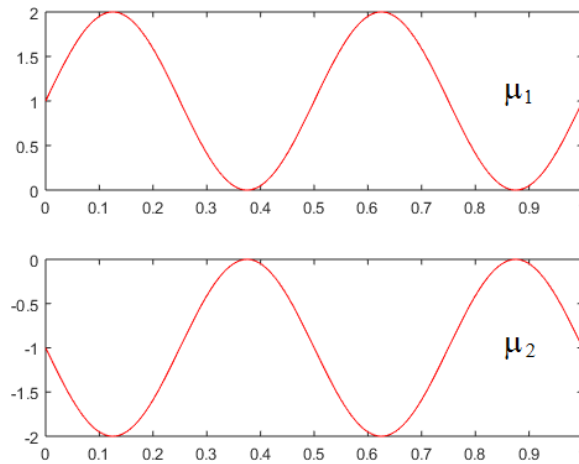


Figure A.3.1. Two entangled waves for the 2-partite case.

Next, Eq.(A.3.2) will be the denominator of Eq.(A.3.3)

$$\mu_{|\Rightarrow\rangle} = \mu_1 + \mu_2 = 0 = \mu_0 \quad \forall t, \tag{A.3.2}$$

$$\mu_{|\nabla\rangle} = (\mu_1 \times (-\mu_2)) / \mu_{|\Rightarrow\rangle} = \pm\infty \quad \forall t, \tag{A.3.3}$$

where, “ \times ” means infix version of Hadamard’s product of vectors (discrete waves like signals) [165], and “ $/$ ” represents the infix version of Hadamard’s quotient of vectors (previous id) [165], and whose result can be seen in Fig.A.3.2. This figure shows us $\mu_{|\Rightarrow\rangle}$ and $\mu_{|\nabla\rangle}$ for the 2-partite case.

Besides, in Fig.A.3.3 both states configurations, GHZ and W, coincide.

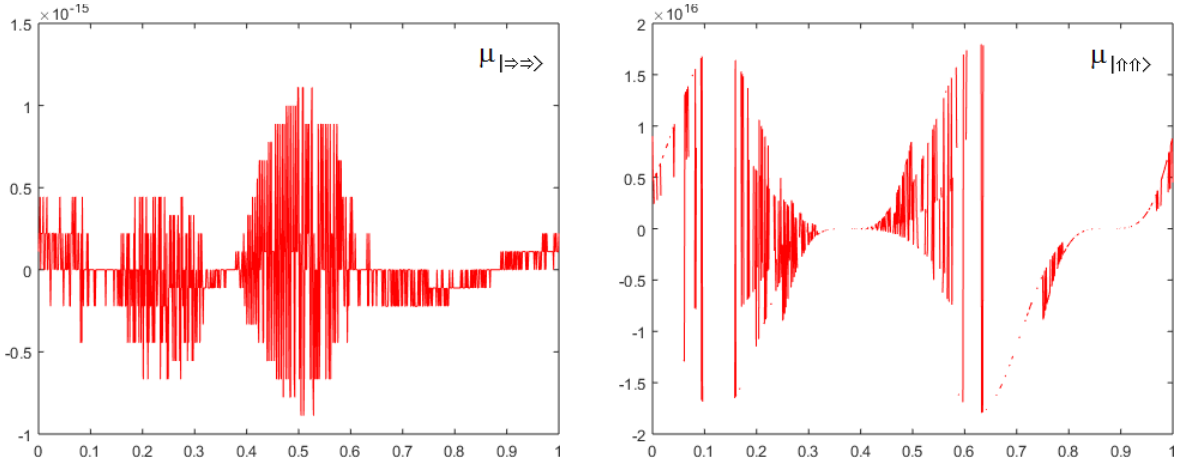


Figure A.3.2. $\mu_{|\psi\rangle\rangle}$ (on the left), and $\mu_{|\phi\rangle\rangle}$ (on the right) for the 2-partite case.

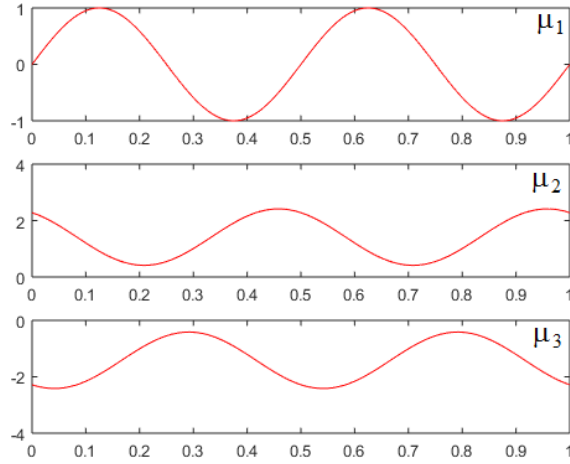


Figure A.3.3. Three entangled waves for the 3-partite GHZ case.

However, for the 3-partite GHZ case the entangled waves will be:

$f = 2$ [hertz],

$A = 1$ (amplitude),

$D = \sqrt{2}$ (baseline),

$N = 1000$ (number of samples), and,

$t = 0:1/(N-1):1$ (from 0 to 1 with a pass = $1/(N-1)$), then,

$$\begin{aligned}
 \mu_1 &= A \sin(2\pi f t) \\
 \mu_2 &= A \sin(2\pi f t + 2\pi / 3) + D \\
 \mu_3 &= A \sin(2\pi f t + 4\pi / 3) - D
 \end{aligned} \tag{A.3.4}$$

In Fig.A.3.3 we can see the three entangled waves μ_1 , μ_2 and μ_3 , with,

$$\mu_{|\psi\rangle\rangle} = \mu_1 + \mu_2 + \mu_3 = 0 = \mu_0 \quad \forall t, \tag{A.3.5}$$

$$\mu_{|\uparrow\uparrow\uparrow\rangle} = \left((\mu_1 \times \mu_2 \times \mu_3) \cdot \mu_{|\Rightarrow\rangle} \right)^{\frac{1}{2}} = \pm\infty \quad \forall t, \quad (\text{A.3.6})$$

where “ $(\cdot)^{\frac{1}{2}}$ ” means infixed version of Hadamard’s square root of vectors (discrete waves like signals), i.e., it is the square root of each and every one of the samples of the discrete wave, and whose result can be seen in Fig.A.3.4. This figure shows us $\mu_{|\Rightarrow\rangle}$ and $\mu_{|\uparrow\uparrow\uparrow\rangle}$ for the 3-partite GHZ case.

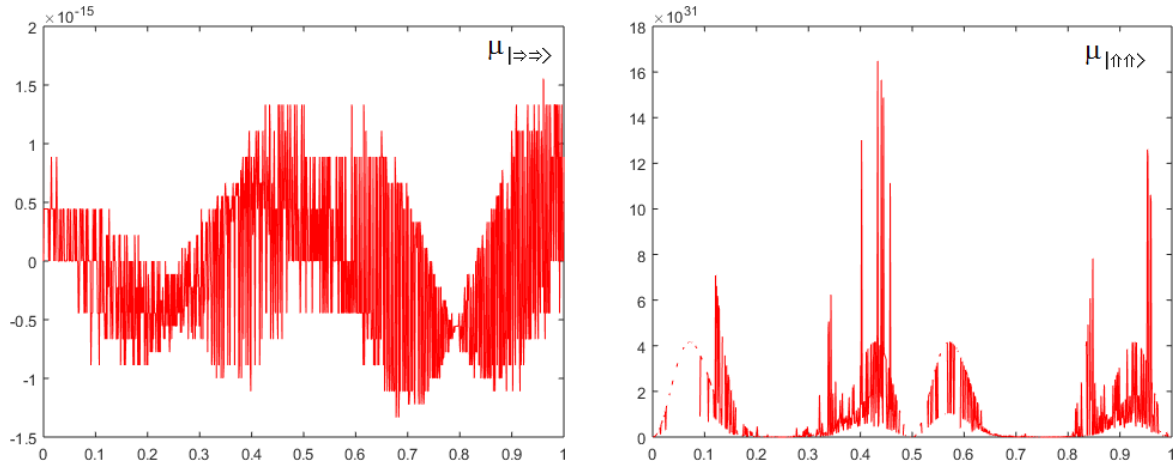


Figure A.3.4. $\mu_{|\Rightarrow\rangle}$ (on the left), and $\mu_{|\uparrow\uparrow\uparrow\rangle}$ (on the right) for the 3-partite GHZ case.

While for the 3-partite W case the entangled waves may have the following form:

$$f = 2 \text{ [hertz]},$$

$$N = 1000 \text{ (number of samples)},$$

$$\varepsilon = \exp(i \cdot 2 \cdot \pi / 3) \text{ (twiddle factor), and,}$$

$$t = 0:1/(N-1):1 \text{ (from 0 to 1 with a pass = } 1/(N-1)\text{)}.$$

The spins will be,

$$\begin{aligned} \mu_1 &= \varepsilon^0 e^{i(2\pi ft - kx)} \\ \mu_2 &= \varepsilon^1 e^{i(2\pi ft - kx)} \\ \mu_3 &= \varepsilon^2 e^{i(2\pi ft - kx)} \end{aligned} \quad (\text{A.3.7})$$

where, $k = \omega/c$ is the wave number and x is the position, with,

$$\mu_{|\Rightarrow\rangle} = \mu_1 \times \mu_2 + \mu_1 \times \mu_3 + \mu_2 \times \mu_3 = 0 \quad \forall t. \quad (\text{A.3.8})$$

$$\mu_{|\uparrow\uparrow\uparrow\rangle} = (\mu_1 \times \mu_2 \times \mu_3) \cdot \mu_{|\Rightarrow\rangle} = \pm\infty \quad \forall t. \quad (\text{A.3.9})$$

Which can be seen in Fig.A.3.5.

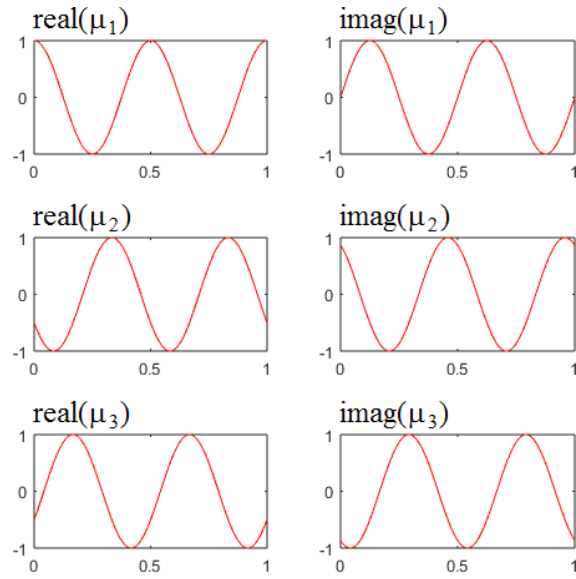


Figure A.3.5. Three entangled waves for the 3-partite W case.

Since the three entangled spins of Eq.(A.3.7) are complex, Fig.A.3.6 shows us $\mu_{|\Rightarrow\rangle}$ and $\mu_{|\Uparrow\rangle}$ for the 3-partite W case, where we have separated the real and the imaginary part of both resulting spins .

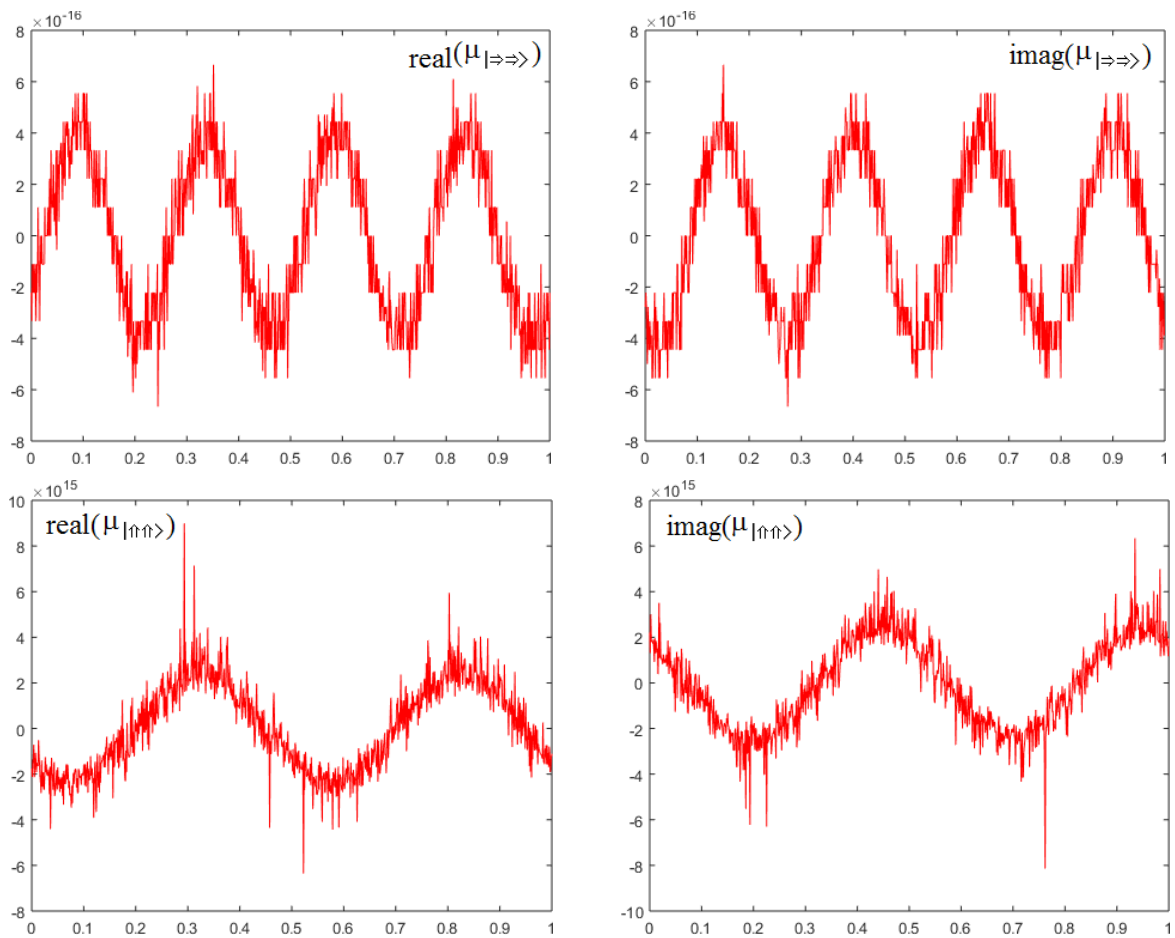


Figure A.3.6. $\mu_{|\Rightarrow\rangle}$ (top), and $\mu_{|\Uparrow\rangle}$ (bottom) for the 3-partite W case.

A.4 N-Dimensional Entanglement

The W states configuration predicts entanglement in N spatial dimensions, i.e., not with respect to a unique dimension but projected on N axes, as long as the entangled spins are always on a same plane, e.g., we can see this in Fig.A.4.1 for 2 dimensions, however, the analysis is easily extendable to N dimensions.

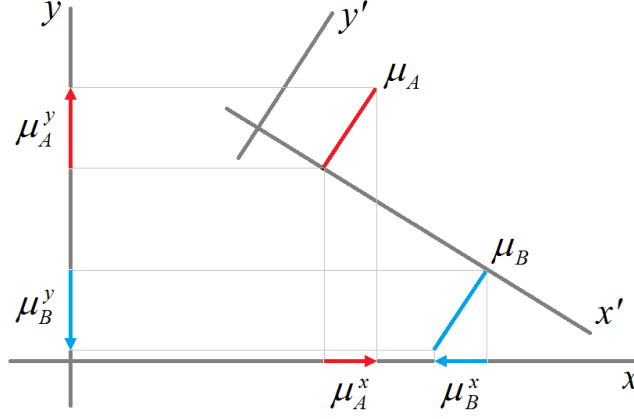


Figure A.4.1. 2-partite entanglement regarding 2 spatial axes.

Figure A.4.1 shows us two entangled spins μ_A (in red) and μ_B (in blue), with projection on one of their original axis (x' , y'): y' , however, they have projections on two new axes (x , y), therefore, for their original axes the spins $\mu_{|\Rightarrow\rangle}$ and $\mu_{|\Uparrow\rangle}$ will be,

$$\mu_{|\Rightarrow\rangle} = \mu_A + \mu_B = (\mu_A^{x'} + \mu_A^{y'}) + (\mu_B^{x'} + \mu_B^{y'}) = (\mu_A^{x'} + \mu_B^{x'}) + (\mu_A^{y'} + \mu_B^{y'}) = 0 \quad (\text{A.4.1})$$

where,

$$\begin{aligned} \mu_A &= \mu_A^{x'} + \mu_A^{y'} \\ \mu_B &= \mu_B^{x'} + \mu_B^{y'} \end{aligned} \quad (\text{A.4.2})$$

with,

$$\begin{aligned} \mu_A^{x'} &= -\mu_B^{x'} \quad , \quad \mu_A^{y'} = \mu_B^{y'} = 0 \\ \mu_A^{y'} &= -\mu_B^{y'} \end{aligned} \quad (\text{A.4.3})$$

The second line of the Eq.(A.4.3), in relation to the original axes (x' , y'), is the unique projection which records a perceptible value for the entanglement. That is, they are equal in modulus, parallel, opposites, and in principle, nonzero. Then, considering the equalities of Eq.(A.4.3), we will have,

$$\mu_{|\Uparrow\rangle} = \frac{\mu_A(-\mu_B)}{\mu_A + \mu_B} = \frac{(\mu_A^{x'} + \mu_A^{y'})(-(\mu_B^{x'} + \mu_B^{y'}))}{(\mu_A^{x'} + \mu_A^{y'}) + (\mu_B^{x'} + \mu_B^{y'})} = \frac{\mu_A^{y'}(-\mu_B^{y'})}{\mu_A^{y'} + \mu_B^{y'}} = \frac{(\mu_A^{y'})^2}{0} = \pm\infty \quad (\text{A.4.4})$$

While for the new pair of axes (x , y), $\mu_{|\Rightarrow\rangle}$ and $\mu_{|\Uparrow\rangle}$ will be,

$$\mu_{|\Rightarrow\rangle} = \mu_A + \mu_B = (\mu_A^x + \mu_A^y) + (\mu_B^x + \mu_B^y) = (\mu_A^x + \mu_B^x) + (\mu_A^y + \mu_B^y) = 0, \quad (\text{A.4.5})$$

where,

$$\begin{aligned}\mu_A &= \mu_A^x + \mu_A^y \\ \mu_B &= \mu_B^x + \mu_B^y\end{aligned}\tag{A.4.6}$$

with,

$$\begin{aligned}\mu_A^x &= -\mu_B^x \\ \mu_A^y &= -\mu_B^y\end{aligned}\tag{A.4.7}$$

Both lines of the Eq.(A.4.7), in relation to the new axes (x, y) , record a perceptible projection for the entanglement. That is, in both cases, they are equal in modulus, parallel, opposites, and in principle, nonzero. Then, considering the equalities of Eq.(A.4.7), we will have,

$$\mu_{|\uparrow\uparrow\rangle}^x = \frac{\mu_A(-\mu_B)}{\mu_A + \mu_B} = \frac{(\mu_A^x + \mu_A^y)(-(\mu_B^x + \mu_B^y))}{(\mu_A^x + \mu_A^y) + (\mu_B^x + \mu_B^y)} = \frac{(\mu_A^x + \mu_A^y)(\mu_A^x + \mu_A^y)}{(\mu_A^x + \mu_B^x) + (\mu_A^y + \mu_B^y)} = \frac{(\mu_A^x + \mu_A^y)^2}{0} = \pm\infty\tag{A.4.8}$$

This shows us several things at once since the W states configuration predicts:

- the multidimensional entanglement [8] exists, as long as, the spins are on the same plane and are parallel, with equal modulus and are opposites,
- the parallel operator can be applied individually: projection by projection, provided that each and every one of the projections complies with

$$\begin{aligned}\mu_{|\Rightarrow\rangle}^x &= \mu_A^x + \mu_B^x = 0 \\ \mu_{|\uparrow\uparrow\rangle}^x &= \frac{\mu_A^x(-\mu_B^x)}{\mu_A^x + \mu_B^x} = \frac{(\mu_A^x)^2}{0} = \pm\infty\end{aligned}\tag{A.4.9}$$

and

$$\begin{aligned}\mu_{|\Rightarrow\rangle}^y &= \mu_A^y + \mu_B^y = 0 \\ \mu_{|\uparrow\uparrow\rangle}^y &= \frac{\mu_A^y(-\mu_B^y)}{\mu_A^y + \mu_B^y} = \frac{(\mu_A^y)^2}{0} = \pm\infty\end{aligned}\tag{A.4.10}$$

- the application to K -partite of N dimensional entanglement as a natural extension of Equations (A.4.9) and (A.4.10) but applying the respective operators on $\mu_{|\Rightarrow\rangle}$ and $\mu_{|\uparrow\uparrow\rangle}$ according to K -partite case, see Appendix A.1.

In terms of applications, as in the case of quantum radar, the orientation is also critical, since in all equations of this work despite having implicitly assumed an analysis strictly on a single plane, we have dispensed with the analysis of the projections on the three spatial axes. This last analysis is what really corresponds in the treatment of signals of any radar, including (of course) its quantum version. Similar considerations can be made and similar results can be obtained for the GHZ states model in relation to K -partite/ N -dimensional cases. In other words, the analysis performed is totally generalizable to N dimensions individually for each dimension. In this context a question arises: can entanglement occur independently in one direction (projection) and in another not as indicated in Fig.A.4.2? As we can see in Fig.A.4.2, at first sight, μ_A (in light blue) and μ_B (in blue) cannot

entangle because they have different orientations and values in their spins. However, the new theory says that we can consider the projections individually and thus establish an entanglement between $\mu_B \equiv \mu_B^y$ (in blue) and μ_A^y (in red), discarding the x axis completely and any eventual projection on it as μ_A^x . If this is verified experimentally, we would be in the presence of an oriented entanglement or entanglement by projection with all the applications that this would allow in practice. The Theory of Dilated Locality contemplates what has been said, however, what about practical reality? This possibility is within the sphere of possibilities that this new theory contemplates as it did with the case of Fig.11 of Section 2.6.

All this should not surprise us because there are other forms of partially entangled pairs [166-169].

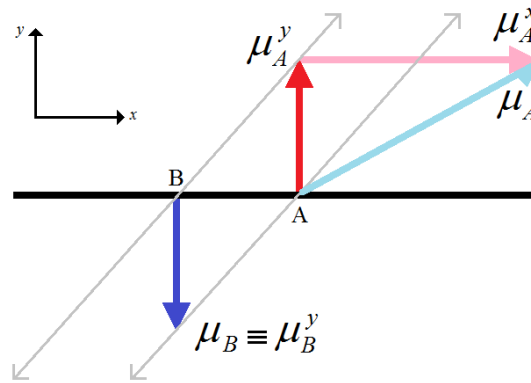


Figure A.4.2. Oriented entanglement or entanglement by projection.

A.5 Deduction of the parallel operator from other entropies

The entropy employed in Section 2.1 to obtain the alter-egos and known as von Neumann's entropy can be deduced as a limit case of the Rényi's entropy [170]. In fact, the α th order Rényi is defined as

$$S_\alpha \equiv \frac{1}{1-\alpha} \log [Tr(\rho^\alpha)] \quad (\text{A.5.1})$$

The zeroth-order ($\alpha = 0$) Rényi's entropy is related to the rank, namely, the number of nonzero singular values of ρ . When $\alpha \rightarrow 1$, the first-order Rényi's entropy reduces to the von Neumann's entropy,

$$S_1 \equiv -Tr(\rho \log \rho), \quad (\text{A.5.2})$$

also known as Shannon's entropy. The latter can also be represented as

$$-Tr(\rho \log \rho) = -\langle \log \rho \rangle. \quad (\text{A.5.3})$$

If we remember Eq.(37) and considering that for the scalar case

$$-\langle \log \rho \rangle = -\log r, \quad (\text{A.5.4})$$

then, replacing Eq.(A.5.4) into Eq.(37) in each case, we will have,

$$S^{A \cap B} = S^A + S^B - S^{A \cup B} = -\log r^A - \log r^B + \log r^{A \cup B}. \quad (\text{A.5.5})$$

Now, from Eq.(7) we can consider, among many other possibilities,

$$r^A = \frac{1}{2} \left(\frac{\mu_{|0\rangle}^2 + \mu_{|1\rangle}^2}{2} \right) = \frac{\mu_{|0\rangle}^2}{2}, \text{ and} \quad (\text{A.5.6a})$$

$$r^B = \frac{1}{2} \left(\frac{\mu_{|0\rangle}^2 + \mu_{|1\rangle}^2}{2} \right) = \frac{\mu_{|1\rangle}^2}{2}, \quad (\text{A.5.6b})$$

given that $\mu_{|0\rangle}^2 = \mu_{|1\rangle}^2 = 1$ for photons. If we replace Equations (A.5.6) and (38) into Eq.(A.5.5), we will have,

$$S^{A \cap B} = -\log \frac{\mu_{|0\rangle}^2}{2} - \log \frac{\mu_{|1\rangle}^2}{2} + \log \left(\frac{\mu_{|0\rangle}^2 - \mu_{|1\rangle}^2}{4} \right)^2. \quad (\text{A.5.7})$$

If we make the appropriate additions and subtractions to Eq.(A.5.7), we will have:

$$S^{A \cap B} = \log \frac{\mu_{|0\rangle}^2}{2} + \log \frac{\mu_{|1\rangle}^2}{2} - \log \left(\frac{\mu_{|0\rangle}^2 - \mu_{|1\rangle}^2}{4} \right) + \left[-2\log \frac{\mu_{|0\rangle}^2}{2} - 2\log \frac{\mu_{|1\rangle}^2}{2} + 3\log \left(\frac{\mu_{|0\rangle}^2 - \mu_{|1\rangle}^2}{4} \right) \right] \quad (\text{A.5.8})$$

Sending to the other side of the equal sign that is in brackets,

$$S^{A \cap B} + 2\log \frac{\mu_{|0\rangle}^2}{2} + 2\log \frac{\mu_{|1\rangle}^2}{2} - 3\log \left(\frac{\mu_{|0\rangle}^2 - \mu_{|1\rangle}^2}{4} \right) = \log \frac{\mu_{|0\rangle}^2}{2} + \log \frac{\mu_{|1\rangle}^2}{2} - \log \left(\frac{\mu_{|0\rangle}^2 - \mu_{|1\rangle}^2}{4} \right). \quad (\text{A.5.9})$$

Replacing the corresponding values of each term of Eq.(A.5.9):

$$S^{A \cap B} - 2 - 2 - 3\infty = \infty = \log \frac{\mu_{|0\rangle}^2 \mu_{|1\rangle}^2}{\mu_{|0\rangle}^2 - \mu_{|1\rangle}^2}. \quad (\text{A.5.10})$$

Finally, we obtain

$$\mu_{|\uparrow\uparrow\rangle} = \frac{\mu_{|0\rangle}^2 \mu_{|1\rangle}^2}{\mu_{|0\rangle}^2 - \mu_{|1\rangle}^2} = \frac{-\mu_{|00\rangle} \mu_{|11\rangle}}{\mu_{|00\rangle} + \mu_{|11\rangle}} = 2^\infty = \infty, \quad (\text{A.5.11})$$

which is exactly equal to Eq.(43).

On the other hand, another version of the entanglement Hamiltonian can be seen in [170]

$$H_{ent} \equiv -\log \rho, \quad (\text{A.5.12})$$

which has a matrix structure. Then, if we consider its scalar version, we will have,

$$S = h_{ent} \equiv -\log r, \quad (\text{A.5.13})$$

As we can see, Eq.(A.5.13) matches completely with Eq.(A.5.4), the deduction starts again and ends with the same result, that is, Eq.(A.5.11).

A.6 Loss and Restoration of Entanglement

We know that an entanglement link is established between elements of an EPR pairs. Figure A.6.1 represents such link as two tank tuned LC circuits based on the guidelines of Appendix A.2.

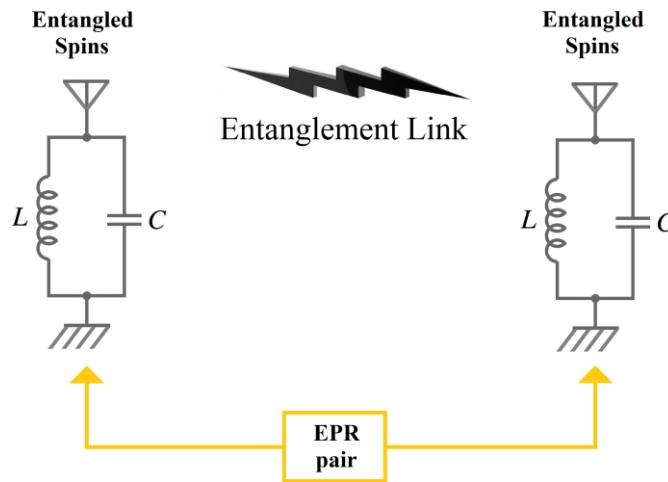


Figure A.6.1. Entanglement link between an EPR pair. This pair is tuned.

A problem arises when we want to measure the state of one of the elements of the entangled pair. In this circumstance, the entanglement is interrupted. In Fig.A.6.2 the intervention of the quantum measurement is represented as resistors in the LC (inductor-capacitor) pairs. These resistors tell us about the direct intervention of the environment on these pairs. As a result of this, the spins become completely independent and the alter-egos disappear.

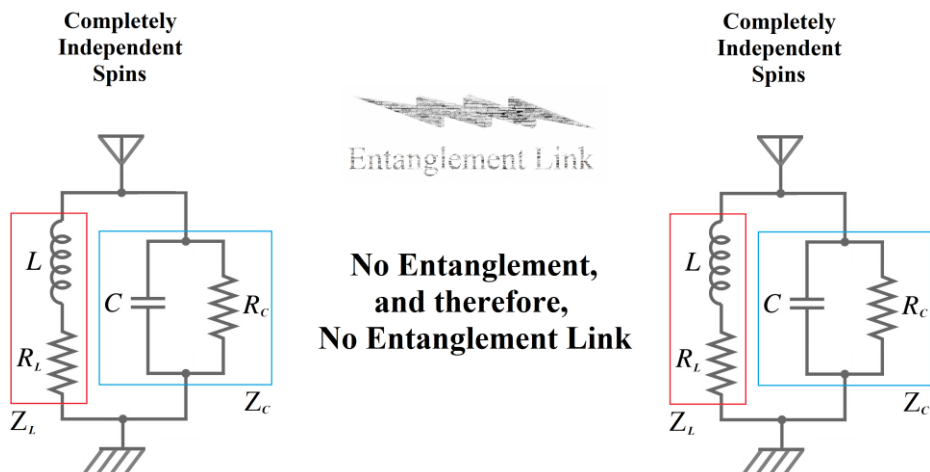


Figure A.6.2. After quantum measurement the entanglement link is disrupted, however, this persists in a ghostly way. Both resulting spins will be completely independent, and the action of the decoherence is represented with resistors in inductors and capacitors.

As we can see in Fig.A.6.3, the resistor components (in green) of the original entangled spins μ_A (in red) and μ_B (in blue) generate two new resulting spins (in pink and in light blue, respectively) which are not entangled. Effectively, the resistive components misalign the original spins (they are not parallel), making them independent and thus interrupting the entanglement. See Appendix A.2.

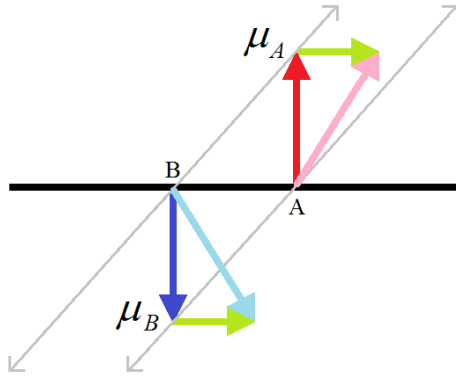


Figure A.6.3. Original entangled spins μ_A (in red) and μ_B (in blue) with their respective resistor components in green, which generate two new resulting spins (in pink and in light blue, respectively) not collinear and hence not entangled.

This is also known as decoherence and is associated with the collapse of the wavefunction. Besides, noise as a consequence of an interaction with the environment or with operations on imperfect gates generally reduces both purity and entanglement itself of a given state. However, if one has several copies of some less than maximally entangled state available, it is possible that both parties Alice and Bob concentrate or distill the entanglement, by acting locally on their parts in relation to the states and exchanging classical information on a classical channel. Thus, by using the so-called local operations and classical communication (LOCC) they can create fewer pairs with higher entanglement and higher degree of purity. This process is called entanglement purification or entanglement distillation [1, 3, 13, 171-177]. So far, this was the only known technique to improve entanglement, even, in part. However, the Theory of Dilated Locality tells us that the loss of entanglement is a completely reversible process, that is, the entanglement can be restored and the link re-established. On the other hand, and given that the resistors are directly associated with heat dissipation, the technique that is suggested as a remedy for the problem is laser cooling [178-180]. Returning to Fig.A.6.2, the Theory of Dilated Locality tells us that the decoherence can be overcome with a direct and local action on the spins (local cooling), although these are independent with an apparent irreversibility.

Everything said so far is indicating that quantum entanglement remains latent after decoherence in a ghostly state, and besides that such entanglement can resurrect with a direct and individual action on the spins as we can see in Fig.A.6.4, which has never been predicted in such a direct way by Quantum Theory. However, this must be verified even experimentally.

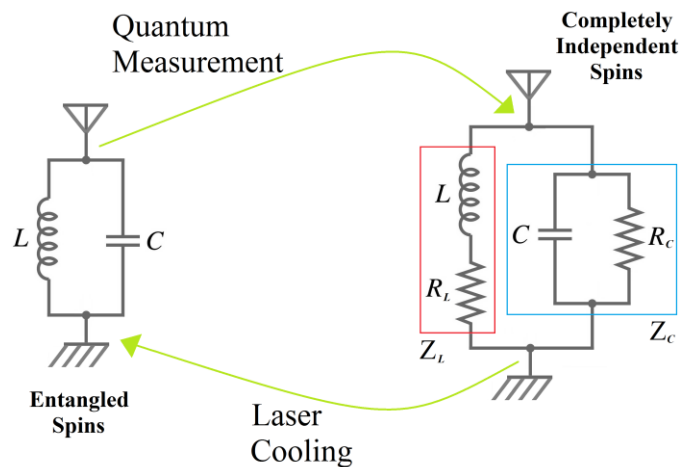


Figure A.6.4. For a given EPR element, the upper green arrow shows the pass from the entangled spins to completely independent spins via quantum measurement, while, the bottom green arrow indicates the transition from completely independent spins to entangled spins thanks to laser cooling. Laser cooling eliminates the resistors factors that inhibit the entanglement.

In a more general context: is the entanglement trainable? Can we make a supervised or unsupervised purification or distillation? In the supervised case the objective is to try to reach a target, and in the unsupervised case minimize an energetic functional. The answer to these questions constitutes a bridge between Quantum Information Processing and Artificial Intelligence.

Finally, when we return to the scheme of Fig.A.6.1 thanks to the laser cooling technique, the range of the locality completely shelters the EPR pair and the alter-egos according to what was developed in Section 3.1, which constitutes an important longing in all quantum optics experiments [181] and their potential applications.

A.7 New protocols for Teleportation and Superdense Coding

A.7.1 Teleportation

A.7.1.1 Standard protocol with two classical bits for desambiguation

The quantum teleportation begins with the distribution of the EPR pair to Alice and Bob. This distribution constitutes the entanglement link between Alice and Bob, and after that, we continue with the complete sketch of quantum teleportation of Fig.A.7.1, where the green line indicates the border between the sides of Alice and Bob, that is, both extremes of the entanglement link. In Fig.A.7.1, a single fine line represents a wire carrying one qubit, while a double line represents a wire carrying one classical bit [13]. Besides, the classical channel is really a control classical channel for disambiguation purposes (as we will see below through two bits), while the entanglement link is really an entanglement data link. Besides, in this figure, the block with an H represents a Hadamard's gate, and $|\beta_{00}\rangle \equiv |\Phi_+^{A \cup B}\rangle$ of Eq.(5).

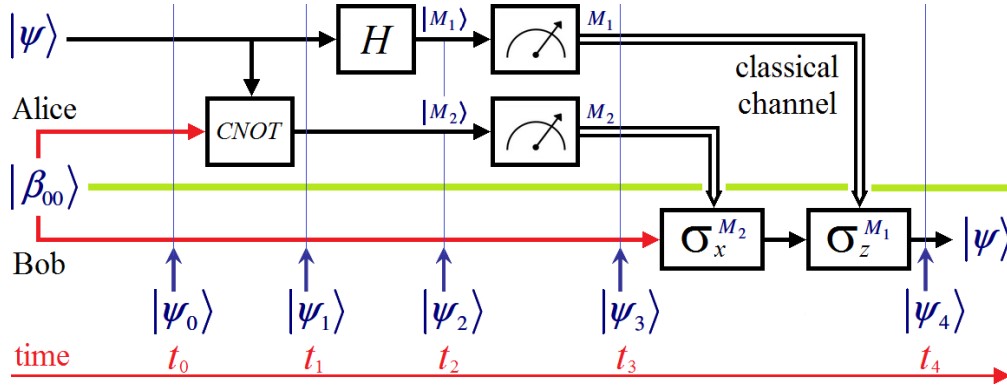


Figure A.7.1. Standard Teleportation protocol using an EPR pair and two classical bits for disambiguation.

If the arbitrary state to be teleported is $|\psi\rangle = \alpha|0\rangle + \beta|1\rangle$, then, the initial state (3-partite state) will be,

$$\begin{aligned} |\psi_0\rangle &= |\psi\rangle|\beta_{00}\rangle = \frac{1}{\sqrt{2}}[\alpha|0\rangle(|00\rangle + |11\rangle) + \beta|1\rangle(|00\rangle + |11\rangle)] \\ &= \frac{1}{\sqrt{2}}[\alpha|000\rangle + \alpha|011\rangle + \beta|100\rangle + \beta|111\rangle] \end{aligned} \quad (\text{A.7.1})$$

where for simplicity and in a generic form $|x\rangle \otimes |y\rangle = |xy\rangle$. Now, CNOT gate is applied to Eq.(A.7.1),

$$|\psi_1\rangle = \frac{1}{\sqrt{2}}[\alpha|000\rangle + \alpha|011\rangle + \beta|110\rangle + \beta|101\rangle]. \quad (\text{A.7.2})$$

At this time, we apply a Hadamard's gate to the elements of Eq.(A.7.2),

$$\begin{aligned}
|\psi_2\rangle &= \frac{1}{2} [|00\rangle \sigma_x^0 \sigma_z^0 |\psi\rangle + |01\rangle \sigma_x^1 \sigma_z^0 |\psi\rangle + |10\rangle \sigma_x^0 \sigma_z^1 |\psi\rangle + |11\rangle \sigma_x^1 \sigma_z^1 |\psi\rangle] \\
&= \frac{1}{2} [|\Phi^+\rangle \sigma_x^0 \sigma_z^0 |\psi\rangle + |\Phi^-\rangle \sigma_x^0 \sigma_z^1 |\psi\rangle + |\Psi^+\rangle \sigma_x^1 \sigma_z^0 |\psi\rangle + |\Psi^-\rangle \sigma_x^1 \sigma_z^1 |\psi\rangle]
\end{aligned} \tag{A.7.3}$$

Finally, Table A.7.I synthesizes the complete process of quantum teleportation, where Alice measures two of the possible qubits of the basis $\{|\Phi^+\rangle, |\Phi^-\rangle, |\Psi^+\rangle, |\Psi^-\rangle\} \equiv \{|\beta_{00}\rangle, |\beta_{01}\rangle, |\beta_{10}\rangle, |\beta_{11}\rangle\}$ and therefore she transmits the corresponding bits M_1 and M_2 via classical channel to Bob. The quantum measurement process is imperative in order to make the wavefunction of the original arbitrary state collapse since this is necessary not to violate the No-Cloning Theorem. In other words, the quantum measurement process destroys the original arbitrary state [13].

TABLE A.7.I

ALICE'S SIDE: MEASUREMENT OF BASE, CLASSICAL TRANSMISSION OF BITS, AND COLLAPSE OF STATES,		BOB'S SIDE: CLASSICAL RECEPTION OF BITS, GATES APPLICATION FOR THE FINAL RECOVERY OF THE ARBITRARY STATE.		
Alice's measurement	Alice transmits	This happens with probability	Collapsed state	Bob applies $\sigma_x^{M_1} \sigma_z^{M_2}$
$ \Phi^+\rangle \rightarrow 00$	$M_2 M_1 = 00$	$\left\ \frac{1}{2} \sigma_x^0 \sigma_z^0 \psi\rangle \right\ ^2 = \frac{1}{4}$	$ \Phi^+\rangle \sigma_x^0 \sigma_z^0 \psi\rangle$	$\sigma_x^0 \sigma_z^0 \psi\rangle = \psi\rangle$
$ \Psi^+\rangle \rightarrow 01$	$M_2 M_1 = 01$	$\left\ \frac{1}{2} \sigma_x^1 \sigma_z^0 \psi\rangle \right\ ^2 = \frac{1}{4}$	$ \Psi^+\rangle \sigma_x^1 \sigma_z^0 \psi\rangle$	$\sigma_x^1 \sigma_z^0 \psi\rangle = \sigma_x \psi\rangle$
$ \Phi^-\rangle \rightarrow 10$	$M_2 M_1 = 10$	$\left\ \frac{1}{2} \sigma_x^0 \sigma_z^1 \psi\rangle \right\ ^2 = \frac{1}{4}$	$ \Phi^-\rangle \sigma_x^0 \sigma_z^1 \psi\rangle$	$\sigma_x^0 \sigma_z^1 \psi\rangle = \sigma_z \psi\rangle$
$ \Psi^-\rangle \rightarrow 11$	$M_2 M_1 = 11$	$\left\ \frac{1}{2} \sigma_x^1 \sigma_z^1 \psi\rangle \right\ ^2 = \frac{1}{4}$	$ \Psi^-\rangle \sigma_x^1 \sigma_z^1 \psi\rangle$	$\sigma_x^1 \sigma_z^1 \psi\rangle = \sigma_x \sigma_z \psi\rangle$

At this point, it is important to mention that in literature there are several concerns regarding the implementation of teleportation protocols using a greater or lesser dimensional commitment but always with two classical bits for disambiguation. An interesting example can be found in [182], which shows that the one-qubit teleportation can be considered as a state transfer between subspaces of the whole Hilbert space of an indivisible eight-dimensional system. However, this as well as the rest of the works that manipulate high dimensional quantum systems for the implementation of teleportation protocols do it with two classical bits for disambiguation.

A.7.1.2 New protocol with only one classical bit for disambiguation

Next, we present a new teleportation protocol with a single bit of disambiguation which is based on Fig.A.7.2, where the block with the symbol “ \otimes ” represents the correlation between $|\psi\rangle$ and $|\beta_{00}\rangle$.

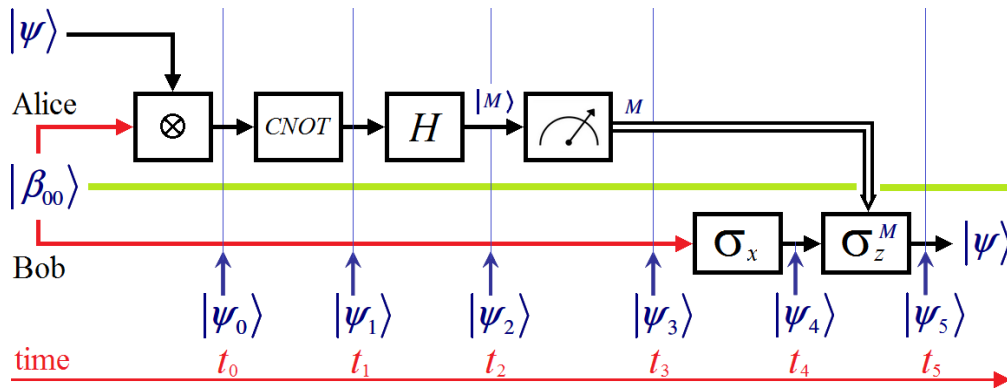


Figure A.7.2. Proposed Teleportation protocol with only one classical bit of disambiguation and using an EPR pair.

Then, we will have the following procedure:

Alice's side:

$$\begin{aligned} |\psi_0\rangle &= |\psi\rangle|\beta_{00}\rangle = \frac{1}{\sqrt{2}}[\alpha|0\rangle(|00\rangle+|11\rangle) + \beta|1\rangle(|00\rangle+|11\rangle)] \\ &= \frac{1}{\sqrt{2}}[\alpha|000\rangle + \alpha|011\rangle + \beta|100\rangle + \beta|111\rangle] \end{aligned} \quad (\text{A.7.4})$$

Applying CNOT gate to Eq.(A.7.4):

$$|\psi_1\rangle = \frac{1}{\sqrt{2}}[\alpha|000\rangle + \alpha|011\rangle + \beta|110\rangle + \beta|101\rangle] \quad (\text{A.7.5})$$

Now, we apply Hadamard's gate to Eq.(A.7.5):

$$\begin{aligned} |\psi_2\rangle &= \frac{1}{2}[\alpha|000\rangle + \alpha|100\rangle + \alpha|011\rangle + \alpha|111\rangle + \beta|010\rangle - \beta|110\rangle + \beta|001\rangle - \beta|101\rangle] \\ &= \frac{1}{2}[|00\rangle(\alpha|0\rangle + \beta|1\rangle) + |10\rangle(\alpha|0\rangle - \beta|1\rangle) + |01\rangle(\alpha|1\rangle + \beta|0\rangle) + |11\rangle(\alpha|1\rangle - \beta|0\rangle)] \end{aligned} \quad (\text{A.7.6})$$

In the instant t_3 , Alice measures, obtains M , and transmits it. In fact, the first qubit of the basis is associated with the application of σ_z gate, and the second one with the application of σ_x gate, then, Alice only measures the first qubit of those bases that end in 1 as $|01\rangle$ and $|11\rangle$, since Bob will always apply the σ_x gate.

Bob's side:

In the same instant t_3 , Bob applies σ_x gate to Eq.(A.7.6):

$$|\psi_4\rangle = \frac{1}{2}[|00\rangle(\alpha|1\rangle + \beta|0\rangle) + |10\rangle(\alpha|1\rangle - \beta|0\rangle) + |01\rangle(\alpha|0\rangle + \beta|1\rangle) + |11\rangle(\alpha|0\rangle - \beta|1\rangle)] \quad (\text{A.7.7})$$

Finally, in the instant t_4 , if $M = 1$, Bob applies σ_z gate to the state associated to the $|11\rangle$ basis of Eq.(A.7.7), and, if $M = 0$, Bob does not apply σ_z gate to the state associated to the $|01\rangle$ basis of Eq.(A.7.7), and in this way we recover the teleported state. The states associated with bases $|00\rangle$ and $|10\rangle$ are completely discarded.

A.7.1.3 Testing the Theory of Dilated Locality

Next, we are going to try to show that for the new protocol proposed is the same use of $(|0\rangle, |1\rangle)$ pair as an EPR pair. This peculiarity says us that this protocol respects the individuality of the entangled particles that are distributed to Alice and Bob and that is consistent with what has been seen so far in the Theory of Dilated Locality. This new protocol can be seen in Fig.A.7.2, and it starts with the correlation between $|\psi\rangle$ and $|0\rangle$ thanks to the operator " \otimes ".

Alice's side:

If the arbitrary state to teleport is $|\psi\rangle = \alpha|0\rangle + \beta|1\rangle$ again, then, the initial state (2-partite state) will be,

$$|\psi_0\rangle = |\psi\rangle \otimes |0\rangle = |\psi\rangle|0\rangle = (\alpha|0\rangle + \beta|1\rangle)|0\rangle = \alpha|00\rangle + \beta|10\rangle \quad (\text{A.7.8})$$

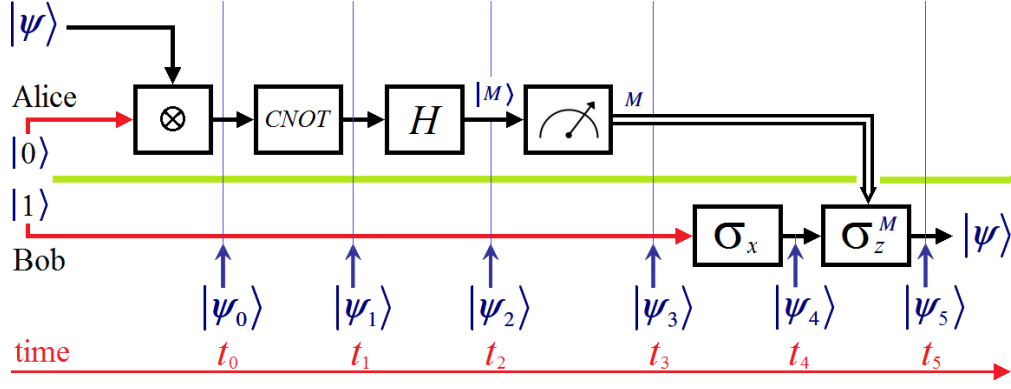


Figure A.7.3. Proposed Teleportation protocol with only one classical bit of disambiguation and using a $(|0\rangle, |1\rangle)$ pair.

Applying CNOT gate to Eq.(A.7.8):

$$|\psi_1\rangle = \alpha|00\rangle + \beta|11\rangle \quad (\text{A.7.9})$$

Now, applying Hadamard's gate to Eq.(A.7.9):

$$|\psi_2\rangle = \frac{1}{\sqrt{2}}[\alpha|00\rangle + \alpha|10\rangle + \beta|01\rangle - \beta|11\rangle] = \frac{1}{\sqrt{2}}[|0\rangle(\alpha|0\rangle + \beta|1\rangle) + |1\rangle(\alpha|0\rangle - \beta|1\rangle)] \quad (\text{A.7.10})$$

Equation (A.7.10) and Fig.A.7.3 show us that if in the instant t_3 Alice measures $|0\rangle$, then she transmits 0, and if she measures $|1\rangle$, then she transmits 1.

Bob's side:

Next, we will establish the state of the wavefunction on Bob's side for each instant.

$$|\psi_0\rangle = |\psi\rangle \otimes |1\rangle = |\psi\rangle|1\rangle = (\alpha|0\rangle + \beta|1\rangle)|1\rangle = \alpha|01\rangle + \beta|11\rangle \quad (\text{A.7.11})$$

$$|\psi_1\rangle = \alpha|01\rangle + \beta|10\rangle \quad (\text{A.7.12})$$

$$|\psi_2\rangle = \frac{1}{\sqrt{2}}[\alpha|01\rangle + \alpha|11\rangle + \beta|00\rangle - \beta|10\rangle] = \frac{1}{\sqrt{2}}[|0\rangle(\alpha|1\rangle + \beta|0\rangle) + |1\rangle(\alpha|1\rangle - \beta|0\rangle)] \quad (\text{A.7.13})$$

$$|\psi_3\rangle_0 = \frac{1}{\sqrt{2}}[|0\rangle(\alpha|1\rangle + \beta|0\rangle)] \quad (\text{A.7.14a})$$

$$|\psi_3\rangle_1 = \frac{1}{\sqrt{2}}[|1\rangle(\alpha|1\rangle - \beta|0\rangle)] \quad (\text{A.7.14b})$$

Applying σ_x gate to both rows of Eq.(A.7.14):

$$|\psi_4\rangle_0 = \alpha|0\rangle + \beta|1\rangle \quad (\text{A.7.15a})$$

$$|\psi_4\rangle_1 = \alpha|0\rangle - \beta|1\rangle \quad (\text{A.7.15b})$$

Applying σ_z gate only to Eq.(A.7.15b), i.e., if $M = 1$:

$$|\psi_5\rangle_0 = \alpha|0\rangle + \beta|1\rangle = |\psi\rangle \quad (\text{A.7.16a})$$

$$|\psi_5\rangle_1 = \alpha|0\rangle + \beta|1\rangle = |\psi\rangle \quad (\text{A.7.16b})$$

Therefore, the complete teleportation of the arbitrary state $|\psi\rangle$ is done with a single classical bit of disambiguation and distributing an entangled pair of type $(|0\rangle,|1\rangle)$ between Alice and Bob. In this way, we can obtain an alternative teleportation protocol to the one in current use that endorses the Theory of Dilated Locality. Besides, this demonstrates that it is the same to distribute a $(|0\rangle,|1\rangle)$ or EPR pair between Alice and Bob. Therefore, this also demonstrates that the predictions based on the Theory of Dilated Locality about the non-loss of individuality by the entangled particles is correct.

Here a question automatically arises: is it possible to do the same thing that we did with the $(|0\rangle,|1\rangle)$ pair but instead distributing a pair of type $(|00\rangle,|11\rangle)$ between Alice and Bob?

Alice's side:

In this case we have an initial 3-partite state,

$$|\psi_0\rangle = |\psi\rangle \otimes |00\rangle = |\psi\rangle |00\rangle = (\alpha|0\rangle + \beta|1\rangle)|00\rangle = \alpha|000\rangle + \beta|100\rangle \quad (\text{A.7.17})$$

Applying CNOT gate to Eq.(A.7.17):

$$|\psi_1\rangle = \alpha|000\rangle + \beta|110\rangle \quad (\text{A.7.18})$$

Now, applying Hadamard's gate to Eq.(A.7.18):

$$|\psi_2\rangle = \frac{1}{\sqrt{2}}[\alpha|000\rangle + \alpha|100\rangle + \beta|010\rangle - \beta|110\rangle] = \frac{1}{\sqrt{2}}[|0\rangle(\alpha|0\rangle + \beta|1\rangle)|0\rangle + |1\rangle(\alpha|0\rangle - \beta|1\rangle)|0\rangle] \quad (\text{A.7.19})$$

Equations (A.7.19) and (A.7.10) are clearly equivalent. Besides, here too, if in the instant t_3 Alice measures $|0\rangle$, then she transmits 0, and if she measures $|1\rangle$, then she transmits 1.

Bob's side:

Next, we will establish the state of the wavefunction on Bob's side for each instant.

$$|\psi_0\rangle = |\psi\rangle \otimes |11\rangle = |\psi\rangle |11\rangle = (\alpha|0\rangle + \beta|1\rangle)|11\rangle = \alpha|011\rangle + \beta|111\rangle \quad (\text{A.7.20})$$

$$|\psi_1\rangle = \alpha|011\rangle + \beta|101\rangle \quad (\text{A.7.21})$$

$$|\psi_2\rangle = \frac{1}{\sqrt{2}}[\alpha|011\rangle + \alpha|111\rangle + \beta|001\rangle - \beta|101\rangle] = \frac{1}{\sqrt{2}}[|0\rangle(\alpha|1\rangle + \beta|0\rangle)|1\rangle + |1\rangle(\alpha|1\rangle - \beta|0\rangle)|1\rangle] \quad (\text{A.7.22})$$

$$|\psi_3\rangle_0 = \frac{1}{\sqrt{2}}[|0\rangle(\alpha|1\rangle + \beta|0\rangle)|1\rangle] \quad (\text{A.7.23a})$$

$$|\psi_3\rangle_1 = \frac{1}{\sqrt{2}}[|1\rangle(\alpha|1\rangle - \beta|0\rangle)|1\rangle] \quad (\text{A.7.23b})$$

Applying σ_x gate to both rows of Eq.(A.7.23):

$$|\psi_4\rangle_0 = \alpha|0\rangle + \beta|1\rangle \quad (\text{A.7.24a})$$

$$|\psi_4\rangle_1 = \alpha|0\rangle - \beta|1\rangle \quad (\text{A.7.24b})$$

Applying σ_z gate only to Eq.(A.7.24b), i.e., if $M = 1$:

$$|\psi_5\rangle_0 = \alpha|0\rangle + \beta|1\rangle = |\psi\rangle \quad (\text{A.7.25a})$$

$$|\psi_5\rangle_1 = \alpha|0\rangle + \beta|1\rangle = |\psi\rangle \quad (\text{A.7.25b})$$

Clearly, the protocols that distribute both of the $(|0\rangle,|1\rangle)$ pairs as well as the $(|00\rangle,|11\rangle)$ pairs between Alice and Bob are equivalent, which is another fact predicted by the Theory of Dilated Locality. In fact, we could do the same with type $(|01\rangle,|10\rangle)$ pairs and even then the protocol would still work perfectly.

A.7.2 Superdense Coding

A.7.2.1 Standard protocol with two classical bits to transmit

Now, we present the standard Superdense Coding (SDC) protocol with two classical bits to transmit and an EPR pair to be distributed between Alice and Bob. This protocol is based on Fig.A.7.4 where after $\sigma_x^{M_2}$ and $\sigma_z^{M_1}$ and depending on the values of M_1 and M_2 , it delivers the Bell's basis $|\beta_{M_1M_2}\rangle$, which is transmitted by an optical channel from the Alice's side to Bob's side. Next, the combination of CNOT gate and Hadamard's gate (in that order) obtains $(|M_1\rangle, |M_2\rangle)$ from $|\beta_{M_1M_2}\rangle$. Finally, quantum measurement allows to reach (M_1, M_2) from $(|M_1\rangle, |M_2\rangle)$.

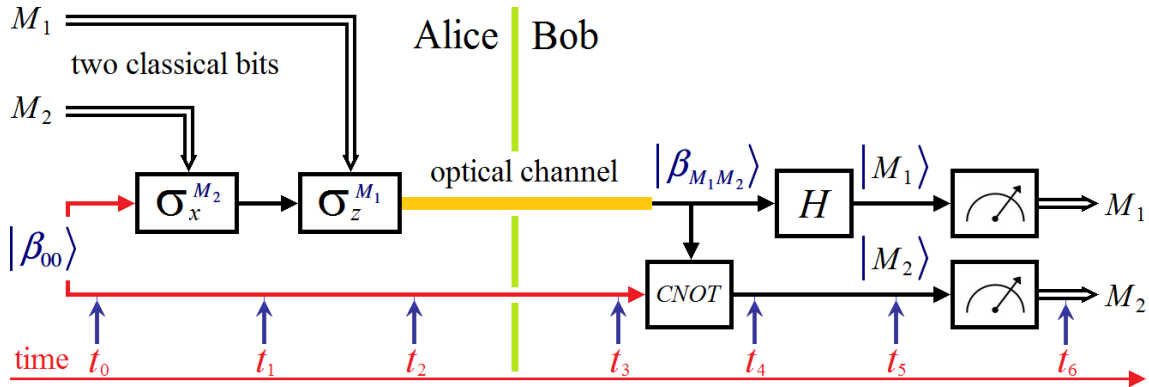


Figure A.7.4. Standard SDC protocol with two classical bits to be transmitted and using an EPR pair.

A.7.2.2 New protocol with only one classical bit to transmit

This protocol can be seen on Fig.A.7.5 and is equivalent to that of Fig.A.7.4 if $M_1 = M$, and $M_2 = 1$. It will be appreciated in the next section. Obviously, if $M_2 = 0$, it would also work.

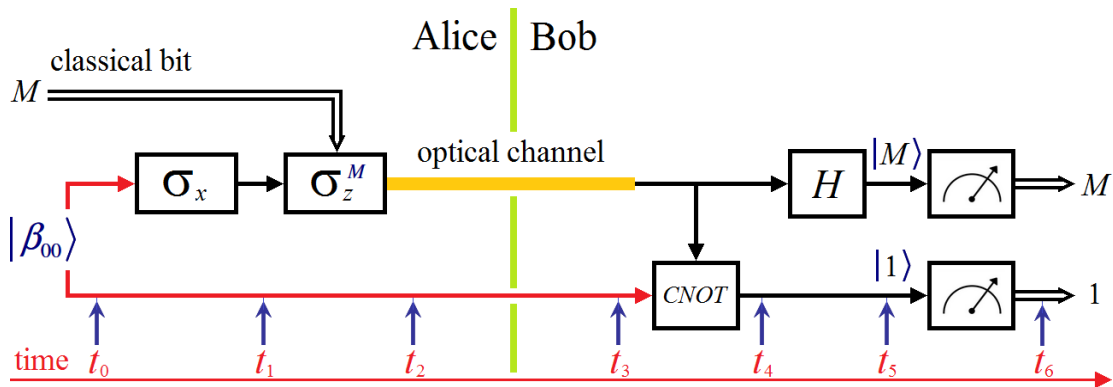


Figure A.7.5. Proposed SDC protocol with only one classical bit to be transmitted using an EPR pair.

A.7.2.3 Testing the Theory of Dilated Locality again

Now, we are going to develop a new protocol for SDC with only one classical bit to transmit and using a $(|0\rangle, |1\rangle)$ pair to distribute between Alice and Bob instead of the traditional EPR pair $|\beta_{00}\rangle$ as in the standard SDC protocol. Figure A.7.6 shows the new SDC protocol which represents the counterpart of the protocol of Fig.A.7.3.

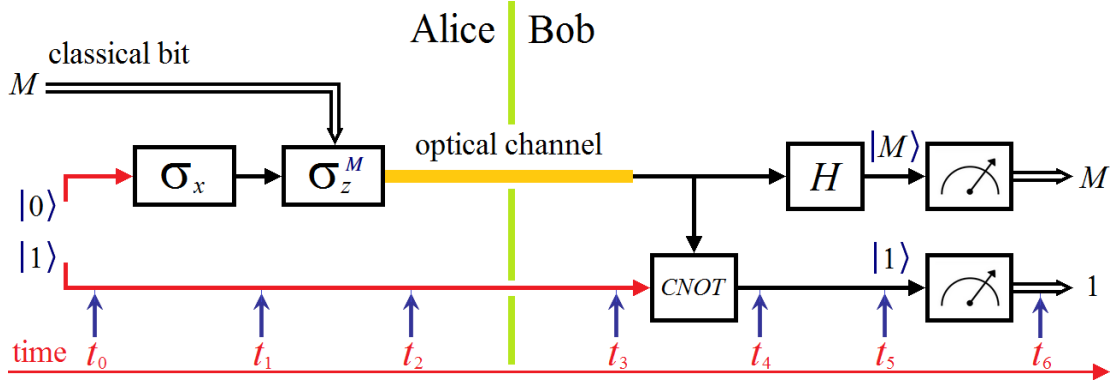


Figure A.7.6. Proposed SDC protocol with only one classical bit to be transmitted using a $(|0\rangle, |1\rangle)$ pair.

Alice's side:

From Fig.A.7.6 we will develop the new protocol instant-by-instant:

Top line:

$$|\psi_0\rangle = |0\rangle \quad (\text{A.7.26})$$

Applying σ_x gate to Eq.(A.7.26):

$$|\psi_1\rangle = |1\rangle \quad (\text{A.7.27})$$

Applying σ_z^M gate to Eq.(A.7.27) and depending on the value of M :

$$|\psi_2\rangle_0 = |1\rangle \quad (\text{A.7.28a})$$

$$|\psi_2\rangle_1 = -|1\rangle \quad (\text{A.7.28b})$$

Bottom line:

$$|\psi_0\rangle = |1\rangle \quad (\text{A.7.29})$$

$$|\psi_1\rangle = |0\rangle \quad (\text{A.7.30})$$

$$|\psi_2\rangle_0 = |0\rangle \quad (\text{A.7.31a})$$

$$|\psi_2\rangle_1 = -|0\rangle \quad (\text{A.7.31b})$$

Bob's side:

From $(|1\rangle, |0\rangle)$ or $(-|1\rangle, -|0\rangle)$ to the input of the combination of Hadamard's gate and CNOT gate, we will obtain $|\beta_{10}\rangle$ or $-|\beta_{10}\rangle$, respectively. Then, and after the quantum measurement, if Bob has an $|\beta_{10}\rangle$, he obtains a 0, and if he has a $-|\beta_{10}\rangle$, he obtains a 1.

This unequivocally establishes the equivalence when we use $(|0\rangle,|1\rangle)$, $(|00\rangle,|11\rangle)$ or EPR pairs for the different protocols of Teleportation and Superdense Coding. Besides, and as a preliminary conclusion, we can say that the entangled spins are not separable, however, they can be distinguishable, where in this context, distinguishable means that the entangled spins can be considered clearly distributable in an individual way between Alice and Bob in the context of protocols like those of Figures A.7.3 and A.7.6 for Teleportation and Superdense Coding, respectively.

On the other hand, and since the locality is dilated for which the EPR pair is local, a question automatically arises: what is the impact of the locality on the distinguishability defined above for the entangled EPR pair? In other words, if they are local: are they distinguishable according to the definition suggested above? Or: are they not?

Finally, an exhaustive analysis is pending on the possibility of developing both Teleportation and Superdense Coding protocols using Mixed Entangled Pairs [183].

References

1. Audretsch, J. Entangled Systems: New Directions in Quantum Physics. Wiley-VCH Verlag GmbH & Co (2007).
2. Jaeger, G. Entanglement, Information, and the Interpretation of Quantum Mechanics. Springer (2009).
3. Horodecki, R. et al. Quantum entanglement. Preprint at arXiv:quant-ph/0702225v2 (2007).
4. Greenberger, D. M., Horne, M. A. & Zeilinger, A. Going Beyond Bell's Theorem in M. Kafatos (Ed.) Bell Theorem, Quantum Theory, and Conceptions of the Universe, S. 69–72, Kluwer, Dordrecht (1989).
5. Greenberger, D. M., Horne, M. A., Shimony, A. & Zeilinger, A. Bell's Theorem without inequalities, Am. J. Phys., Vol.58, pp.1131–1143 (1990).
6. Barreiro, J. T. & Kwiat, P. G. Hyperentanglement for advanced quantum communication. Quantum Communications and Quantum Imaging VI, edited by Ronald E. Meyers, Yanhua Shih, Keith S. Deacon, Proc. of SPIE Vol. 7092, 70920P (2008).
7. Denga, F. G., Renb, B. C. & Li, X. H. Quantum hyperentanglement and its applications in quantum information processing. Preprint at arXiv:quant-ph/1610.09896v5 (2017).
8. Krenna, M. et al. Generation and confirmation of a (100×100) -dimensional entangled quantum system. PNAS, Vol.111, No.17, pp.6243–6247 (2014).
9. Coffman, V., Kundu, J. & Wootters, W. K. Distributed Entanglement. Preprint at arXiv:quant-ph/9907047v2 (1999).
10. Buscemi, F., Gour, G. & Kim, J. S. Polygamy of Distributed Entanglement. Preprint at arXiv:quant-ph/0903.4413v2 (2009).
11. Megidish, E. et al. Entanglement Between Photons that have Never Coexisted. Preprint at arXiv:quant-ph/1209.4191v1 (2012).
12. Rab, A. D. et al. Entanglement of photons in their dual wave-particle nature. Preprint at arXiv:quant-ph/1702.04146v1 (2017).
13. Nielsen, M. A. & Chuang, I. L. Quantum Computation and Quantum Information. Cambridge University Press, Cambridge (2004).
14. Preskill, J. Lecture Notes for Physics 229: Quantum Information and Computation. CreateSpace Independent Publishing Platform (2015).
15. Weedbrook, C. et al. Gaussian quantum information. Rev. Mod. Phys. 84, 621 (2012).
16. Kaye, P., Laflamme, R. & Mosca, M. An Introduction to Quantum Computing. Oxford University Press, Oxford (2004).
17. Stolze, J. & Suter, D. Quantum Computing: A Short Course from Theory to Experiment. WILEY-VCH Verlag GmbH & Co. KGaA, Weinheim (2007).
18. NIST. Quantum Computing and Communication. CreateSpace Independent Publishing Platform (2014).
19. Pathak, A. Elements of Quantum Computation and Quantum Communication. CRC Press (2013).
20. Anderson, R. & Brady, R. Why quantum computing is hard - and quantum cryptography is not probably secure. Preprint at arXiv:quant-ph/1301.7351v1 (2013).
21. Cariolaro, G. Quantum Communications. Springer International Publishing (2015).

22. Mishra, V. K. *An Introduction to Quantum Communication*. Momentum Press (2016).
23. Imre, S. & Gyongyosi, L. *Advanced Quantum Communications: An Engineering Approach*. Wiley-IEEE Press (2012).
24. Einstein, A., Lorentz, H. A., Minkowski, H. & Weyl, H. *The Principle of Relativity: a collection of original memoirs on the special and general theory of relativity*. Courier Dover Publications (1952).
25. Bell, J. On the Einstein Podolsky Rosen paradox. *Physics*. 1:195 (1964).
26. Vaidman, L. *Quantum theory and determinism*. Quantum Stud.: Math. Found. Springer (2014).
27. Einstein, A., Podolsky, B. & Rosen, N. Can Quantum-Mechanical Description of Physical Reality Be Considered Complete? *Physical Review*. 47 (10): 777–780 (1935).
28. Dieks, D. Communication by EPR devices. *Physics Letters A*, vol.92, issue 6, pp. 271-272 (1982).
29. Ghirardi, G. C., Grassi, R., Rimini, A. & Weber, T. Experiments of the EPR Type Involving CP-Violation Do not Allow Faster-than-Light Communication between Distant Observers. *Europhys. Lett.* Vol.6, pp.95-100 (1988).
30. Aspect, A., Grangier, P. & Roger, G. Experimental Realization of Einstein-Podolsky-Rosen-Bohm Gedankenexperiment: A New Violation of Bell's Inequalities. *Physical Review Letters*. Vol. 49, Iss. 2, pp. 91–94 (1982).
31. Peres, A. & Terno, D. R. Quantum Information and Relativity Theory. Preprint at arXiv:quant-ph/0212023v2 (2003).
32. Grodsky, I. T. & Streater, R. F. No-Go Theorem. *Phys. Rev. Lett.*, Vol.20, Num.13, pp.695-698 (1968).
33. Van Raamsdonk, M. Lectures on Gravity and Entanglement. Preprint at arXiv:hep-th/1609.00026v1 (2016).
34. Lin, J., Marcolli, M., Ooguri, H. & Stoica, B. Locality of Gravitational Systems from Entanglement of Conformal Field Theories. *Physical Review Letters*, PRL 114, 221601 (2015).
35. Castro Ruiz, E., Giacomina, F. & Brukner, C. Entanglement of quantum clocks through gravity. *PNAS*, pp.E2303–E2309 (2017).
36. Maldacena, J., Susskind, L. Cool horizons for entangled black holes. Preprint at arXiv:1306.0533v2 [hep-th] (2013).
37. Maldacena, J. Black Holes and Wormholes and the Secrets of Quantum Spacetime. *Scientific American*. 315. 26-31 (2016).
38. Preskill, J. Quantum information and black holes Quantum information and black holes seminar at MIT. Available at <http://www.theory.caltech.edu/people/preskill/talks/MIT-2014-blackholes.pdf> (2014).
39. De Aquino, F. TOE: Theory of Everything. Available at: <https://arxiv.org/ftp/gr-qc/papers/9910/9910036.pdf> (2012).
40. Newton, R. G. *Quantum Physics: A text for Graduate Students*. Springer (2002).
41. Gasiorowicz, S. *Quantum Physics*. John Wiley and Sons (2003).
42. Peres, A. *Quantum Theory: Concepts and Methods*. Kluwer Academic Publishers (2002).
43. - *Compendium of Quantum Physics: Concepts, Experiments, History and Philosophy*. Greenberger, Daniel, Hentschel, Klaus, Weinert, Friedel (Eds.) pp.404-405. Springer (2009).
44. Sadiq, M. *Experiments with Entangled Photons: Bell Inequalities, Non-local Games and Bound Entanglement* PhD Thesis Stockholm University (2016).
45. Doplicher, S. The Principle of Locality. Effectiveness, fate and challenges. Preprint at arXiv:math-ph /0911.5136v1 (2009).
46. Herbert, N. FLASH—A superluminal communicator based upon a new kind of quantum measurement. *Foundations of Physics*. 12(12), pp.1171-1179 (1982),
47. Eberhard, P. H. & Ross, R. R. Quantum field theory cannot provide faster-than-light communication. *Foundations of Physics Letters* 2: 127 (1989).
48. Blaylock, G. The EPR paradox, Bell's inequality, and the question of locality. Preprint at arXiv:quant-ph/0902.3827v4 (2009).
49. Aspect, A., Dalibard, J. & Roger, G. Experimental Test of Bell's Inequalities Using Time-Varying Analyzers. *Physical Review Letters*. Vol. 49, Iss. 25, pp. 1804–1807 (1982).

50. Hanson, R. Loophole-free Bell inequality violation using electron spins separated by 1.3 kilometres. *Nature*. 526: 682–686 (2015).
51. Clauser, J. F., Horne, M. A., Shimony, A. & Holt, R. A. Proposed experiment to test local hidden-variable theories. *Physical Review Letters*, Vol.23, No.15, pp.880-884 (1969).
52. Fuwa, M. et al. Experimental proof of nonlocal wavefunction collapse for a single particle using homodyne measurements. *Nature Communications*. 6:6665 (2015).
53. Aspect, A. Quantum mechanics: To be or not to be local. *Nature*. 446 (7138): 866–867 (2007).
54. Horodecki, R., Horodecki, M. & Horodecki, P. Quantum information isomorphism: Beyond the dilemma of the Scylla of ontology and the Charybdis of instrumentalism. *IBM J. RES. & DEV.*, Vol.48, No.1, pp.139-147 (2004).
55. Oppenheim, J. et al. Thermodynamical Approach to Quantifying Quantum Correlations. *Physical Review Letter*, Vol.89, 180402 (2002).
56. Horodecki, M. et al. Local information as a resource in distributed quantum systems. *Physical Review Letter*, Vol.90, 100402 (2003).
57. Bennett, C. H. et al. Teleporting an Unknown Quantum State via Dual Classical and Einstein-Podolsky-Rosen Channels. *Phys. Rev. Lett.* 70, 1895 (1993).
58. Bouwmeester, D. et al. Experimental Quantum Teleportation. *Nature*, 390, 575–579 (1997).
59. Boschi, D. et al. Experimental Realization of Teleporting an Unknown Pure Quantum State via Dual Classical and Einstein-Podolsky-Rosen Channels. *Phys. Rev. Lett.*, 80, 1121 (1998).
60. Yin, J. et al. Bounding the speed of ‘spooky action at a distance’. Preprint at arXiv:1303.0614v1 [quant-ph] (2013).
61. Al-Khalili, J. *Black Holes, Wormholes and Time Machines*, 2nd Edition, CRC Press. (1999).
62. Phillips, A. C. *Introduction to Quantum Mechanics*. Wiley. (2003).
63. Ellis, G.F.R., Williams, R.M. *Flat and Curved Space Times*. Oxford University Press, Oxford. p.104 (1988).
64. Minkowski, H. *Space and Time*. In: Lorentz, H.A.E., Minkowski, A.H., Weyl, H. (eds.) *The Principle of Relativity*. Dover, New York (1952).
65. Wald, R.M. Resource letter TMGR-1: teaching the mathematics of general relativity. *Am. J. Phys.* 74, 471–477 (2006).
66. Weingard, R. Relativity and the reality of past and future events. *Br. J. Philos. Sci.* 23, 119–121 (1972).
67. Petkov, V. *Relativity and the Nature of Spacetime*. Springer, Berlin. Chap. 10. (2005).
68. Rindler, W. *Essential Relativity*, 2nd edn. Springer, Berlin. p. 244. (1977).
69. Synge, J.L. *Relativity: The General Theory*. Nord-Holand, Amsterdam. p.109. (1960).
70. Edgren, L., Marnelius, R. & Salomonson, P. Infinite spin particles. Preprint at arXiv:hep-th/0503136v1 (2005).
71. Longo, R., Morinelli, V. & Rehren, K-H. Where Infinite Spin Particles are Localizable, *Commun.Math. Phys.* 345, 587–614 (2016).
72. Zinoviev, Y. M. Infinite Spin Fields in $d = 3$ and Beyond, *Universe*, 3, 63 (2017).
73. Bengtsson, A. K. H. BRST Theory for Continuous Spin. Preprint at arXiv:1303.3799v2 [hep-th] (2014).
74. Bekaert, X. & Skvortsov, E. Elementary particles with continuous spin. Preprint at arXiv:1708.01030v2 [hep-th] (2017).
75. Chashchina, O. I. & Silagadze, Z. K. Breaking the light speed barrier. Preprint at arXiv:1112.4714v2 [hep-ph] (2012).
76. Porrati, M. Universal Limits on Massless High-Spin Particles. Preprint at arXiv:0804.4672v3 [hep-th] (2008).
77. Baskal, S. & Kim, Y. S. Little groups and Maxwell-type tensors for massive and massless particles, *Europhys. Lett.*, 40 (4), pp.375-380 (1997).
78. Schroer, B. Wigner’s infinite spin representations and inert matter, *Eur. Phys. J. C* 77:362 (2017).
79. Schuster, P. & Toro, N. A Gauge Field Theory of Continuous-Spin Particles. Preprint at arXiv:1302.3225v2 [hep-th] (2013).
80. Schuster, P. & Toro, N. A CSP Field Theory with Helicity Correspondence. Preprint at arXiv:1404.0675v1 [hep-th] (2014).

81. Schroer, B. Dark matter and Wigner's third positive energy representation class. Preprint at arXiv:1306.3876v5 [gr-qc] (2014).
82. Fernando, S. & Günaydin, M. Massless conformal fields, AdS(d+1)/CFTd higher spin algebras and their deformations, Nuclear Physics B 904, 494–526 (2016).
83. Pashnev, A. & Tsulaia, M. Dimensional reduction and BRST approach to the description of a Regge trajectory. Preprint at arXiv:hep-th/9703010v1 (1997).
84. Abbott, L. F. Massless particles with continuous spin indices, Physical Review D, Vol.13, No.8, 2291-2294 (1976).
85. Brink, L. Continuous Spin Representations of the Poincare and Super-Poincare Groups. Preprint at arXiv:hep-th/0205145v1 (2002).
86. Schuster, P. & Toro, N. On the Theory of Continuous-Spin Particles: Helicity Correspondence in Radiation and Forces. Preprint at arXiv:1302.1577v2 [hep-th] (2013).
87. Külske, C. & Orlandi, E. A simple fluctuation lower bound for a disordered massless random continuous spin model in $d = 2$. Preprint at arXiv:math/0604068v2 [math.PR] (2006).
88. Hirata, K. Quantization of Massless Fields with Continuous Spin, Progress of Theoretical Physics, Vol. 58, No. 2, 652-666 (1977).
89. Ünsal, M. Topological symmetry, spin liquids and CFT duals of Polyakov model with massless fermions. Preprint at arXiv:0804.4664v1 [cond-mat.str-el] (2008).
90. Didenko, V. E. Skvortsov, E. D. Elements of Vasiliev theory. Preprint at arXiv:1401.2975v5 [hep-th] (2015).
91. Peach, A. MSc Particles, Strings & Cosmology: Dissertation Higher-Spin Gauge Theories, Vasiliev Theory and Holography, Durham University. (2013).
92. Boulanger, N. et al. Higher spin interactions in four-dimensions: Vasiliev versus Fronsdal, J. Phys. A: Math. Theor. 49, 095402 (52pp). (2016).
93. Moradi, H. Higher-Spin Holographic Dualities and W-Algebras, Master's Thesis Faculty of Science, University of Copenhagen. (2012).
94. Kessel, P. The Physics of Higher-Spin Theories, Ph.D. Thesis, Humboldt-Universität zu Berlin. (2016).
95. Lepage-Jutier, A. Black Holes and Toy Cosmologies in Higher Spin Gravity, Ph.D. Thesis, McGill University. (2014).
96. Bauke, H. et al. What is the relativistic spin operator? Preprint at arXiv:1303.3862v2 [quant-ph] (2014).
97. Börner, G., Ehlers, J. & Rudolph, E. Relativistic Spin Precession in Two-body Systems, Astro. & Astrophys. 44, 417-420 (1975).
98. Weder, R. A. Spectral properties of one-body relativistic spin-zero hamiltonians, Ann. Inst. Henri Poincaré, Vol. XX no.2, 211-220 (1974).
99. Polyzou, W. N., Glöckle, W. & Witala, H. Spin in relativistic quantum theory. Preprint at arXiv:1208.5840v1 [nucl-th] (2012).
100. Hamdan, N., Chamaa, A. & López-Bonilla, J. On the Relativistic Concept of the Dirac's electron Spin, Lat. Am. J. Phys. Educ. Vol.2, No.1, 65-70 (2008).
101. Koelling, D. D. & Harmon, B. N. A technique for relativistic spin-polarised calculations? J. Phys. C: Solid State Phys., Vol.10. 3107-3114 (1977).
102. Feshbach, H. & Villars, F. Elementary Relativistic Wave Mechanics of Spin 0 and Spin 1/2 Particles. Reviews of Modern Physics, Vol.30, No.1, 24-45 (1958).
103. Choi, T. Relativistic Spin Operator and Lorentz Transformation of the Spin State of a Massive Dirac Particle. Journal of the Korean Physical Society, Vol. 62, No. 8, pp. 1085-1092 (2013).
104. McKenzie, C-A. An Interpretation of Relativistic Spin Entanglement Using Geometric Algebra. Electronic Theses and Dissertations. 5652 (2015).
105. Alsing, P. M. & Milburn, G. J. Lorentz Invariance of Entanglement. Preprint at arXiv:quant-ph/0203051v1 (2002).
106. Ahn, D., Lee, H-J. & Hwang, S. W. Relativistic entanglement of quantum states and nonlocality of Einstein-Podolsky-Rosen (EPR) paradox. Preprint at arXiv:quant-ph/0207018v2 (2002).
107. Alba, D., Crater, H. W. & Lusanna, L. Relativistic Quantum Mechanics in the Rest-Frame Instant Form of Dynamics. Preprint at arXiv:0907.1816v2 [hep-th] (2010).

108. Friis, N. et al. Relativistic entanglement of two massive particles. Preprint at arXiv:0912.4863v2 [quant-ph] (2010)
109. Lusanna, L. Relativistic Entanglement from Relativistic Quantum Mechanics in the Rest-Frame Instant Form of Dynamics. Preprint at arXiv:1012.3374v1 [quant-ph] (2010).
110. Crater, H. W. & Lusanna, L. On Relativistic Entanglement and Localization of Particles and on their Comparison with the Non-Relativistic Theory. Preprint at arXiv:1306.6524v4 [quant-ph] (2014).
111. Horwitz, L. & Arshansky, R. I. Relativistic Entanglement. Preprint at arXiv:1707.03294v3 [quant-ph] (2017).
112. Barrett, J. A. Entanglement and Disentanglement in Relativistic Quantum Mechanics, *Studies in History and Philosophy of Science Part B: Studies in History and Philosophy of Modern Physics*, Vol.48, 168-174 (2015).
113. Palge, V. Relativistic entanglement of single and two particle systems, Ph.D. Thesis, University of Leeds. (2013).
114. Dunningham, J. & Vedral, V. Entanglement and nonlocality of a single relativistic particle. Preprint at arXiv:0901.0844v1 [quant-ph] (2009).
115. Palge, V. & Dunningham, J. Surveying relativistic entanglement of two particles with continuous momenta. Preprint at arXiv:1409.1316v1 [quant-ph] (2014).
116. Lusanna, L. Relativistic entanglement from relativistic quantum mechanics in the rest-frame instant form of dynamics, 5th International Workshop DICE2010, *Journal of Physics: Conference Series* 306, 012039 (2011).
117. Jafarizadeh, M. A. & Mahdian, M. Quantifying entanglement of two relativistic particles using optimal entanglement witness, *Quantum Inf Process*, 10:501–518 (2011).
118. Zych, M. et al. Quantum interferometric visibility as a witness of general relativistic proper time. Preprint at arXiv:1105.4531v2 [quant-ph] (2011).
119. Pikovski, I. et al. Universal decoherence due to gravitational time dilation. Preprint at arXiv:1311.1095v2 [quant-ph] (2015).
120. Ruiza, E. C., Giacomina, F. & Brukner, C. Entanglement of quantum clocks through gravity, *PNAS*, E2303–E2309 (2017).
121. Anastopoulos, C. & Hu, B. L. Problems with the Newton–Schrödinger equations, *New Journal of Physics* 16, 085007 (2014).
122. Smerlak, M. & Rovelli, C. Relational EPR. Preprint at arXiv:quant-ph/0604064v3 (2007).
123. Hamel, J. S. Relativity as a Consequence of Quantum Entanglement: A Quantum Logic Gate Space Model for the Universe. Preprint at arXiv:0905.1119v2 [physics.gen-ph] (2009).
124. Friis, N. Relativistic Effects in Quantum Entanglement. Preprint at arXiv:1003.1874v1 [quant-ph] (2010)
125. Nikolic, H. EPR before EPR: a 1930 Einstein-Bohr thought experiment revisited. Preprint at arXiv:1203.1139v4 [quant-ph] (2012).
126. Susskind, L. Copenhagen vs Everett, Teleportation, and ER=EPR. Preprint at arXiv:1604.02589v2 [hep-th] (2016).
127. Cowen, R. Space, time, entanglement. *Nature*. Vol.527, 290-293 (2015).
128. Bancal, J-D. et al. Quantum non-locality based on finite-speed causal influences leads to superluminal signalling. *Nature Physics*. Vol.8, 867-870 (2012).
129. Goulart, P. Massless black holes and charged wormholes in string theory. Preprint at arXiv:1611.03164v3 [hep-th] (2017).
130. Strominger, A. Massless black holes and conifolds in String Theory. Preprint at arXiv:hep-th/9504090v1 (1995).
131. Emparan, R. Massless black hole pairs in string theory. Preprint at arXiv:hep-th/9607102v3 (1996).
132. Balasubramanian, V., Kraus, P. & Shigemori, M. Massless black holes and black rings as effective geometries of the D1–D5 system, *Class. Quantum Grav.* 22, 4803–4837 (2005).
133. Hull, C. M. Duality, Enhanced Symmetry and Massless Black Holes. *Proceedings of Strings'95: Future Perspectives in String Theory* (World Scientific, I. Bars et al. eds.), p. 230. (1996).
134. Van Raamsdonk, M. Building up spacetime with quantum entanglement, *Gen Relativ Gravit.* 42:2323–2329 (2010).

135. Jensen K. & Karch, A. The holographic dual of an EPR pair has a wormhole. Preprint at arXiv:1307.1132v2 [hep-th] (2013).
136. Balasubramanian, V. et al. Multiboundary Wormholes and Holographic Entanglement. Preprint at arXiv:1406.2663v2 [hep-th] (2014).
137. Yin, J. et al. Bounding the speed of 'spooky action at a distance'. arXiv:1303.0614v1 [quant-ph] (2013).
138. Popescu, S. & Rohrlich, D. Causality and Nonlocality as Axioms for Quantum Mechanics. arXiv:quant-ph/9709026v2 (1997).
139. Peacock, K. A. & Hepburn, B. Begging the Signalling Question: Quantum Signalling and the Dynamics of Multiparticle Systems. arXiv:quant-ph/9906036v1 (1999).
140. Ghirardi, G. C. et al. Experiments of the EPR Type Involving CP-Violation Do not Allow Faster-than-Light Communication between Distant Observers. *Europhys. Lett.* Vol.6, pp.95-100 (1988).
141. Eberhard, P. H. & Ross, R. R. Quantum field theory cannot provide faster-than-light communication. *Foundations of Physics Letters* 2: 127 (1989).
142. Hawking, S. A brief history of time. Bantam Books. (1998).
143. Steinhauer, J. Observation of quantum Hawking radiation and its entanglement in an analogue black hole. *Nature Physics*, 12, 959–965 (2016).
144. Mastriani, M. Quantum spectral analysis: frequency in time. (2018) <hal-01655209v2>
145. Mastriani, M.: Quantum spectral analysis: frequency in time with applications to signal and image processing (2018) <hal-01654125v2>
146. Schrödinger, E. Die gegenwaertige Situation in der Quantenmechanik, *Die Naturwissenschaften* 23, 807. (1935).
147. Schrödinger, E. Discussion of probability relations between separated systems, *Proc. Cambridge Philos. Soc.* 32, 446. (1935).
148. Tolimieri, R., An, M. & Lu, C. Algorithms for Discrete Fourier Transform and convolution. Springer Verlag, New York (1997).
149. Briggs, W. L. & Van Emden, H. The DFT: An Owner's Manual for the Discrete Fourier Transform. SIAM, Philadelphia (1995).
150. Hsu, H. P. Fourier Analysis. Simon & Schuster, New York (1970).
151. Oppenheim, A. V, Willsky, A. S. & Nawab, S. H. Signals and Systems. Second Edition, Prentice Hall, Upper Saddle River, NJ (1997).
152. Oppenheim, A. V. & Schaffer, R. W. Digital Signal Processing. Prentice Hall, Englewood Cliffs, NJ (1975).
153. Van Loan, C. Computational Frameworks for the Fast Fourier Transform, SIAM (1992).
154. Heideman, M. T., Johnson, D. H. & Burrus, C. S. Gauss and the history of the fast Fourier transform. *IEEE ASSP Magazine* 1(4), 14–21. (1984).
155. Hawking, S. W. Black holes and thermodynamics *Physical Review D* **13**(2):191-197. (1976).
156. MacKay, D. J. C. Information Theory, Inference, and Learning Algorithms Cambridge University Press. (2003).
157. Roston, G. B. Quantum entanglement, spin-1/2 and the Stern–Gerlach experiment. *Eur. J. Phys.* 26, 657–672. (2005).
158. Castro Ruiz, E., Giacomini, F. & Brukner, C. Entanglement of quantum clocks through gravity. *PNAS*, E2303–E2309 (2017).
159. Micadei, K., et al, Reversing the thermodynamic arrow of time using quantum correlations, arXiv:1711.03323v1 [quant-ph] (2017)
160. Weston, M. M., et al. Heralded quantum steering over a high-loss channel. *Science Advances*. Vol.4, No.1, e1701230 (2018)
161. Sackett, C. A., et al. Experimental entanglement of four particles. *Nature* **404**, 256-259 (2000).
162. Huggins, E. R. Geometrical Optics, Physics 2000, Moose Mountain Digital Press, New Hampshire 03750 (2000)
163. Karris, S. T. Circuit Analysis I with MATLAB® Applications. Orchard Publications, Fremont, California (2004)
164. Busch, P., Lahti, P., Pellonpää, J. P. and Ylisen, K. Quantum Measurement. Springer (2016)
165. De Graeve, R. and Parrisé, B. Symbolic algebra and Mathematics with Xcas. University of Grenoble I (2007) https://www-fourier.ujf-grenoble.fr/~parrisé/giac/cascmd_en.pdf

166. Kurucz, Z., Koniorczyk, Z. and Janszky, J. Teleportation with partially entangled states. *Fortschr. Phys.* 49, No.10–11, 1019–1025 (2001)
167. Yu, X.-T., Zhang, Z.-C. and Xu J. Distributed wireless quantum communication networks with partially entangled pairs. *Chin. Phys. B*, Vol.23, No.1 (2014) 010303
168. Li, W.-D., Zhang, J.-L. and Gu, Y.-J. Quantum circuits for realizing deterministic and exact teleportation via two partially entangled pairs particles. *IOP Chinese Physics*, Vol.5, No.3 (2006)
169. Cai, X.-F., Yu, X.-T., Shi, L.-H. and Zhang, Z.-C.. Partially entangled states bridge in quantum teleportation. *Springer Front. Phys.*, 2014, 9(5): 646–651.
170. Deng, D. L., Li, X. and Das Sarma, S. Quantum Entanglement in Neural Network States, *Physical Review X* 7, 021021 (2017)
171. Horodecki, P. L., Horodecki, R. Distillation and Bound Entanglement, *Quantum Information and Computation*, Vol.1, No.1, pp.45-75, Rinton Press (2001)
172. Kalb, N., et al. Entanglement Distillation between Solid-State Quantum Network Nodes. *arXiv:1703.03244v1 [quant-ph]* (2017)
173. Briegel, H. J., et al. Entanglement Purification. In: Bouwmeester D., Ekert A., Zeilinger A. (eds) *The Physics of Quantum Information*. Springer, Berlin, Heidelberg. (2000)
174. Parker, S., Bose, S. and Plenio M. B. Entanglement Purification via Entanglement Swapping. In: Braunstein S. L., Pati A. K. Eds. *Quantum Information with Continuous Variables*. Springer, Dordrecht (2003)
175. Dür, W. and Briegel, Hans.-J. Purification and Distillation, in *Lectures on Quantum Information*. D. Bruß and G. Leuchs Eds. Wiley-VCH Verlag GmbH, Weinheim, Germany. (2006)
176. Dür, W. and Briegel, H. J. Entanglement purification and quantum error correction, *arXiv:0705.4165v2 [quant-ph]* (2007)
177. Bernád, J. Z., Torres, J. M., Kunz, L. and Alber, G. Multiphoton-state-assisted entanglement purification of material qubits, *Physical Review A* 93, 032317 (2016)
178. Foot, C. J. *Atomic Physics*, Oxford University Press, N.Y. (2005)
179. Metcalf, H. J. and van der Straten, P. Laser Cooling and Trapping. *Journal of the Optical Society of America B*. 20. 10.1364/JOSAB.20.000887. (2003)
180. Vuletic, V. and Chu, S. Laser Cooling of Atoms, Ions, or Molecules by Coherent Scattering, Vol.84, No.17 *Physical Review Letters*. (2000)
181. Rideout, D., et al. Fundamental quantum optics experiments conceivable with satellites - reaching relativistic distances and velocities. *arXiv:1206.4949v2 [quant-ph]* (2012)
182. Kiktenko, E. O., Fedorov, A. K. and Manko, V. I. Teleportation in an indivisible quantum system, *arXiv:1512.05168v2* (2016)
183. Zheng, S.-B. Teleportation of Quantum States through Mixed Entangled Pairs. *Chinese Physics Letters*. Vol.23, No.9, 2356 (2006)